WFPC2 Instrument Science Report 96-05[1]

Wavelength / Aperture Calibration of the WFPC2 Linear Ramp Filters

J. Biretta, C. Ritchie, S. Baggett, and J. MacKenty
May 23, 1996

ABSTRACT

We derive transformations between central wavelengths on the linear ramp filters and aperture locations in the WFPC2 focal plane. Tables containing appropriate HST pointing offsets are then generated for use by the TRANS observation planning software. In closing we review software tools and calibration procedures for linear ramp filter data.

1. Introduction

The WFPC2 Linear Ramp Filters (LRFs) offer a narrow band imaging capability which is tunable from ~3700 to ~9800 Angstroms with bandpass FWHM $\Delta\lambda/\lambda$~0.013. They provide a unique tool for study of problems ranging from planetary absorption bands to emission lines in high-z galaxies and quasars.

The LRF filter set contains four narrow band interference filters whose central wavelength varies as a function of position on the filter surface. Utilization of these filters requires an accurate mapping from bandpass central wavelength to telescope pointing offset. This mapping is the subject of the present report.

In Section 2 we derive a generalized model which allows mapping of LRF wavelengths into both the (V2,V3) planes and WFPC2 CCD pixel coordinates. Ingredients of this model are the physical specifications of the filters and filter mechanisms, laboratory wavelength calibrations for the filters, and on-orbit calibrations of the WFPC2 focal plane geometry. In Section 3 we refine the generalized model using ground-based and on-orbit observations of wavelength and geometric calibrations. Sections 4, 5, and 6 use the refined model to assemble the tables which convert proposal LRF central wavelengths to HST pointing offsets. Finally, Section 7 gives information for observers, including details on the implementation of early LRF science proposals, descriptions of LRF software tools, and flat field and photometric calibration procedures.

1. Copies of this report may be obtained from the Science Support Division, Space Telescope Science Institute, 3700 San Martin Drive, Baltimore MD 21218, by e-mail to help@stsci.edu, by anonymous FTP to stsci.edu directory instrument_news/WFPC2, and by WWW at http://www.stsci.edu/instruments.html

Table of Contents

2. A Model for Mapping LRF Wavelengths onto Aperture Locations.

In this section we develop a geometric mapping of the linear ramp filters onto the (V2,V3) coordinate system and WFPC2 CCD pixel locations. We begin with a detailed description of the filters, the effects of vignetting, filter wheel rotation, and a geometric model for projecting the filters onto the (V2,V3) focal plane. The section closes with the other essential ingredient, a geometric model mapping WFPC2 CCD pixel locations onto the (V2,V3) plane. The approach will be to establish coordinates of important features of each linear ramp filter, and then map these into the focal plane with a simple series of geometric coordinate transformations.

2.1 Properties of the Linear Ramp Filters.

There are four separate linear ramp filters, named FR418N, FR533N, FR680N, and FR868N, which occupy four slots in wheel 12 of the Selectable Optical Filter Assembly (SOFA). Each of these filters is a sandwich of colored glass, a thin film, epoxy, a second thin film, and BK7 (clear glass). The thin films are deposited in four strips side-by-side, where the central wavelength varies linearly along each strip. Figure 1 illustrates the typical layout of each filter. In the design specifications, wavelengths are set at two “strip locations” for each ramp, for example points 1A and 1B in Figure 1. The filters are designed to provide a 6% wavelength run between these points. The direction of wavelength increase reverses on each adjacent ramp, so that points 1B and 2A have the same wavelength, and so forth.

Figure 1. Drawing of the linear ramp filter physical design specifications. All units are inches. The outer periphery of the filter glass constitutes a 2.256 inch square with rounded corners. Ramps #2 and #3 are 0.490 inches wide, while the outer ramps (#1 and #4) are approximately 0.638 inches wide. Central wavelength increases in direction shown by arrows on ramps. "Strip locations" 1B and 2A have same wavelength, and so forth. From JPL Drawing 10136830.

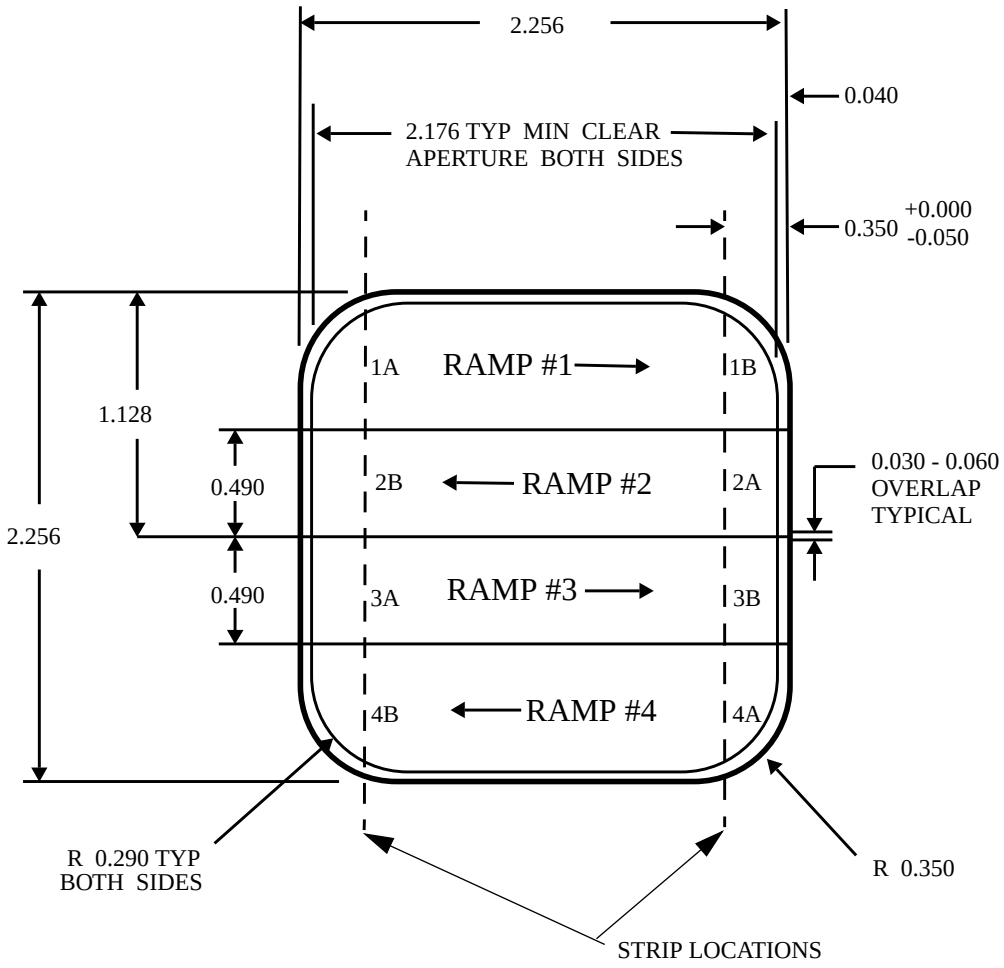

Wavelength calibration is provided by a set of measurements made at JPL using a monochrometer with a narrow slit to provide illumination, and a micrometer to provide position information (See Evans 1992). The central wavelength of each ramp was measured at five equally spaced points along the length of the ramp. The resulting data were later integrated over an annular aperture to simulate the Optical Telescope Assembly (OTA) beam. Second order polynomials of the form

$$\lambda_0 = A_0 + A_1 Y + A_2 Y^2$$

were fit to the results of the integration, where λ_0 is the local central wavelength, and Y is the distance in inches measured from the edge of the filter glass. The parameters A_0, A_1, and A_2 are given in Table 1 (from Evans 1992).

Table 1: Coefficients for second-order wavelength equations.

Filter	Ramp #	A_0	A_1	A_2
FR418N	1	3657.7	138.7	0.6178
FR418N	2	3876.9	158.6	0.5472
FR418N	3	4130.5	168.8	-0.7389
FR418N	4	4371.3	185.8	0.2913
FR533N	1	4677.7	177.3	-1.125
FR533N	2	4948.4	199.2	0.6484
FR533N	3	5257.3	217.9	-1.481
FR533N	4	5596.9	220.9	-0.6938
FR680N	1	5916.0	269.4	0.3460
FR680N	2	6290.8	275.6	0.7184
FR680N	3	6673.5	301.6	0.3321
FR680N	4	7141.9	289.3	-0.2999
FR868N	1	7555.5	320.4	1.906
FR868N	2	8014.3	350.5	-0.7500
FR868N	3	8510.7	375.6	0.3706
FR868N	4	9034.3	387.2	0.8722

The TRANS system for processing proposals assumes wavelength varies linearly with distance, hence for simplicity we have used a linear approximation of the form

$$\lambda_0 = B_0 + B_1 Y$$

where the coefficients B_0 and B_1 are given in Table 2. Hereinafter we use this linear wavelength relation. Typical differences between the second-order equation and the linear approximation are ~0.3 Angstrom; the maximum difference occurs on the FR868N #1 ramp and is 1.5 Angstrom. These differences are all insignificant compared to the ~100 Angstrom bandpass FWHM.

.

Table 2: Coefficients for linearized wavelength equations.

Filter	Ramp #	B_0 (Angstroms)	B_1 (Angstroms / inch)
FR418N	1	3657.2	140.08
FR418N	2	3876.5	159.82
FR418N	3	4131.1	167.15
FR418N	4	4371.1	186.45
FR533N	1	4678.6	174.79
FR533N	2	4947.9	200.65
FR533N	3	5258.5	214.60
FR533N	4	5597.5	219.35
FR680N	1	5915.7	270.17
FR680N	2	6290.2	277.20
FR680N	3	6673.2	302.34
FR680N	4	7142.1	288.63
FR868N	1	7554.0	324.64
FR868N	2	8014.9	348.83
FR868N	3	8510.4	376.43
FR868N	4	9033.6	389.14

2.2 Vignetting and cross-talk at the filters.

An additional factor governing the placement of targets in the WFPC2 field of view is the avoidance of vignetted regions on the filter, and regions where light from the OTA passes through more than one ramp (i.e. cross-talk regions).

The ramp filters are located in wheel 12 of the SOFA, which is about 7.20 inches from the OTA focal plane (the focal plane here being defined as the focal position of the 4th K-spot; Trauger 1993). Hence for the F/24 OTA focal ratio an unaberrated OTA beam would have a diameter of 0.300 inch at the ramp filters, or about 27.4 arcseconds, assuming an OTA focal length of 57.6 meters. Some additional allowance is needed for spherical aberration, since the OTA beam is aberrated at the filter; we have assumed spherical aberration gives a blur diameter of 5.0 arcseconds at the focal plane (i.e. diameter containing 100% of light). Thus we have adopted 0.355 inches, or 32.4 arcseconds, as the diameter of the aberrated OTA beam at the filter.

The outer edge of the unvignetted field is determined by the clear aperture of the filter, which is defined by the retaining lip on the SOFA filter wheel. This retaining lip forms a

2.069 inch square with 0.239 inch radius rounded corners. This, together with the OTA beam size described above, leads to an approximately square unvignetted field of 1.714 inches or 156.40 arcseconds on a side.

The two inner ramps on each filter (ramps #2 and #3) are 0.490 inches wide, though about 0.030 inches of width are lost to the "dead" overlap region between ramps (Figure 1). Given an OTA beam diameter of 0.355 inches, the clear field-of-view of the inner two ramps has a width of 0.105 inches or 9.6 arcseconds at the focal plane.

The outer two ramps (#1 and #4 ramps) are physically wider, and hence give a wider clear field-of-view at the focal plane. If we include the blockage from the filter wheel retaining lip (recall the 2.069 inch square aperture), and the "dead" overlap region, the physical width of the ramp is about 0.515 inches, leading to an unvignetted field of 0.160 inches or 14.6 arcseconds at the focal plane.

It should be noted that the appearance in images of the ramp boundary regions will depend on the light source. For monochromatic light, the part of the OTA beam passing through an adjacent ramp will generally be far from the central wavelength for the adjacent ramp, and hence is blocked, causing a vignetting. On the other hand, for a continuum light source, there will generally be only slight dimming of the image in the boundary regions; the light lost from one ramp is simply made up by light passing through the adjacent ramp at a different wavelength. The width of this "cross-talk" region is the OTA beam diameter at the filter, which is 0.355 inches or 32.4 arcseconds wide.

2.3 Rotation of the filter wheel

It will be necessary to rotate the filter wheel to move some wavelengths closer to the CCD centers. Otherwise these wavelengths might fall between CCDs, or just outside the region imaged by the CCDs. There are three possible rotated positions, besides the nominal zero rotation: -33, -18, and +15 degree rotations. The first two are already implemented in the commanding software, while new commanding was developed to support the +15 degree rotation. This will be discussed further in Section 5.

In addition, it is necessary to know the location of the rotation axis. According to JPL blue prints of the filter wheel, the rotation axis is 2.165 inches above, and 0.704 inches left, of the filter cavity center, in a system where X and Y run parallel to the edges of the square filter cavity, with Y parallel to the direction of wavelength run.

2.4 Projection of the Ramp Filters into the (V2,V3) focal plane

Once specification of the filter and filter wheel is complete, it is a simple matter to project the filter into the (V2,V3) plane. Wavelengths and other filter attributes are mapped into the (V2,V3) plane using a series of generalized coordinate transformations. These transformations include shift, linear scale changes, and rotations, and are given by equations:

$$Y_{(n+1)} = -C_{n,3} \cdot (X_n + C_{n,1}) \cdot \sin(-C_{n,5}) + C_{n,4} \cdot (Y_n + C_{n,2}) \cdot \cos(-C_{n,5}) \quad (1)$$

$$X_{(n+1)} = C_{n,3} \cdot (X_n + C_{n,1}) \cdot \cos(-C_{n,5}) + C_{n,4} \cdot (Y_n + C_{n,2}) \cdot \sin(-C_{n,5})$$

Here the $C_{n,1}$ and $C_{n,2}$ terms specify translations; the $C_{n,3}$ and $C_{n,4}$ terms specify linear scale changes; and the $C_{n,5}$ term specifies a rotation about the origin. A ramp central wavelength would be mapped into the (V2,V3) plane using nine (n=1 to 9) serial applications of the above transformations, along with the coefficients in Table 3. For example, setting X_1= 0 and Y_1 = λ (the desired LRF wavelength) and performing the n=1 to n=9 transformations, results in (V2,V3) coordinates for the target. This formality may seem cumbersome, but the function of the individual terms is easily understood, and the transformation can be rapidly evaluated by computer.

While Table 3 contains 720 coefficients (16 ramp segments each with 45 parameters), few of them are actually utilized. Many are inert, and are set to either 0 or 1. Other parameters are shared by different ramps on the same filter, or are shared by different filters. Only ten of the parameters are considered “free” and will be adjusted as described in Section 3. These are $C_{7,1}$ and $C_{7,2}$, which are the same for all filters, and $C_{3,1}$ and $C_{3,2}$ for which each filter has an independent set. The filter wheel rotation angle is given by θ.

Table 3: LRF Wavelength / (V2,V3) Transformation Coefficients.

Filter & Ramp #	λmin	λmax	n	$C_{n,1}$	$C_{n,2}$	$C_{n,3}$	$C_{n,4}$	$C_{n,5}$	Type
FR418N1	3672	3961	1	0.7698	-3657.2	1	0.00713888	0	0
			2	0	-1.128	1	1	0	0
			3	$C_{3,1}$	$C_{3,2}$	1	1	0	0
			4	+0.704	-2.165	1	1	θ	0
			5	-0.704	+2.165	1	1	0	0
			6	0	0	91.252	91.252	0	0
			7	$C_{7,1}$	$C_{7,2}$	1	1	0	0
			8	0	0	1	1	-135	0
			9	0	0	-1	1	0	0
FR418N2	3894	4222	1	0.245	-3876.5	1	-0.00625704	0	0
			2	0	1.128	1	1	0	0
			3	$C_{3,1}$	$C_{3,2}$	1	1	0	0
			4	+0.704	-2.165	1	1	θ	0

Filter & Ramp #	λmin	λmax	n	$C_{n,1}$	$C_{n,2}$	$C_{n,3}$	$C_{n,4}$	$C_{n,5}$	Type
			5	-0.704	+2.165	1	1	0	0
			6	0	0	91.252	91.252	0	0
			7	$C_{7,1}$	$C_{7,2}$	1	1	0	0
			8	0	0	1	1	-135	0
			9	0	0	-1	1	0	0
FR418N3	4150	4490	1	-0.245	-4131.1	1	0.00598254	0	0
			2	0	-1.128	1	1	0	0
			3	$C_{3,1}$	$C_{3,2}$	1	1	0	0
			4	+0.704	-2.165	1	1	θ	0
			5	-0.704	+2.165	1	1	0	0
			6	0	0	91.252	91.252	0	0
			7	$C_{7,1}$	$C_{7,2}$	1	1	0	0
			8	0	0	1	1	-135	0
			9	0	0	-1	1	0	0
FR418N4	4390	4770	1	-0.7698	-4371.1	1	-0.00536340	0	0
			2	0	1.128	1	1	0	0
			3	$C_{3,1}$	$C_{3,2}$	1	1	0	0
			4	+0.704	-2.165	1	1	θ	0
			5	-0.704	+2.165	1	1	0	0
			6	0	0	91.252	91.252	0	0
			7	$C_{7,1}$	$C_{7,2}$	1	1	0	0
			8	0	0	1	1	-135	0
			9	0	0	-1	1	0	0
FR533N1	4695	5055	1	-0.7698	-4678.6	1	0.00572115	0	0
			2	0	-1.128	1	1	0	0
			3	$C_{3,1}$	$C_{3,2}$	1	1	0	0
			4	+0.704	-2.165	1	1	θ	0
			5	-0.704	+2.165	1	1	0	0
			6	0	0	91.252	91.252	0	0
			7	$C_{7,1}$	$C_{7,2}$	1	1	0	0
			8	0	0	1	1	-135	0

Filter & Ramp #	λmin	λmax	n	$C_{n,1}$	$C_{n,2}$	$C_{n,3}$	$C_{n,4}$	$C_{n,5}$	Type
			9	0	0	-1	1	0	0
FR533N2	4970	5380	1	-0.245	-4947.9	1	-0.00498393	0	0
			2	0	1.128	1	1	0	0
			3	$C_{3,1}$	$C_{3,2}$	1	1	0	0
			4	+0.704	-2.165	1	1	θ	0
			5	-0.704	+2.165	1	1	0	0
			6	0	0	91.252	91.252	0	0
			7	$C_{7,1}$	$C_{7,2}$	1	1	0	0
			8	0	0	1	1	-135	0
			9	0	0	-1	1	0	0
FR533N3	5280	5720	1	0.245	-5258.5	1	0.00465985	0	0
			2	0	-1.128	1	1	0	0
			3	$C_{3,1}$	$C_{3,2}$	1	1	0	0
			4	+0.704	-2.165	1	1	θ	0
			5	-0.704	+2.165	1	1	0	0
			6	0	0	91.252	91.252	0	0
			7	$C_{7,1}$	$C_{7,2}$	1	1	0	0
			8	0	0	1	1	-135	0
			9	0	0	-1	1	0	0
FR533N4	5620	6070	1	0.7698	-5597.5	1	-0.00455886	0	0
			2	0	1.1280	1	1	0	0
			3	$C_{3,1}$	$C_{3,2}$	1	1	0	0
			4	+0.704	-2.165	1	1	θ	0
			5	-0.704	+2.165	1	1	0	0
			6	0	0	91.252	91.252	0	0
			7	$C_{7,1}$	$C_{7,2}$	1	1	0	0
			8	0	0	1	1	-135	0
			9	0	0	-1	1	0	0
FR680N1	5945	6501	1	-0.7698	-5915.7	1	-0.00370137	0	0
			2	0	1.128	1	1	0	0
			3	$C_{3,1}$	$C_{3,2}$	1	1	0	0

Filter & Ramp #	λmin	λmax	n	$C_{n,1}$	$C_{n,2}$	$C_{n,3}$	$C_{n,4}$	$C_{n,5}$	Type
			4	+0.704	-2.165	1	1	θ	0
			5	-0.704	+2.165	1	1	0	0
			6	0	0	91.252	91.252	0	0
			7	$C_{7,1}$	$C_{7,2}$	1	1	0	0
			8	0	0	1	1	-135	0
			9	0	0	-1	1	0	0
FR680N2	6320	6895	1	-0.245	-6290.2	1	0.00360750	0	0
			2	0	-1.128	1	1	0	0
			3	$C_{3,1}$	$C_{3,2}$	1	1	0	0
			4	+0.704	-2.165	1	1	θ	0
			5	-0.704	+2.165	1	1	0	0
			6	0	0	91.252	91.252	0	0
			7	$C_{7,1}$	$C_{7,2}$	1	1	0	0
			8	0	0	1	1	-135	0
			9	0	0	-1	1	0	0
FR680N3	6701	7330	1	0.245	-6673.2	1	-0.00330755	0	0
			2	0	1.128	1	1	0	0
			3	$C_{3,1}$	$C_{3,2}$	1	1	0	0
			4	+0.704	-2.165	1	1	θ	0
			5	-0.704	+2.165	1	1	0	0
			6	0	0	91.252	91.252	0	0
			7	$C_{7,1}$	$C_{7,2}$	1	1	0	0
			8	0	0	1	1	-135	0
			9	0	0	-1	1	0	0
FR680N4	7170	7761	1	0.7698	-7142.1	1	0.00346462	0	0
			2	0	-1.128	1	1	0	0
			3	$C_{3,1}$	$C_{3,2}$	1	1	0	0
			4	+0.704	-2.165	1	1	θ	0
			5	-0.704	+2.165	1	1	0	0
			6	0	0	91.252	91.252	0	0
			7	$C_{7,1}$	$C_{7,2}$	1	1	0	0

Filter & Ramp #	λmin	λmax	n	$C_{n,1}$	$C_{n,2}$	$C_{n,3}$	$C_{n,4}$	$C_{n,5}$	Type
			8	0	0	1	1	-135	0
			9	0	0	-1	1	0	0
FR868N1	7761	8251	1	0.7698	-7554.0	1	0.00308029	0	0
			2	0	-1.128	1	1	0	0
			3	$C_{3,1}$	$C_{3,2}$	1	1	0	0
			4	+0.704	-2.165	1	1	θ	0
			5	-0.704	+2.165	1	1	0	0
			6	0	0	91.252	91.252	0	0
			7	$C_{7,1}$	$C_{7,2}$	1	1	0	0
			8	0	0	1	1	-135	0
			9	0	0	-1	1	0	0
FR868N2	8055	8765	1	0.245	-8014.9	1	-0.00286673	0	0
			2	0	1.128	1	1	0	0
			3	$C_{3,1}$	$C_{3,2}$	1	1	0	0
			4	+0.704	-2.165	1	1	θ	0
			5	-0.704	+2.165	1	1	0	0
			6	0	0	91.252	91.252	0	0
			7	$C_{7,1}$	$C_{7,2}$	1	1	0	0
			8	0	0	1	1	-135	0
			9	0	0	-1	1	0	0
FR868N3	8545	9320	1	-0.245	-8510.4	1	0.00265657	0	0
			2	0	-1.128	1	1	0	0
			3	$C_{3,1}$	$C_{3,2}$	1	1	0	0
			4	+0.704	-2.165	1	1	θ	0
			5	-0.704	+2.165	1	1	0	0
			6	0	0	91.252	91.252	0	0
			7	$C_{7,1}$	$C_{7,2}$	1	1	0	0
			8	0	0	1	1	-135	0
			9	0	0	-1	1	0	0
FR868N4	9070	9862	1	-0.7698	-9033.6	1	-0.00256976	0	0
			2	0	1.128	1	1	0	0

Filter & Ramp #	λmin	λmax	n	$C_{n,1}$	$C_{n,2}$	$C_{n,3}$	$C_{n,4}$	$C_{n,5}$	Type
			3	$C_{3,1}$	$C_{3,2}$	1	1	0	0
			4	+0.704	-2.165	1	1	θ	0
			5	-0.704	+2.165	1	1	0	0
			6	0	0	91.252	91.252	0	0
			7	$C_{7,1}$	$C_{7,2}$	1	1	0	0
			8	0	0	1	1	-135	0
			9	0	0	-1	1	0	0

The nine serial transformations used to map LRF central wavelengths into the (V2,V3) plane can be summarized as follows:

(n=1): Convert Y from wavelength (Angstroms) to offset (inches) from low-wavelength end of the filter glass. It should be apparent that $C_{1,2} = (-B_0)$ and $C_{1,4} = B_1^{-1}$, where B_0 and B_1 are given in Table 2. Note that the sign of $C_{1,4}$ can be either positive or negative, depending on whether wavelength increases with increasing Y, or with decreasing Y. Also, transform X coordinate (inches) from origin at ramp center to origin at filter center.

(n=2): Complete transformation from wavelength to (x,y) system with origin at filter center, and with units of inches. $C_{2,2}$ is either -1.128 or +1.128, depending on whether the low wavelength end of the ramp is at the top or bottom.

(n=3): Transform from origin at filter center, to origin at filter wheel cavity center. This should be a very small shift, and allows for any decenter of the filter in the filter wheel cavity.

(n=4): Translate origin to filter wheel rotation point, and rotate filter by angle $C_{4,5} = \theta$ if necessary. $C_{4,1}$ = 0.704 inches, and $C_{4,2}$ = 2.165 inches, always.

(n=5): Translate from filter wheel rotation axis to SOFA optical axis.

(n=6): Scale coordinates from inches to arcseconds in focal plane. Assuming the nominal focal length for a 2.4 meter, F/24, telescope we have $C_{6,3} = C_{6,4} = 91.252$ arcseconds per inch.

(n=7): Translate origin from SOFA optical axis to (V2,V3) origin. This effectively allows for a decenter of the SOFA relative to the (V2,V3) origin by $C_{7,1}$ and $C_{7,2}$ arcseconds.

(n=8, 9): Finally, rotate about origin and flip X axis, to obtain formal (V2,V3) coordinates.

Coordinates other than wavelength (e.g. ramp filter edges; limits of unvignetted regions) are mapped in the same way, by merely omitting the (n=1) and (n=2) transformations, and supplying coordinates referenced to the filter center in units of inches.

Figure 2 shows the resulting mapping of the F418N filter into the (V2,V3) focal plane. Wavelengths are indicated by “+” marks every 10 Angstroms and are labeled every 50 Angstroms. Dotted lines outline the approximate unvignetted regions. To make the plot easier to read and interpret, we have placed the +V2 direction towards the lower right of the figure, and the +V3 direction towards the lower left. The small x near the center indicates the origin.

Figure 2. FR418N filter projected into the (V2,V3) plane.

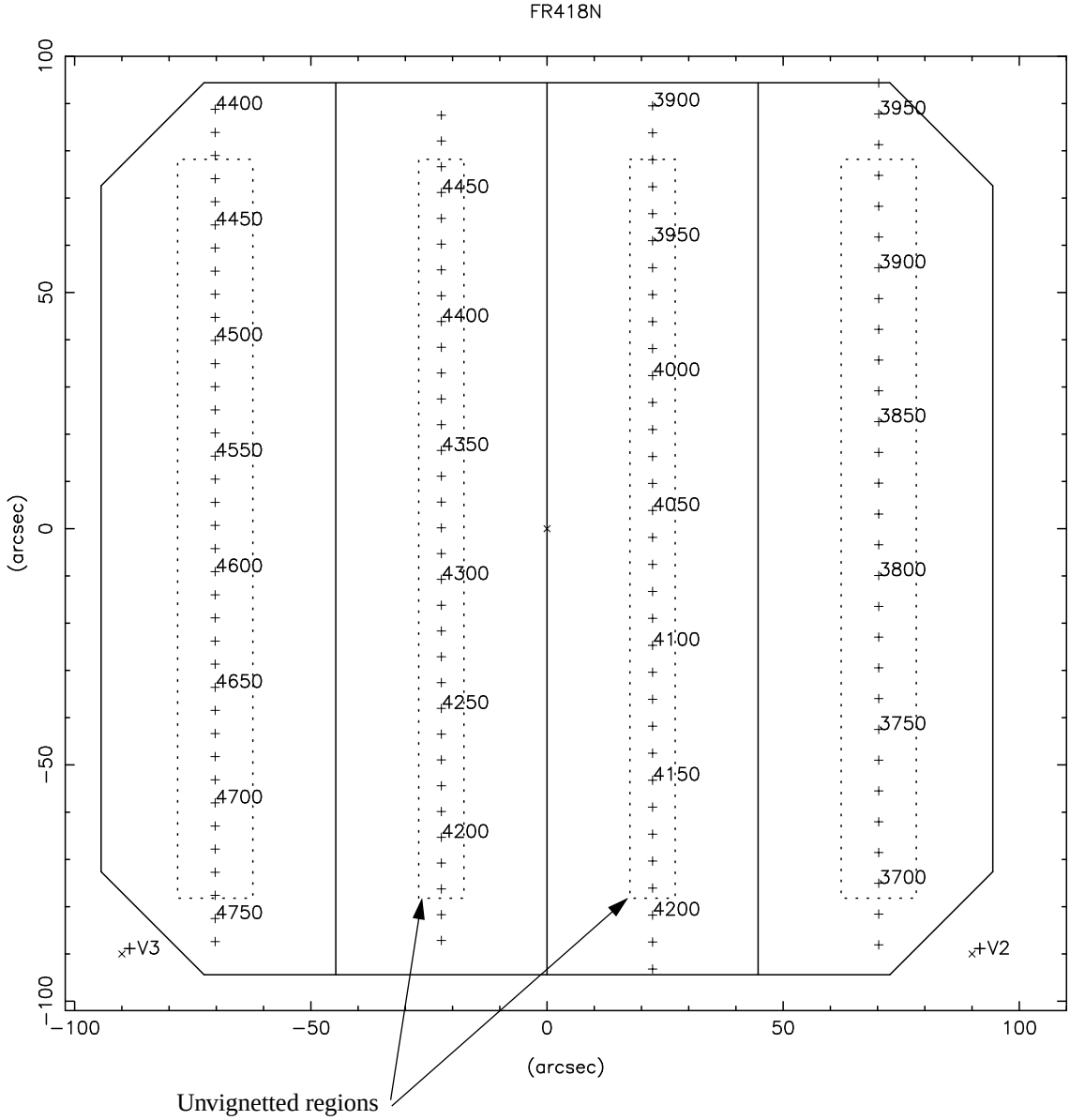

2.5 Geometry of the WFPC2 focal plane

We also require an accurate transformation between CCD pixel coordinates and (V2,V3). We have used the results of Cox (1994) for our model, which includes small differences in pixel scale, and small rotations of the CCDs from their nominal alignments. We also allow for a six arcsecond wide vignetted region along the pyramid vertices where the CCDs adjoin.

Again a series of coordinate transformations are used to relate pixel positions to (V2,V3).

There are two transformations used in series, and the coefficients are given in Table 4. Two different types of transformations are used. When $Type = 0$ a normal transformation is used:

$$X_{(n+1)} = C_{n,3} \cdot (X_n + C_{n,1}) \cdot \cos(-C_{n,5}) + C_{n,4} \cdot (Y_n + C_{n,2}) \cdot \sin(-C_{n,5})$$
$$Y_{(n+1)} = -C_{n,3} \cdot (X_n + C_{n,1}) \cdot \sin(-C_{n,5}) + C_{n,4} \cdot (Y_n + C_{n,2}) \cdot \cos(-C_{n,5}) \quad (2)$$

But when $Type = 1$ we use a parity-reversed transformation, to allow transformation from right-handed CCD coordinates to the left-handed (V2,V3) system:

$$X_{(n+1)} = -C_{n,3} \cdot (X_n - C_{n,1}) \cdot \cos(-C_{n,5}) + C_{n,4} \cdot (Y_n - C_{n,2}) \cdot \sin(-C_{n,5})$$
$$Y_{(n+1)} = C_{n,3} \cdot (X_n - C_{n,1}) \cdot \sin(-C_{n,5}) + C_{n,4} \cdot (Y_n - C_{n,2}) \cdot \cos(-C_{n,5}) \quad (3)$$

We have ignored the complication of geometric distortion in the cameras. This causes a maximum error of ~0.3 arcseconds, which is small in comparison with normal telescope pointing errors.

Table 4: Coefficients for transforming CCD pixel coordinates to (V2,V3).

CCD	*n*	$C_{n,1}$	$C_{n,2}$	$C_{n,3}$	$C_{n,4}$	$C_{n,5}$	*Type*
PC1	1	420	424.5	0.04553	0.04553	224.69	1
	2	1.8051	-30.8958	1	1	0	0
WF2	1	423.5	414.0	0.09959	0.09959	314.22	1
	2	-51.9649	-6.4458	1	1	0	0
WF3	1	436.0	424.5	0.09956	0.09956	44.52	1
	2	-0.7149	48.0942	1	1	0	0
WF4	1	423.0	421.0	0.09963	0.09963	135.09	1
	2	54.4351	-6.5758	1	1	0	0

Figure 3 shows the resulting model of the WFPC2 focal plane. Again +V3 is towards the lower left, and +V2 is towards the lower right.

Figure 3. WFPC2 CCDs projected into the (V2,V3) plane.

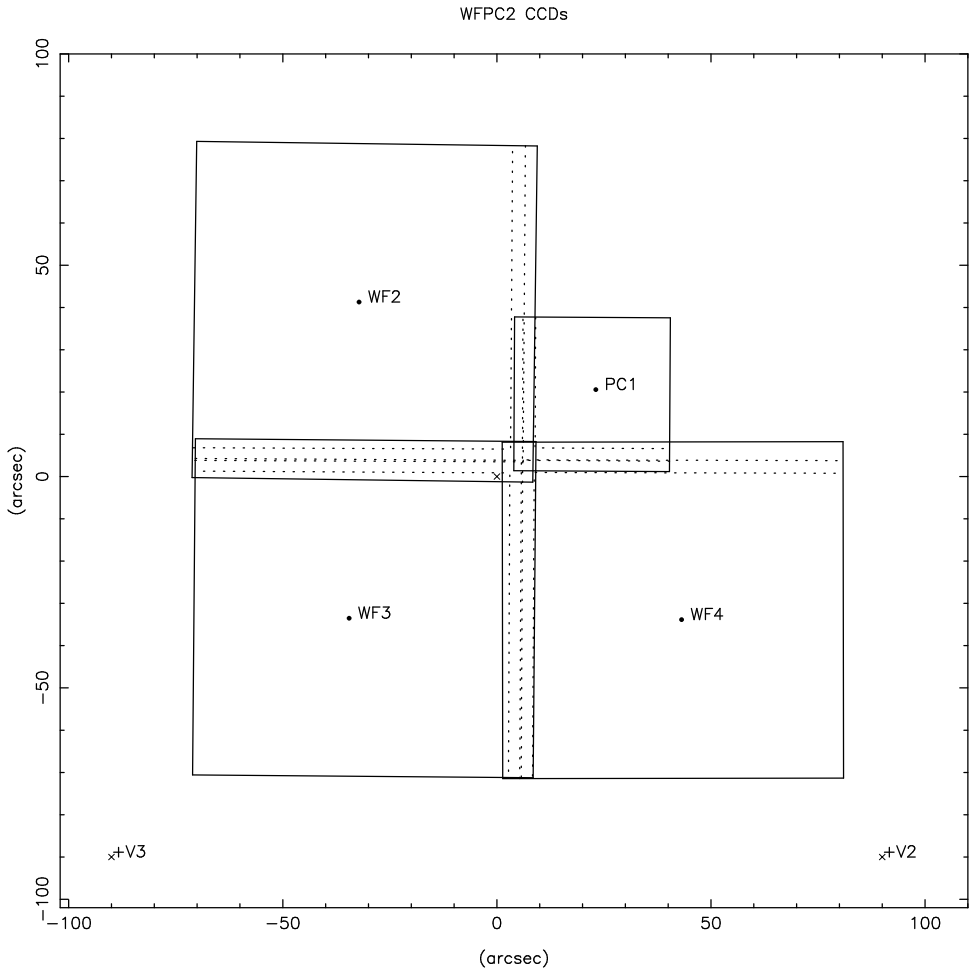

3. Refinement of the Model Through Measurement of Ground-Based and On-Orbit LRF Images.

At this point we are able to map both LRF wavelengths and CCD pixel positions into the (V2,V3) focal plane coordinate system. What remains is comparison of observed wavelength vs. CCD pixel position data, and then adjustment of free parameters as needed to bring the observations and model into agreement. As it turns out, there is relatively little data available to constrain the wavelength / aperture mapping. Hence we will allow only a minimum of free parameters. The following parameters will be varied:

(A) An (x,y) shift of the SOFA optical axis in the (V2,V3) focal plane. From previous work (Biretta and Sparks 1995; Scowen 1995) it is known that there is a misalignment of the SOFA optical axis and CCD focal plane by several arcseconds. We will allow for this misalignment by permitting the $C_{7,1}$ and $C_{7,2}$ parameters (see Table 3) to vary. We will require that all the LRF filters have the same value for these two parameters.

(B) Second, we will allow a small decenter (up to 0.016 inch) of each of the four LRF filters in the filter wheel cavities. Causes for such a shift might be mechanical clearance allowed in the filter wheel cavities, run-out of the SOFA main bearing, and errors during laboratory measurement of the wavelength positions on the ramps. These decenters will be implemented through the $C_{3,1}$ and $C_{3,2}$ parameters of Table 3. There will be a separate pair of these parameters for each filter.

We will use ground-based and on-orbit observations to constrain these parameters. There are several types of data which provide different constraints. We have used on-orbit images of VISFLATs taken through the ramps crossed with narrow band filters, and ground-based arc lamp data, to constrain placement of the filters in the wavelength direction. Placement in the transverse (cross-wavelength or normal) direction is constrained by measurements on VISFLATs without any crossing filter.

At the outset, it is useful to quantify the accuracy required for the wavelength / aperture calibration. The nominal pointing accuracy of HST, as determined by the accuracy of the guide star catalog, is about 1 arcsecond. Hence, our wavelength / aperture calibration needs only comparable accuracy. This also implies that the effects of optical distortion in the camera optics can be neglected, since they contribute offsets only at a level of ~0.3 arcseconds. Less accuracy is required in the direction of wavelength variation, since the filter bandpass FWHM corresponds to about 32 arcseconds at all wavelength settings. While a factor of two light loss would be unacceptable, one might consider a 5% loss as acceptable for the purposes of taking data (provided, of course, that it could be calibrated out later). This would correspond to about 5 arcseconds of pointing error, which we will take to be the maximum acceptable error in the wavelength direction.

3.1 Constraints from on-orbit narrow-band VISFLATs.

VISFLATs taken through ramp filters crossed with narrow band filters provide our most important source of information on the ramp positions in the wavelength direction.

The images used here were taken during February and March 1995 as part of proposal

6140. A typical image is shown in Figure 4. In this case the FR418N ramp is crossed with the F437N filter producing a single spot on WF2 in this mosaicked image. The full-intensity region of the spot is only about 15 arcseconds in size, though the wings extend to a large distance. The broad wings are caused by the ramp filter bandpass, and the ~40 arcsecond cross-dispersion width of the ramp, which are both convolved with the ~32 arcsecond diameter of the OTA beam at the filter.

Quantitative spot positions on the CCDs were measured by averaging a swath of pixels along one CCD axis (typically ~10 pixel wide swath), fitting a polynomial to the averaged values as a function of distance in the other direction, and then computing the spot position as the location of the polynomial peak. This was then repeated to get the position along the other axis. Figure 5 shows fits for the F418N + F437N image of Figure 4.

Figure 4.VISFLAT taken through unrotated FR418N + F437N. The four CCDs have been mosaicked together. A bright spot appears on WF2 due to 4369 Angstrom light transmitted by the F437N filter. Directions of rows and columns of WF2 are as indicated.

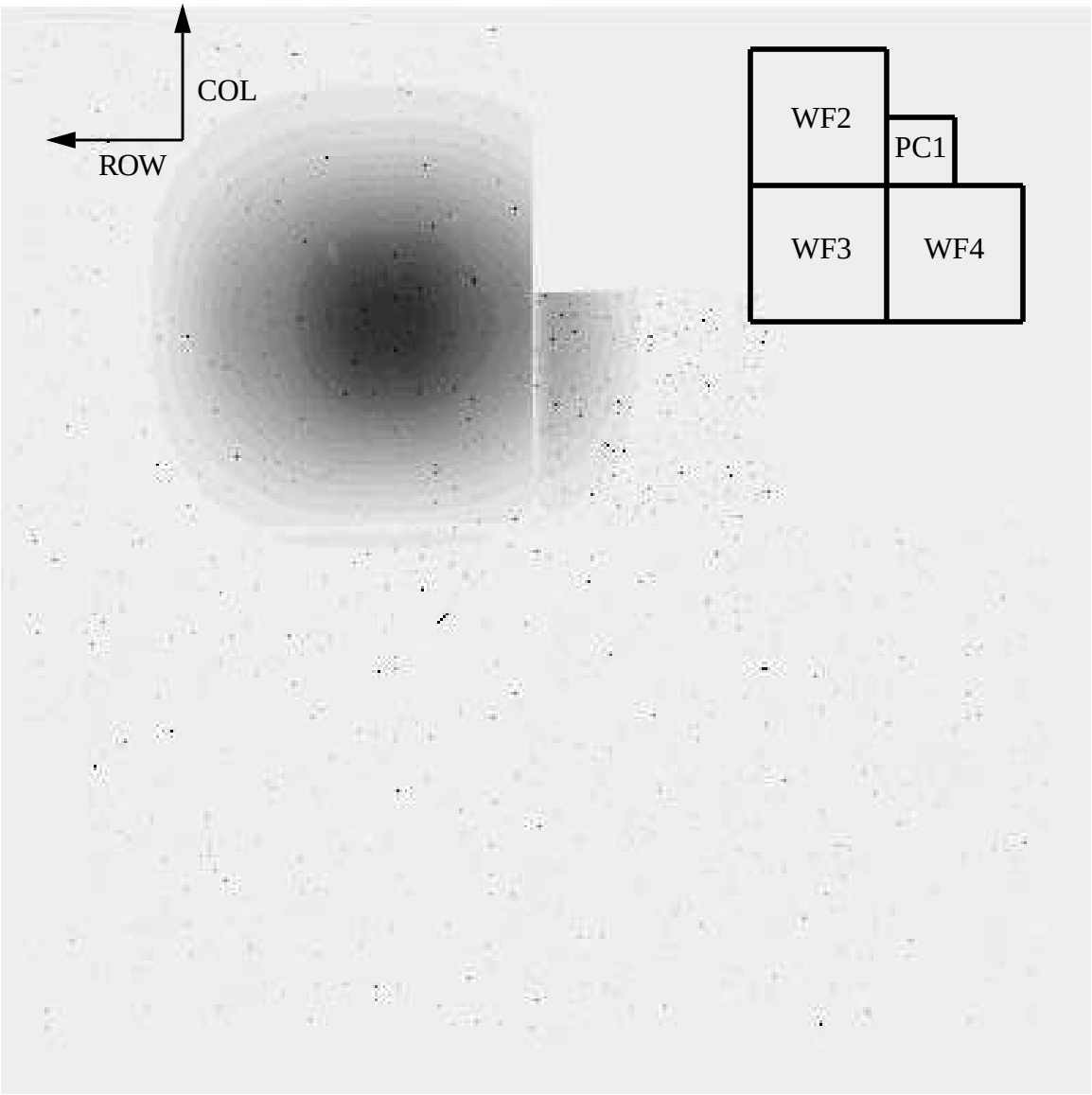

Figure 5. Observed intensity profiles and fitted polynomials for Figure 4 on WF2. Fitted position is (X,Y) = (342.5,238.5). (a.) Profile along CCD Y direction, in direction of constant wavelength. (b.) Profile along CCD X direction, along wavelength variation.

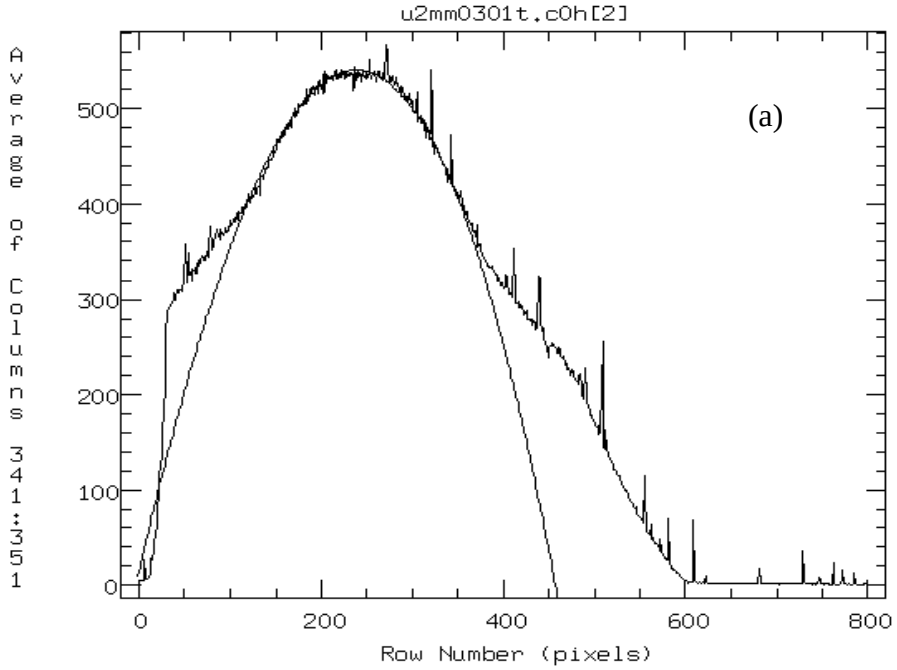

Y (Transverse to wavelength direction)

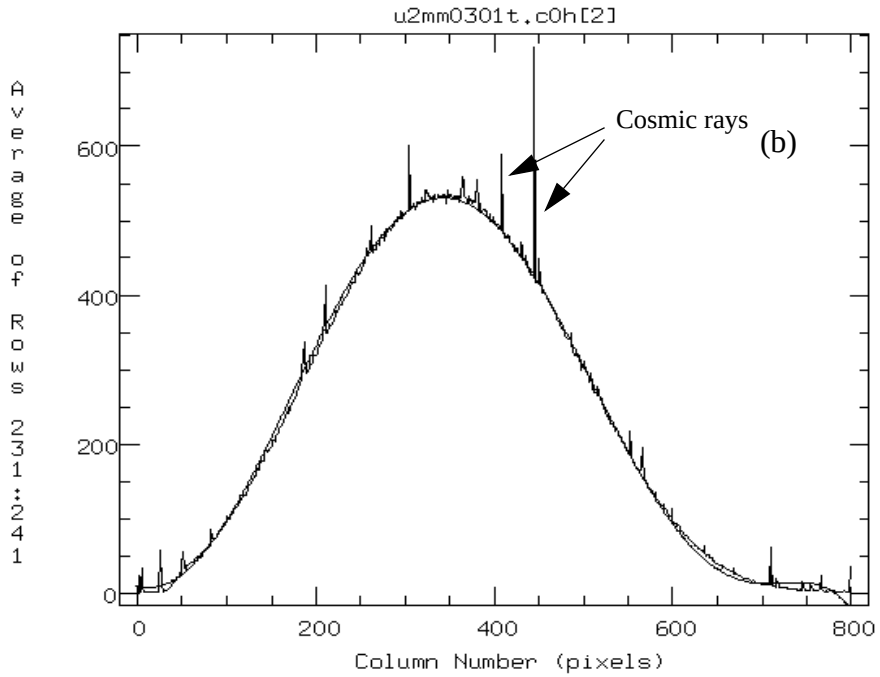

X (Along wavelength direction)

Results for this and other filters are given in Table 5. Measured positions are in units of CCD pixels, where Y is in the direction of "blooming." In the wavelength direction the curves typically have a well-behaved symmetric shape as defined by the filter bandpass, and the uncertainties are only a few pixels. However, the cross-dispersion curves are often highly asymmetric so that the measured peak may not correspond very well to the optical center of the ramp. Systematic errors as large as ~60 pixels can occur in peak locations in the cross-wavelength or transverse direction.

Table 5: Wavelength data from VISFLATS crossed with narrow band filters

Image Name	Ramp Filter	Ramp Filter Rotation	Ramp #	Narrow Band Filter	N. B. Filter λ (Ang.)	CCD	Measured Position of Spot (pixels) X ..... Y	
u2mm0101t	FR418N	0	1	F375N	3737	WF4	565.0	750.0
u2mm0301t	FR418N	0	3	F437N	4370	WF2	342.5	238.5
u2mm0302t	FR418N	0	4	F469N	4695	WF3	725.0	639.0
u2mm0401t	FR533N	0	1	F487N	4865	WF3	676.0	121.0
u2mm0402t	FR533N	0	2	F502N	5012	WF2	796.0	254.0
u2mm0402t	FR533N	0	1	F502N	5012	WF2	748.0	672.0
u2mm0402t	FR533N	0	1	F502N	5012	WF2	730.0	677.0
u2mm0402t	FR533N	0	1	F502N	5012	WF2	748.0	688.0
u2mm0501t	FR533N	-18	2	F502N	5012	WF2	750.0	625.0
u2mm0403t	FR533N	0	4	F588N	5894	WF4	259.0	738.5
u2mm0502t	FR533N	-18	4	F588N	5894	WF3	105.0	569.0
u2mm0502t	FR533N	-18	4	F588N	5894	WF4	593.0	103.0
u2mm0601t	FR533N	-33	4	F588N	5894	WF3	684.0	645.0
u2mm0602t	FR680N	0	1	F631N	6306	WF3	735.0	343.0
u2mm0603t	FR680N	0	2	F656N	6564	WF3	231.5	205.5
u2mm0604t	FR680N	0	2	F658N	6591	WF3	234.5	113.5
u2mm0605t	FR680N	0	2	F673N	6732	WF2	458.0	231.0
u2mm0705t	FR680N	-18	2	F673N	6732	WF2	660.0	187.5
u2mm0705t	FR680N	-18	3	F673N	6732	WF2	393.0	734.0
u2mm0901p	FR680N	-33	3	F673N	6732	WF2	573.5	544.0
u2mm0701t	FR680N	0	4	FQCH4N-C	7279	WF4	661.0	743.0
u2mm0903p	FR868N	0	4	F953N	9544	WF3	721.0	215.5

3.2 Constraints from ground-based arc lamp data.

Given the small number of narrow band filters, we have also used observations of arc lamps taken during thermal vacuum testing at JPL. These observations are perhaps less reliable, since some amount of mechanical "gravity release" may occur after launch, but nonetheless, they provide some additional constriants on the calibration.

The thermal vacuum test exposures were made through the "stimulus" which simulates the OTA focal ratio and illumination pattern, and hence should approximate the on-orbit illumination pattern. The thermal vacuum images are very similar to the on-orbit image shown in Figure 4, and were analyzed in the same way. Table 6 lists the thermal vacuum images used and the corresponding position results. Again typical uncertainties are a few pixels in the wavelength direction, but can be much larger in the cross-wavelength or transverse direction.

Table 6: Wavelength data from thermal vacuum test.

TV Tape	Tape Files	Emission Line (Angstroms)	Filter	Ramp #	CCD	Measured Position of Spot (pixels) X ..... Y	
119	57-60	Hδ 4101	FR418N	2	WF4	343	304
119	57-60	Hγ 4340	FR418N	3	WF2	163	253
119	53-56	Hg 4358	FR418N	3	WF2	263	257
120	37-40	Hβ 4861	FR533N	1	WF3	723	163
120	29-32	Hg 5461	FR533N	3	WF4	285	314
121	57-60	Hα 6563	FR680N	2	WF3	260	223
121	61-64	Ar 7067	FR680N	3	WF4	240	297
121	61-64	Ar 7384	FR680N	4	WF4	382	745
122	53-56	Ar 8408	FR868N	1	WF4	92.5	320
122	53-56	Ar 9123	FR868N	3	WF2	486	244
122	53-56	Ar 9658	FR868N	4	WF3	707	502

3.3 Location of ramp centers in the cross-wavelength direction -- 10" apertures.

For the purpose of locating the ramp filters in the focal plane along the direction normal to the wavelength runs, we have used on-orbit VISFLATs taken through the ramp filters without any second filter in place. These provide numerous points along each ramp strip where the centroid can be measured. The method for locating the ramp center deserves some attention. As can be seen in Figure 5(a), the intensity profiles in the direction normal to the wavelength run have rather flat peaks, and hence identifying the ramp centroid as the profile peak would be a poor method; slight flat field variations or noise would cause

large errors in the measured centroid position. A better method would be to look at the edges of the intensity profile. We have used two methods which essentially do this. The first measures the location of a 10” diameter aperture, which is placed so as to be well-centered in the high-throughput region of the profile. This maximizes the response function across a 10” diameter aperture. Table 7 gives these results. Typically the centroids are measured at several locations along the wavelength run, for example, at X=150, 350, 550, and 750 on WF4 for FR680N.

Table 7: Measured Optimal CCD (X,Y) Positions for 10” Wide Apertures

Filter Image	X	Y	X	Y	X	Y	X	Y
FR680N U2MM0B04T								
Ramp #4 on WF4	150	730	350	739	550	734	750	721
Ramp #3 on WF4	150	293	350	294	550	294	750	297
Ramp #2 on WF2	150	242	350	243	550	246	750	251
Ramp #2 on WF3	245	150	244	350	244	550	244	750
Ramp #1 on WF2	150	691	350	702	550	698	750	682
Ramp #1 on WF3	687	150	692	350	688	550	683	750
FR680N18 U2MM0C01T								
Ramp #4 on WF4	75	211	125	195	175	178	225	172
	275	149	375	128	475	120	575	98*
Ramp #4 on WF3	80	525*	105	575	106	625	120	675
	136	725	151	775				
Ramp #3 on WF2	75	378	125	361	175	347	275	316
	375	284	475	252	575	224	675	211
Ramp #3 on WF3	398	75	417	125	433	175	448	225
	462	275	476	325	495	375	509	425
	522	475	537	525	555	575	564	625
	576	675	589	725	606	775		
Ramp #2 on WF2	225	772*	275	763*	375	746	475	722
	575	694	675	659	775	636		
FR680N33 U2MM0C03T								
Ramp #4 on WF2	75	346	125	314	175	265	225	242
Alternate Measurements	75	321	125	281	175	249	225	227
Ramp #4 on WF3	504	325	531	375	560	425	587	475
	616	525	637	575	658	625		

Table 7: Measured Optimal CCD (X,Y) Positions for 10” Wide Apertures

Ramp #3 on WF2	75	774+	175	771+	225	750	275	744
	375	692	475	632	525	607	575	605
FR868N U2MM0C05T								
Ramp #1 on WF4	150	746+	350	750#	550	750#	750	746
Ramp #2 on WF4	150	324	350	324	550	325	750	327
Ramp #3 on WF2	150	216	350	215	550	218	750	224
Ramp #3 on WF3	216	150	215	350	212	550	216	750
Ramp #4 on WF2	150	659	350	672	550	675	750	662
Ramp #4 on WF3	662	150	662	350	656	550	651	750
FR868N18 U2MM0D02T								
Ramp #1 on WF4	75	234	125	220	175	200	225	189
	275	166	375	147	475	130	575	113
	625	111*	675	97*				
Ramp #1 on WF3	74	525*	76	575*	87	625*	99	675
	108	725	124	775				
Ramp #2 on WF2	75	347	125	334	175	317	275	285
	375	255	475	226	575	198	675	192
Ramp #2 on WF3	366	75	383	125	398	175	413	225
	428	275	443	325	462	375	476	425
	495	475	506	525	522	575	539	625
	551	675	564	725	580	775		
Ramp #3 on WF2	225	753*	275	745	325	733	375	721
	475	697	575	671	675	640	775	613
FR868N33 U2MM0D04T								
Ramp #1 on WF2	75	323	125	298	175	267	225	240
Alternate Measurements	75	301	125	269	175	237	225	216
Ramp #1 on WF3	485	325	520	375	549	425	577	475
	603	525	626	575	647	625		
Ramp #2 on WF2	75	773*	175	769*	225	747	275	722
	375	670	475	611	525	582	575	594

* 5” wide image instead of 10” # 4” wide image instead of 10” + off edge in Y

3.4 Location of ramp centers in the cross-wavelength direction-- 95% points.

Ramps may also be located in the direction normal to the wavelength runs by measuring the 95% intensity points on the profiles taken normal, or transverse, to the wavelength run, and then by aligning these with the edges of the unvignetted region on each ramp. We chose 95%, since flat field variations and noise should contribute only 1 or 2% intensity variations over the small regions in question. Also, 95% is high enough on the profiles, so as to limit the effect of cross-talk on the results. Table 8 shows these results. Again, measurements are usually made at several points along each ramp.

Table 8: CCD (X,Y) Positions for 95% Intensity Points

Filter Image	X	Y	X	Y	X	Y	X	Y
FR418N U2MM0A02T								
PC1	438	409						
WF2	781	314	781	205	514	648	514	794
WF3	318	453	199	453	642	454	793	454
WF4	432	196	432	367	242	681	242	795
FR533N33 U2MM0B02T								
WF3	261	175	444	75	335	300	531	192
	436	451	621	350	510	572	696	468
	566	663	740	554				
FR533N18 U2MM0A05T								
PC1	258	233	533	115	298	349	596	216
	349	495	654	357	407	699	729	562
Alternate Measurements	315	413	623	292	359	531	669	376
WF2	345	236	383	351	501	665	533	768
WF3	454	415	563	375				
FR680N U2MM0B04T								
PC1	433	639	433	774				
WF2	633	452	767	452				
FR680N33 U2MM0C03T								
WF3	289	196	479	107	343	288	532	186
	472	481	657	378	545	591	710	489
	622	708	779	594				
FR680N18 U2MM0C01T								
PC1	273	251	575	130	298	322	596	187
	339	448	641	332	373	579	691	457

Table 8: CCD (X,Y) Positions for 95% Intensity Points

WF3	273	251	575	130	298	322	596	187
	339	448	641	332	373	579	691	457
FR868N U2MM0C05T								
PC1	506	420	692	420				
WF2	389	607	389	792				
WF3	604	400	751	400				
WF4	410	271	410	388				
FR868N33 U2MM0D04T								
WF3	282	196	459	104	359	311	538	218
	488	511	656	411	599	676	748	567
	427	410	594	314				
FR868N18 U2MM0D02T								
PC1	305	240	547	133	332	319	608	193
	390	466	648	346	411	547	679	420
	429	638	711	511				

The question may arise as to why there are maxima in the cross-wavelength profiles, since cross-talk from adjacent ramps will tend to fill-in the vignetted light on any given ramp. However, the response functions of the CCDs and the filters naturally lead to some ramps having higher net quantum efficiency than adjacent ones.

3.5 Refinement of the model parameters.

We now use the above data to refine our model. As an example, the measured CCD (X,Y) data points for the unrotated FR418N filter are plotted on the (V2,V3) plane in Figure 6 using the transformations discussed in Section 2.5. The small “x” near the center of the plot indicates the origin of the (V2,V3) plane; the direction of +V2 is towards the lower right, and +V3 is towards the lower left.

Points which constrain position in the wavelength direction are plotted as filled squares. These points are also labeled with the filter in the case of on-orbit VISFLATS (e.g. 4370 F437N), or arc lamp line in the case of thermal vacuum ground-based data (e.g. 4358 TV Hg). The wavelengths are given in Angstroms. Points used to constrain position in the transverse direction (cross-wavelength, or normal direction) are plotted as solid stars or triangles.

The predicted location of the FR418N filter in the (V2,V3) plane is shown in Figure 7. Wavelengths corresponding to measured wavelength data are marked with open squares along the center of the appropriate ramp.

For position determination in the transverse direction, we align according to the edges of the unvignetted regions, which are shown by dotted lines. Our goal is to have the measured 10 arcsecond centers (star symbols) placed near the center of the unvignetted regions (outlined with dashed line). Also, the measured 95% intensity points (triangles) should fall symmetrically about the unvignetted region.

The superposition of the measured and predicted points is shown in Figure 8. This is merely a sandwich of Figures 6 and 7. This "initial model" has all the variable parameters in Table 3 set to zero. As can be seen, the fit is quite poor. For example, the "3737 F375N" observed point near the outer corner of WF4 lies about 6 arcseconds above and right of the predicted location (open square). Also, the star symbols, which represent the optimal locations of 10 arcsecond apertures measured in the VISFLATS, are shifted about 6 arcseconds right of the centers of the unvignetted ramp regions; this is most noticeable on the center two ramps. Finally, the solid triangles, which indicate 95% intensity points in the VISFLATs, are not symmetrically disposed about the unvignetted regions. Similar plots were made for all the filters and filter rotations where data existed.

We then began refining the model by adjusting the $C_{7,1}$ and $C_{7,2}$ coefficients of the LRF filter transformation (see Section 2.4) so as to minimize differences between the observed and predicted positions. These two parameters essentially describe the location of the SOFA optical axis in the (V2,V3) plane. A single set of values were used for all four ramp filters. The quality of the fit was judged by visually inspecting the plots; small adjustments then were made to $C_{7,1}$ and $C_{7,2}$, the model was replotted, and the fits were judged again, and so forth. The best agreement between the model and the observed points appears to occur for $C_{7,1}$ = 7.80 arcseconds, and $C_{7,2}$ = 2.17 arcseconds. The uncertainty on these values is about 0.3 arcseconds.

Once $C_{7,1}$ and $C_{7,2}$ were optimized, we noticed that each individual filter appeared to have a small systematic offset in the transverse direction (i.e. direction normal to wavelength run). We then made small adjustments to the $C_{3,1}$ parameters, until each individual filter was well registered against the observed data points. We judged that there was too little wavelength data to make any reliable adjustments to $C_{3,2}$. The final fit parameters are summarized in Table 9.

Comparisons of the final model and observed data are shown in Figures 9.a. through 9.j. The RMS difference between the model and observations is approximately 1.4 arcseconds in the wavelength direction, and 1 arcsecond in the transverse direction. The uncertainties in the final fitted model are about one-half these values. We have included only the most reliable data in these estimates; the ground-based wavelength data, and the transverse positions of the #1 and #4 ramps are excluded, as discussed below. The quality of this fit is within the requirements set out at the beginning of this Section.

In the wavelength direction, the fits are generally much better than the 5 arcsecond requirement described in the Introduction. The largest errors are for the ground-based thermal vacuum data on CCD WF4. For example, the measured 5461 TV Hg point lies 6 arcseconds below the predicted point (Figure 9.b.). Also, the measured 4101 TV H-delta point lies 3 arcseconds below the predicted point (Figure 9.a.). These large discrepancies may represent gravity release in the WF4 camera, or changes in the articulated fold mirror settings for WF4. These points were given little weight in the final solution. The on-orbit

wavelength data for WF4 are much better, with all differences between the model and observations being <1 arcsecond.

One concern with the wavelength data is that the illumination pattern of the VISFLAT diffuser is different from that of the OTA. This might introduce small wavelength shifts in the ramp interference filters due to different effective angles of incidence. This was checked by taking Earthflats at several settings of the ramps crossed with narrow band filters (specifically images U2MM0E07T, U2MM0F03T, and U2MM0I06T), and then comparing the results against the same settings observed with the VISFLAT lamp. Typical differences in spot maxima were 0.4 ± 0.4 arcseconds between the Earthflats and VISFLATs. Hence the VISFLAT illumination does not appear to introduce any important wavelength shifts when compared to external OTA illumination.

In the transverse direction, we gave the most weight to the central two ramps on each filter (the #2 and #3 ramps). The outer ramps (#1 and #4) appear to have various complications which corrupt the measurements. On each filter, the left-most ramp appears to lie partially outside the region imaged by WF4. Hence, the measured 10 arcsecond aperture centers (star symbols) do not correspond well to the geometric center of the unvignetted region on the filter glass. The effect is especially pronounced on the FR868N filter (Figure 9.h.). There is also a tendency on the left-most ramp, for the measured 10 arcsecond centers to be 1 to 3 arcseconds right of the geometric center of the unvignetted filter glass. This is somewhat puzzling, but might be attributed to roll-off in the VISFLAT illumination near the edges of the field of view. This would have the effect of pushing the measured points towards brighter regions near the field center. The points on both the #1 and #4 ramps show a slight inward bow at the top and bottom of the field of view. This would also be consistent with an illumination roll-off in the VISFLAT diffuser, where brightness depended on distance from the field center. Due to these complications, the #1 and #4 ramps were give less weight when determining the transverse position of the filters.

As previously discussed, the peaks measured in the VISFLATs taken through narrow band filters crossed with the ramps (filled square symbols in plots) are unsuitable for position location in the transverse direction. These were not used in evaluating the transverse fits.

A possible concern with the poor fits in the transverse direction for the #1 and #4 ramps is that the image scale of 91.25 arcseconds per inch might be incorrect. This would cause us to make the filter too large in the model plots. This possibility was checked by measuring the distance between the centers of the FR868N filter rotated -18 degrees on WF2 in image U2MM0D02T. The result, 0.4902 ± 0.0010 inch, is in excellent agreement with the design specification of 0.490 inch. Any errors in image scale would appear negligible.

In conclusion, the equations in Section 2.5 and 2.6, along with coefficients in Tables 3, 4, and 9, provide a mapping between LRF central wavelength and both (V2,V3) and CCD (X,Y) pixel locations. Next we use this information to construct Tables required by the observation planning software.

Figure 6. Observed data points projected into the (V2,V3) plane.

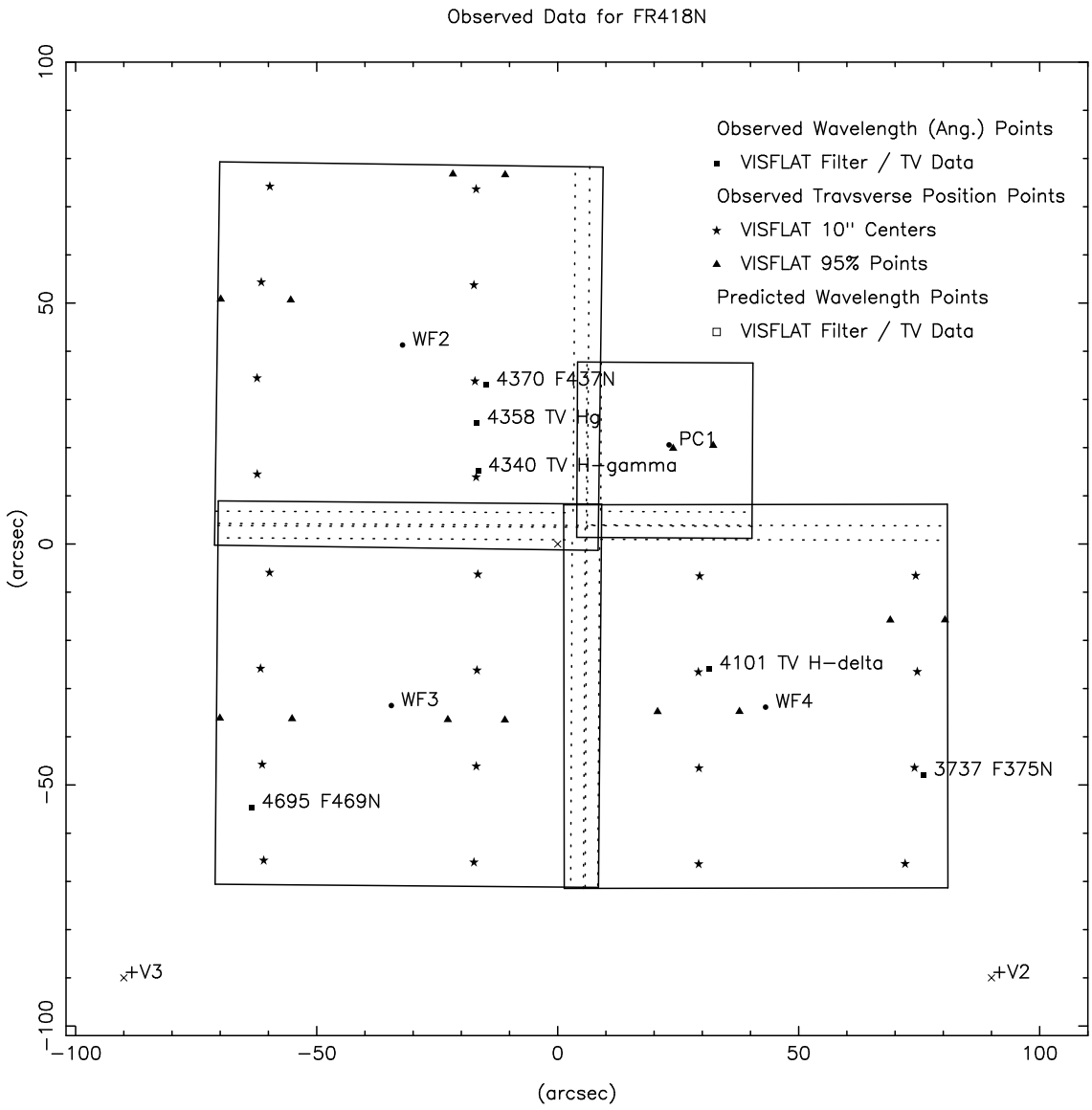

Figure 7. Predicted location of FR418N filter in the (V2,V3) plane.

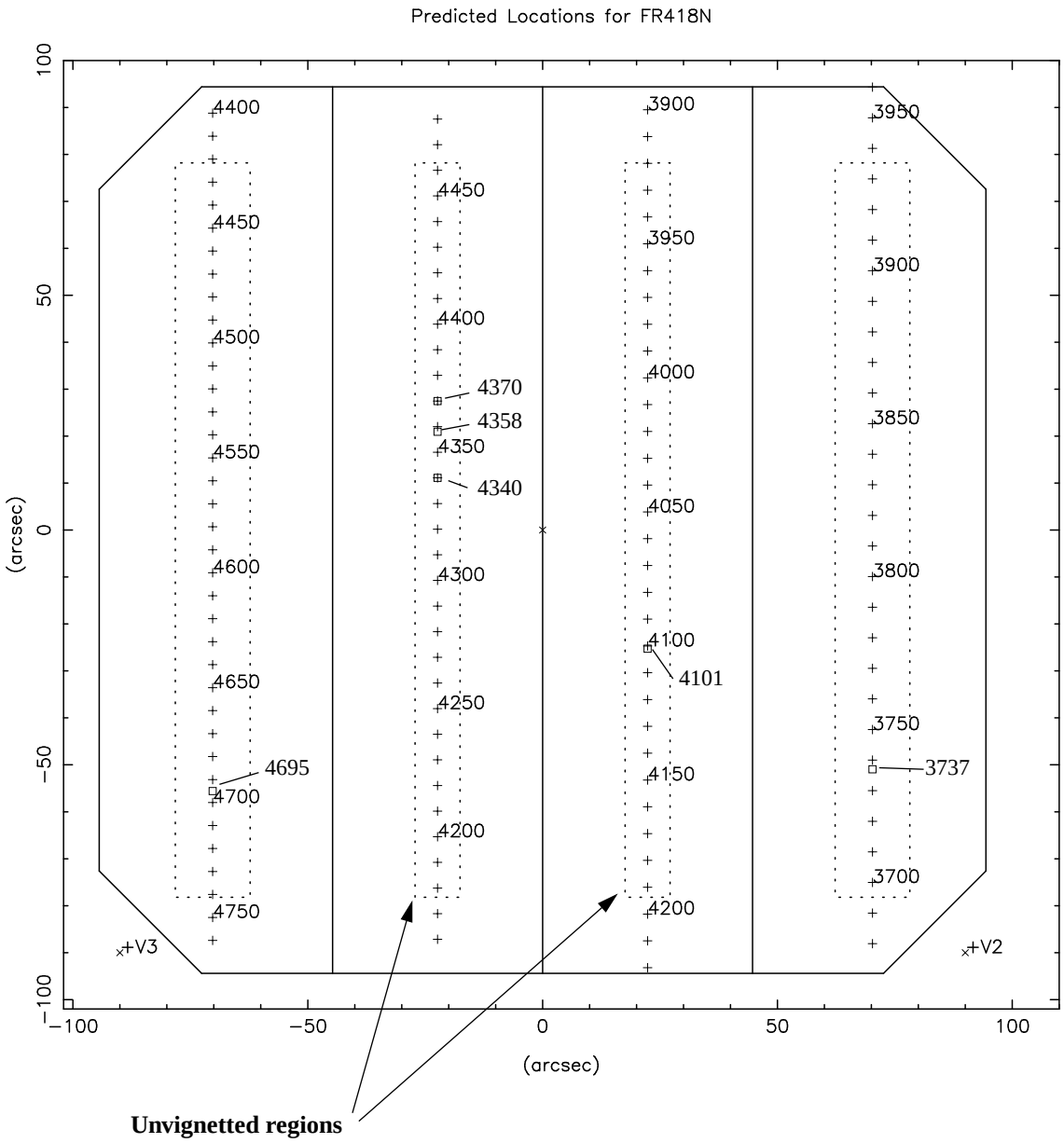

Figure 8. Comparison of initial model with observed data for unrotated FR418N filter.

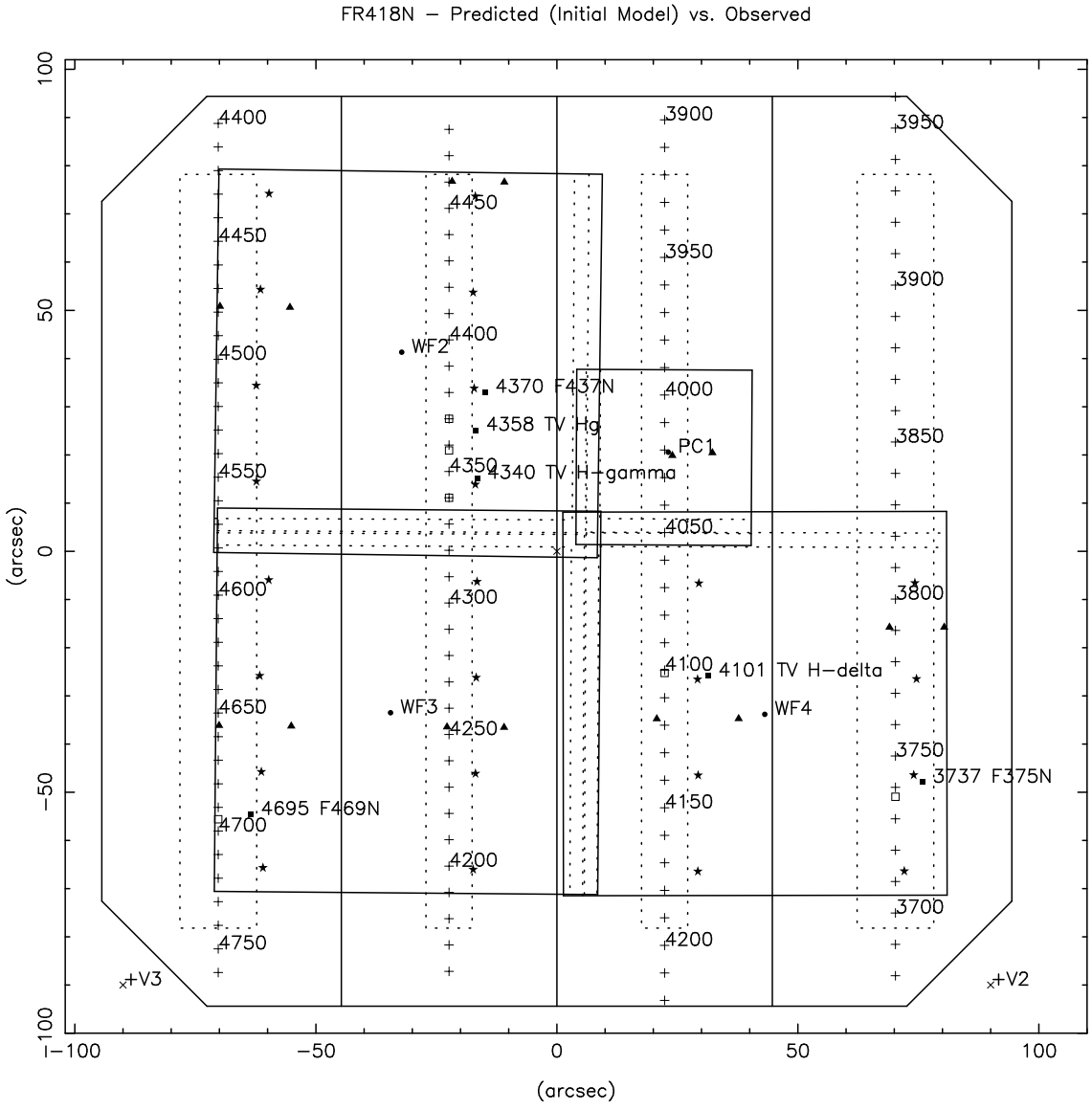

Table 9: Final fitted transformation coefficients.

Filter	$C_{7,1}$ (arcseconds)	$C_{7,2}$ (arcseconds)	$C_{3,1}$ (inches)	$C_{3,2}$ (inches)
FR418N	7.80	2.17	-0.016	0
FR533N	7.80	2.17	0.005	0
FR680N	7.80	2.17	-0.005	0
FR868N	7.80	2.17	0.016	0

Figure 9.a. Comparison of final model with observed data for unrotated FR418N.

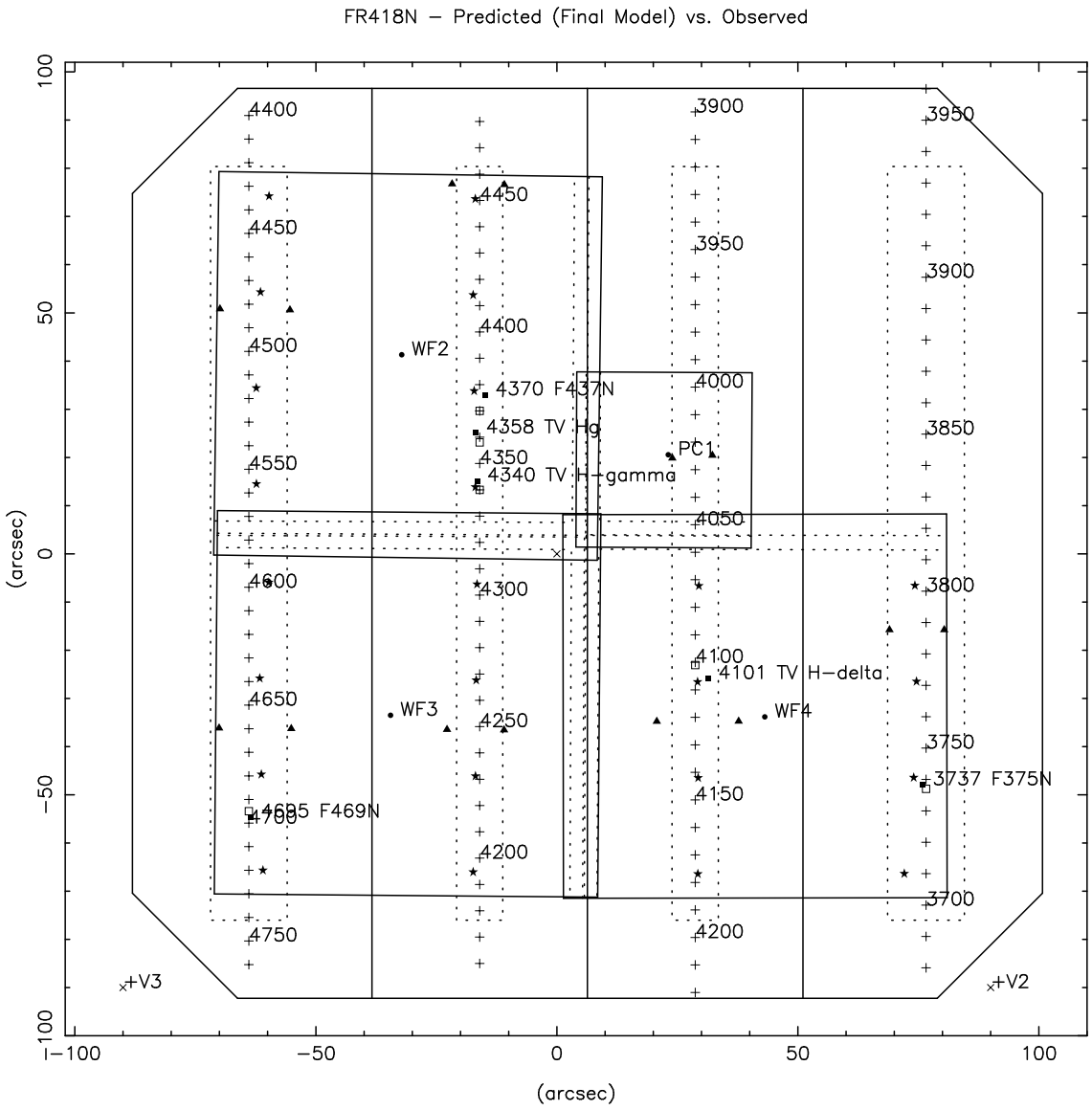

Figure 9.b. Comparison of final model with observed data for unrotated FR533N.

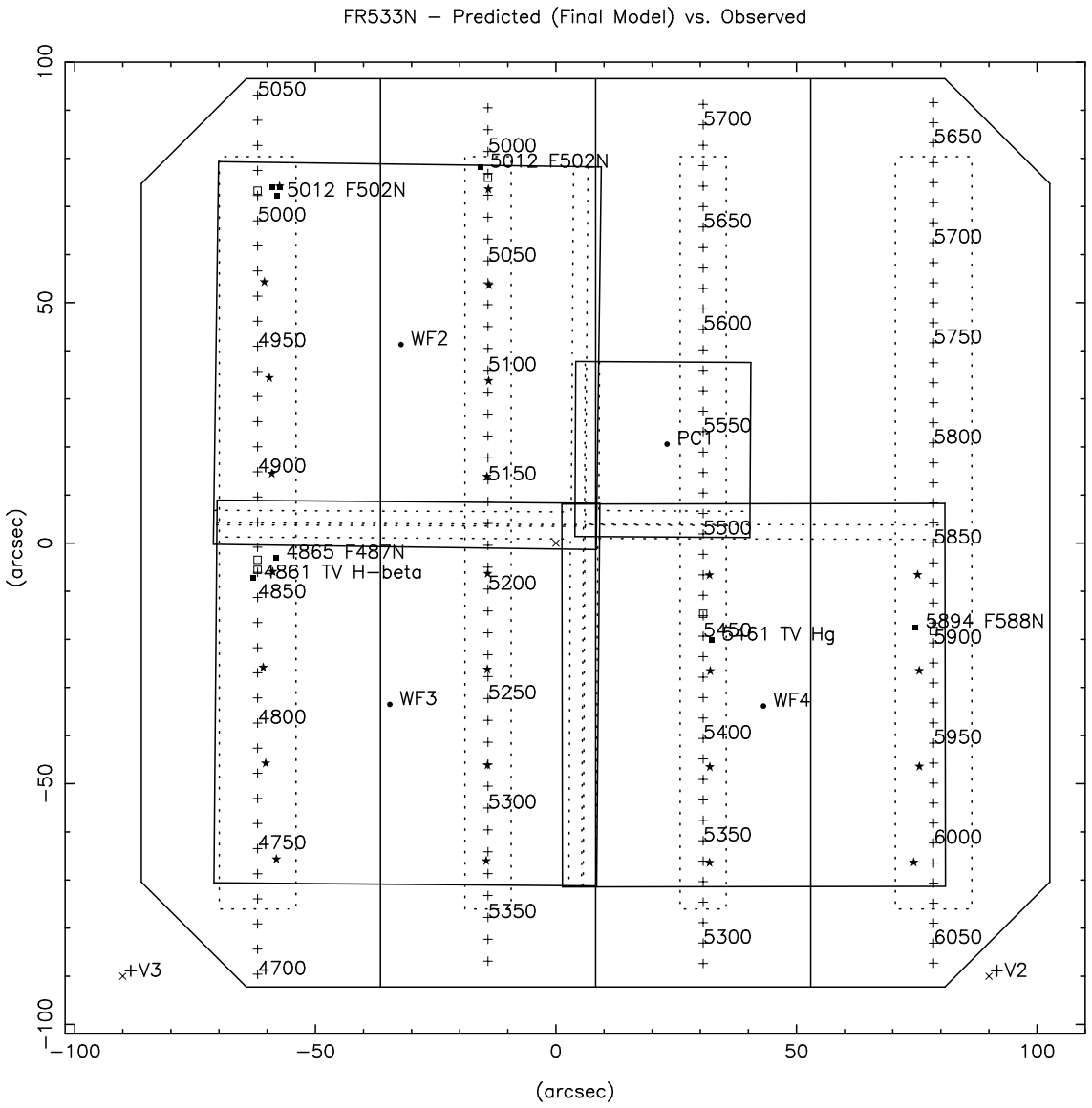

Figure 9.c. Comparison of final model with observed data for rotated FR533N18.

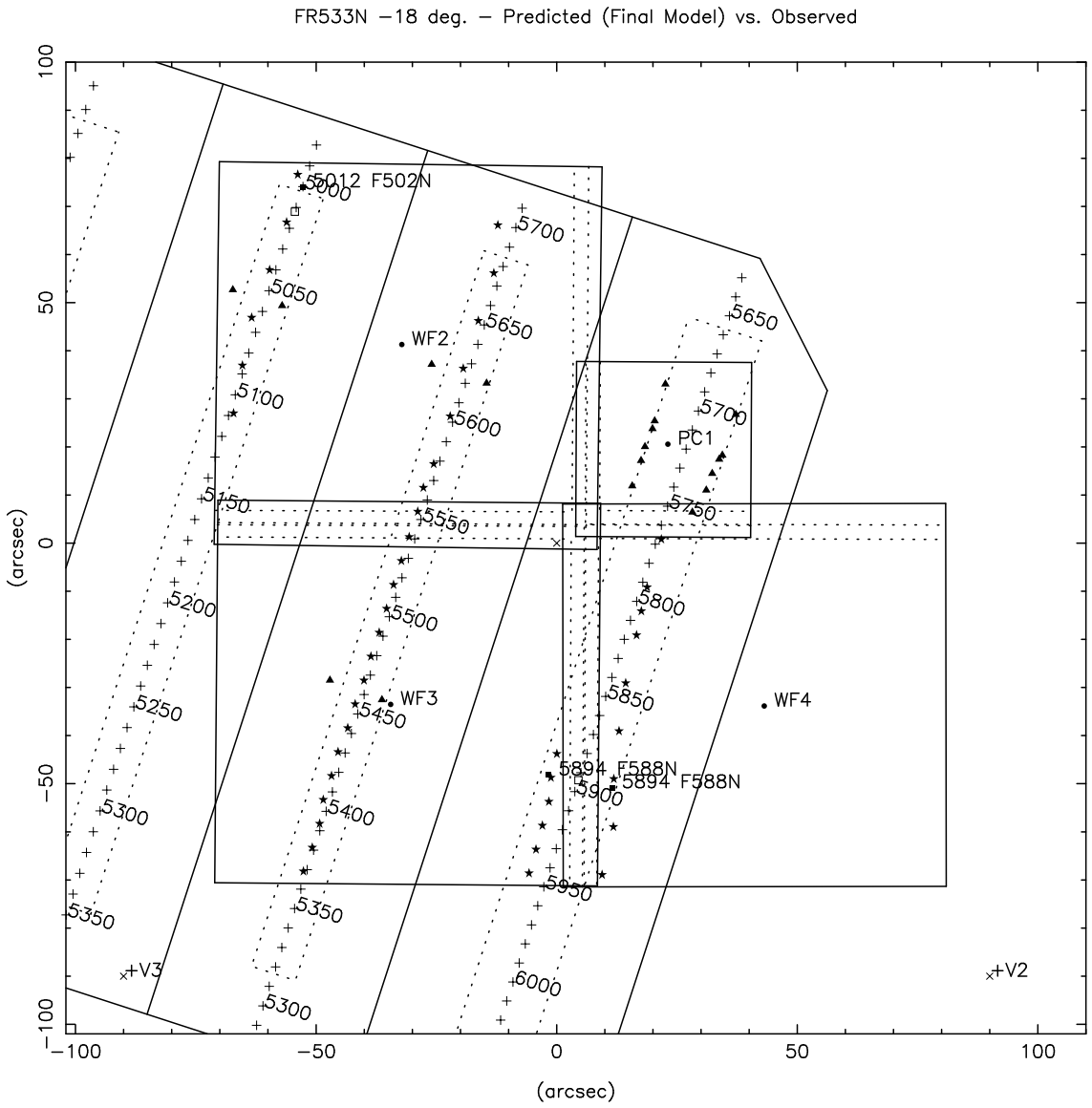

Figure 9.d. Comparison of final model with observed data for rotated FR533N33.

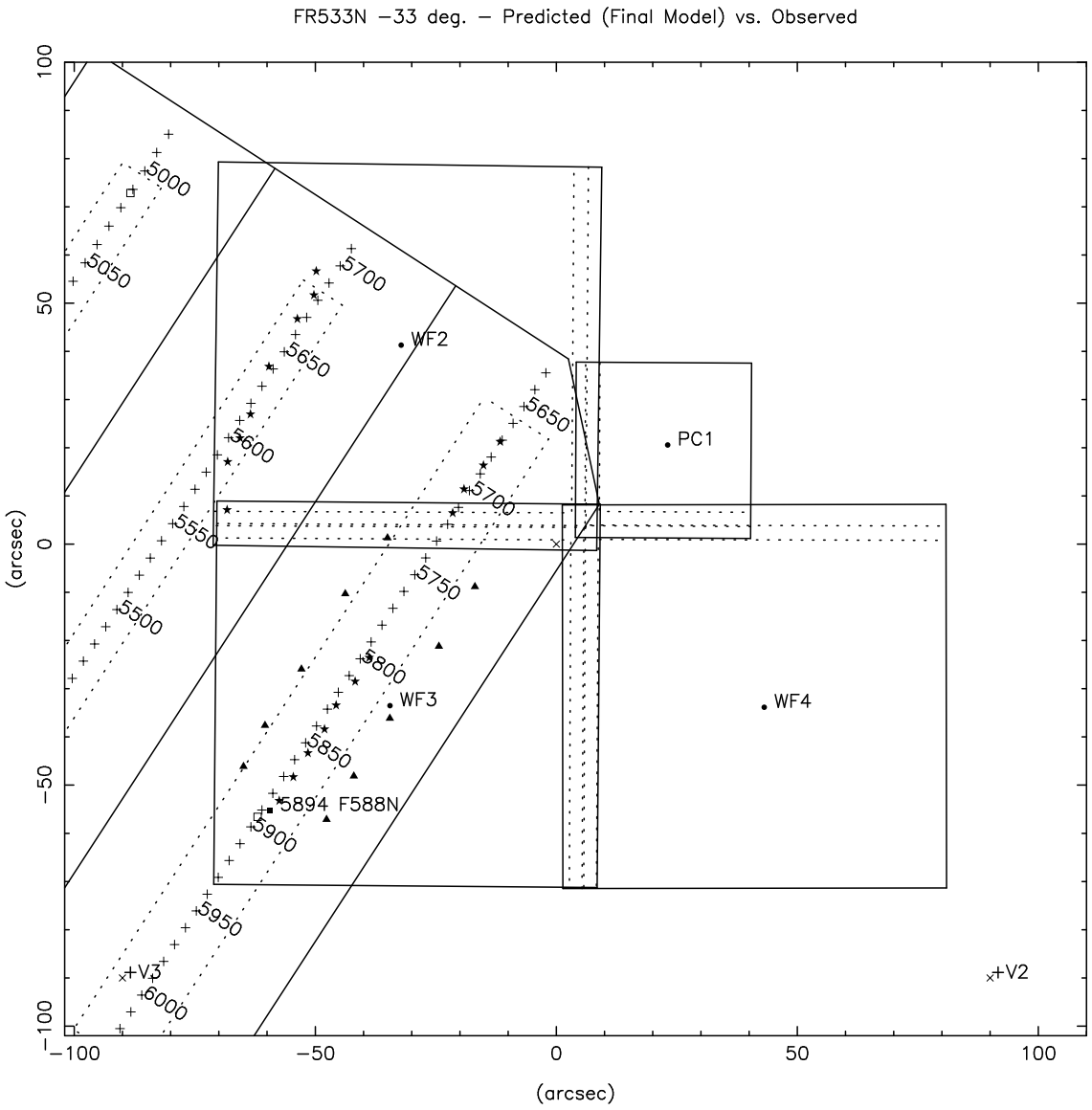

Figure 9.e. Comparison of final model with observed data for unrotated FR680N.

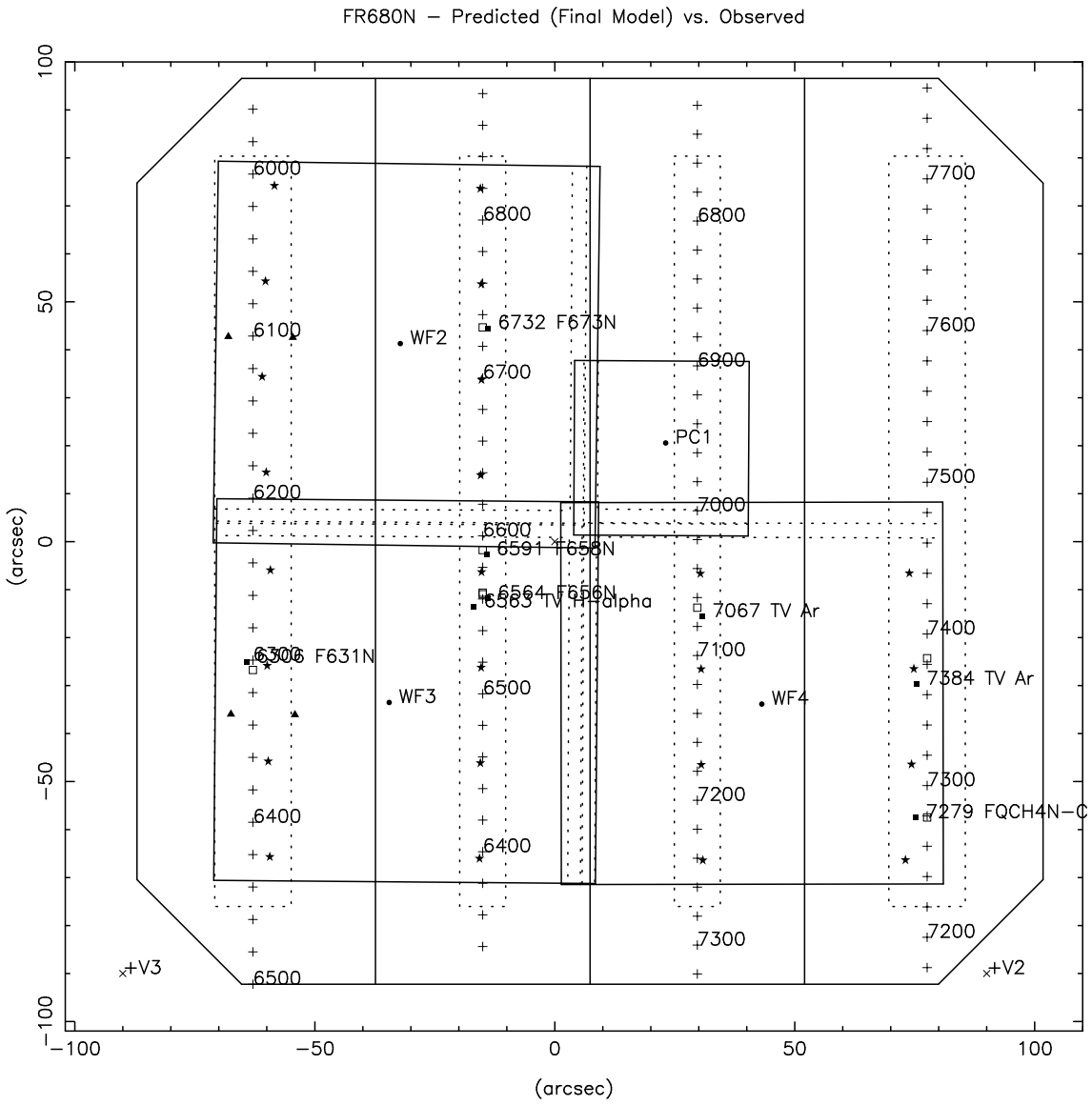

Figure 9.f. Comparison of final model with observed data for rotated FR680N18.

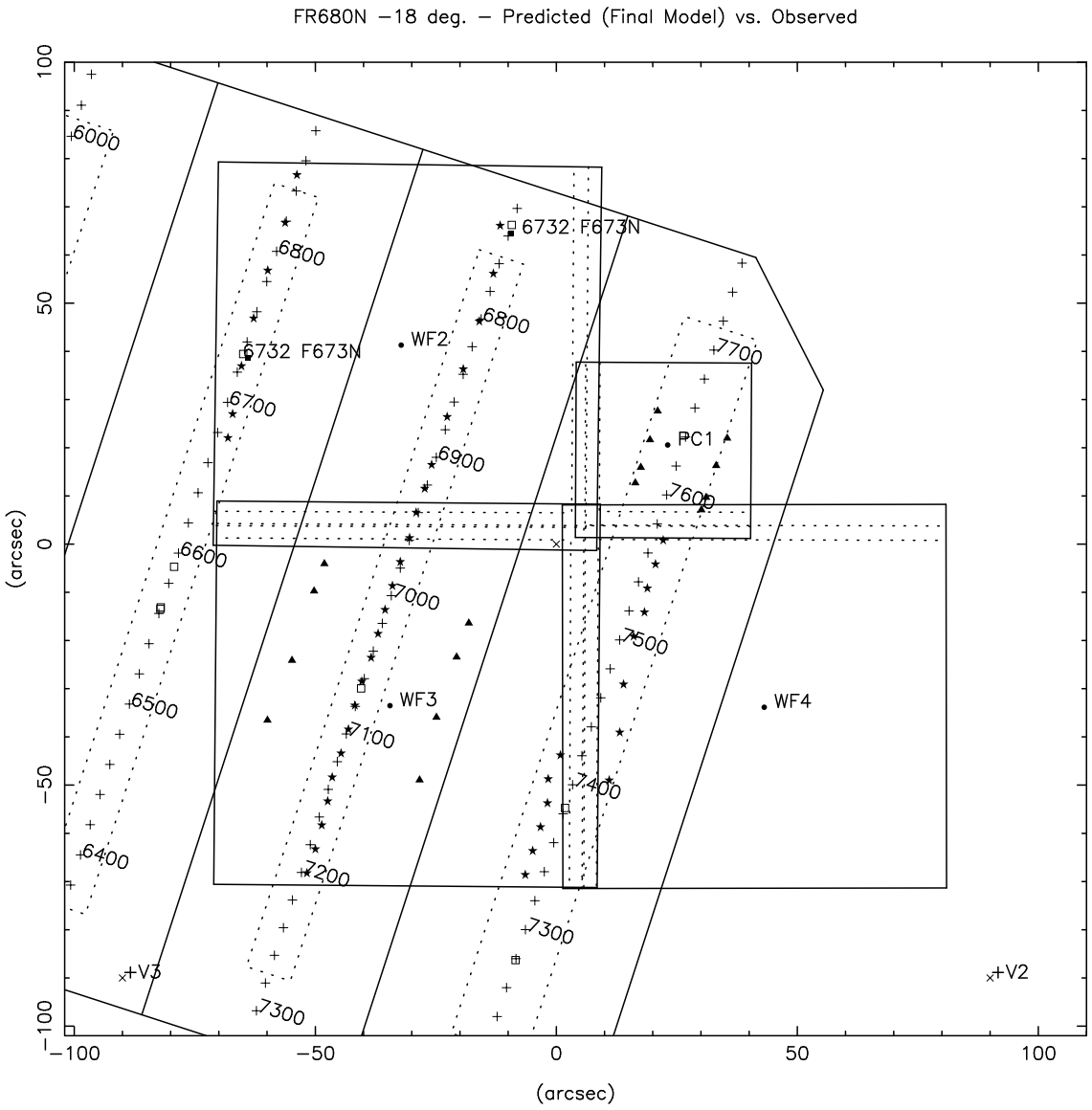

Figure 9.g. Comparison of final model with observed data for rotated FR680N33.

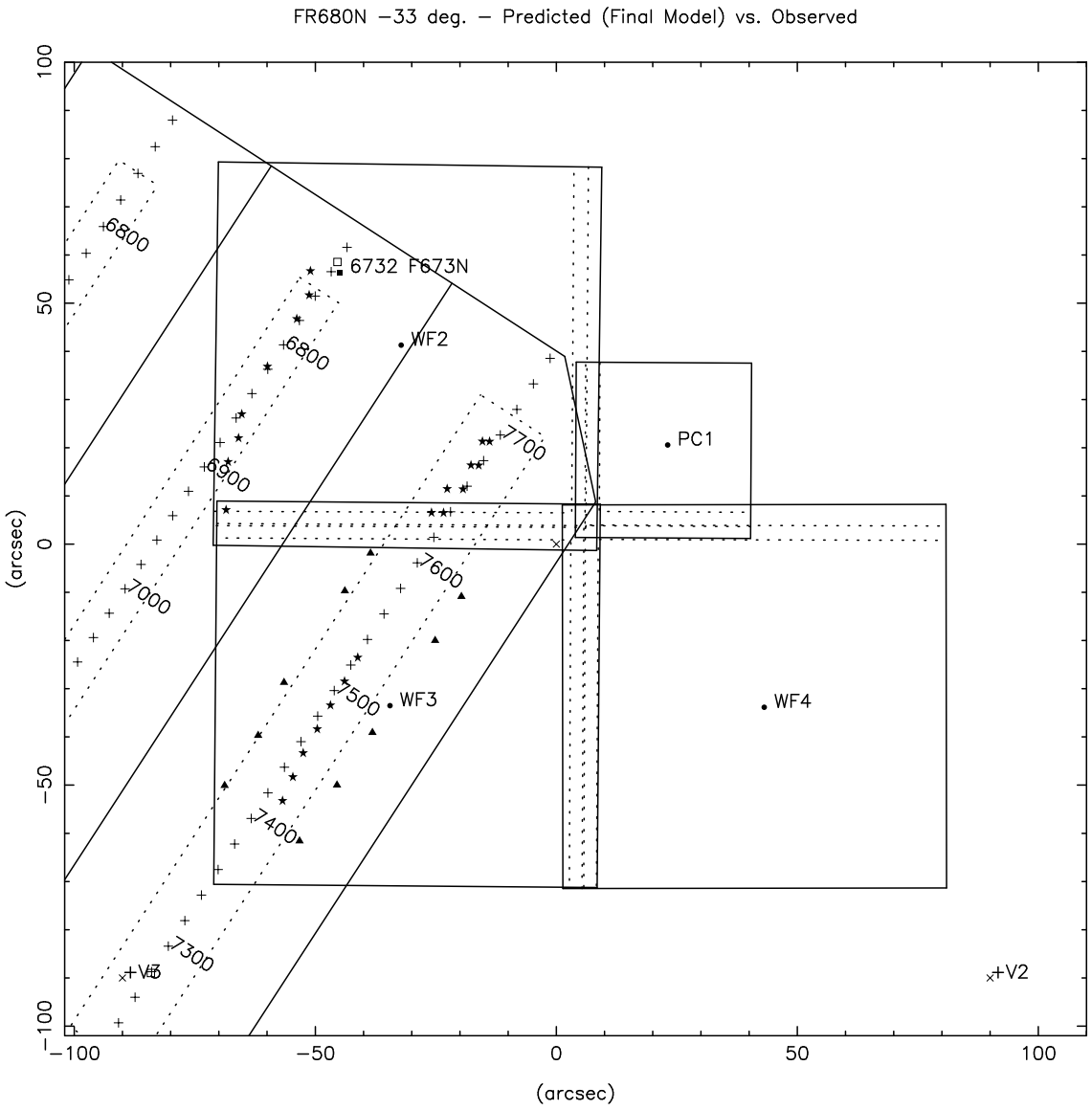

Figure 9.h. Comparison of final model with observed data for unrotated FR868N.

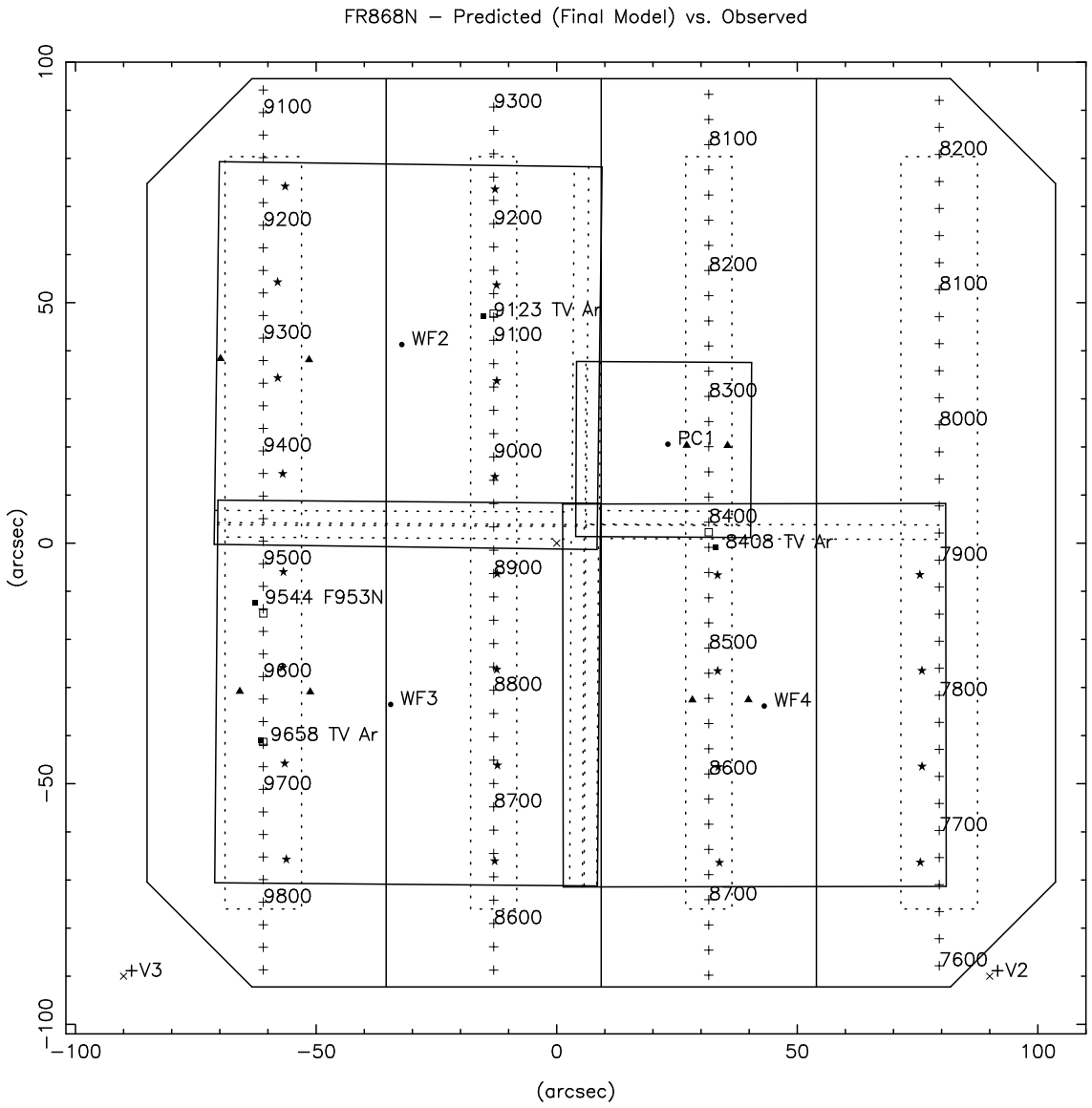

Figure 9.i. Comparison of final model with observed data for rotated FR868N18.

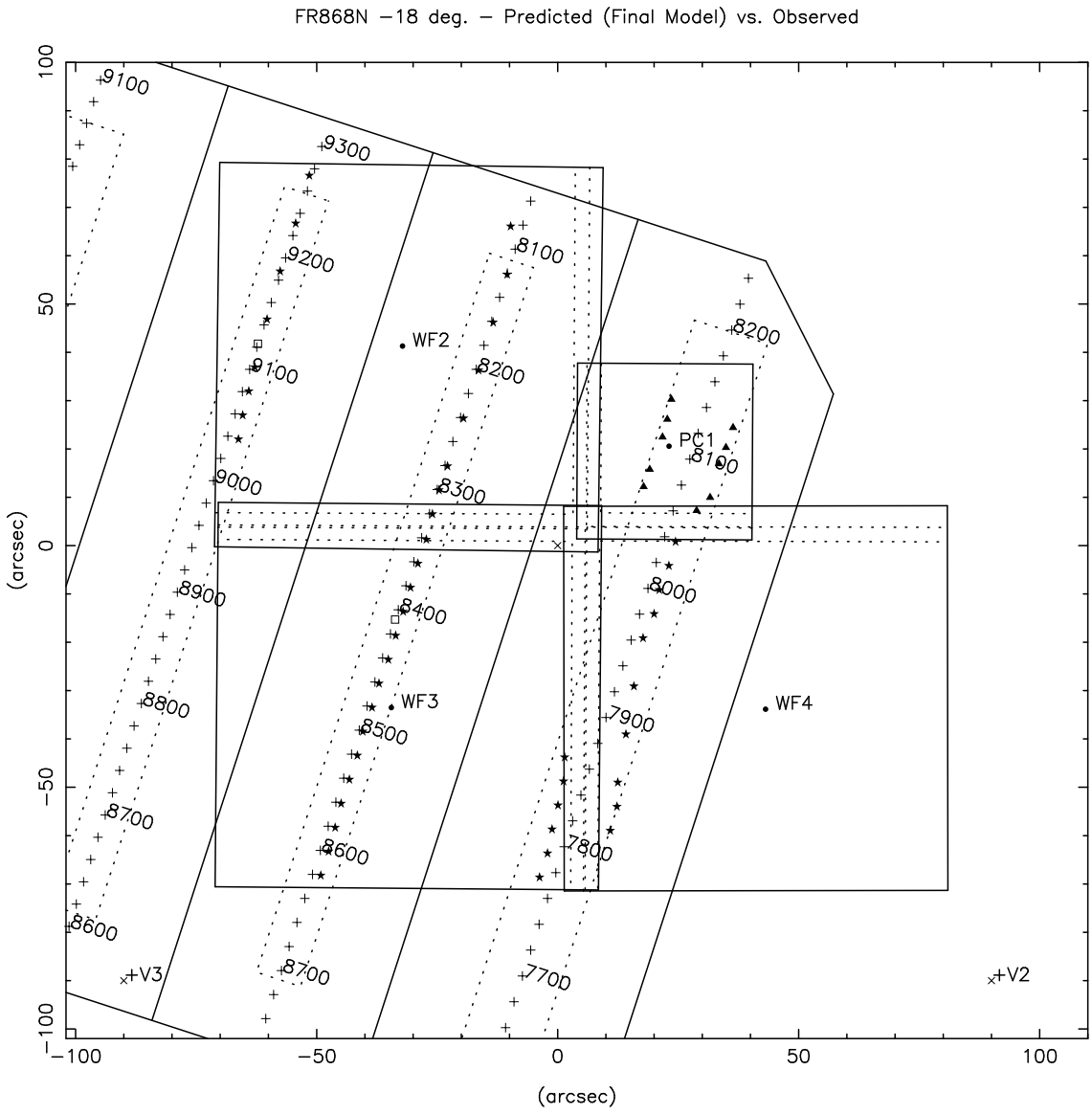

Figure 9.j. Comparison of final model with observed data for rotated FR868N33.

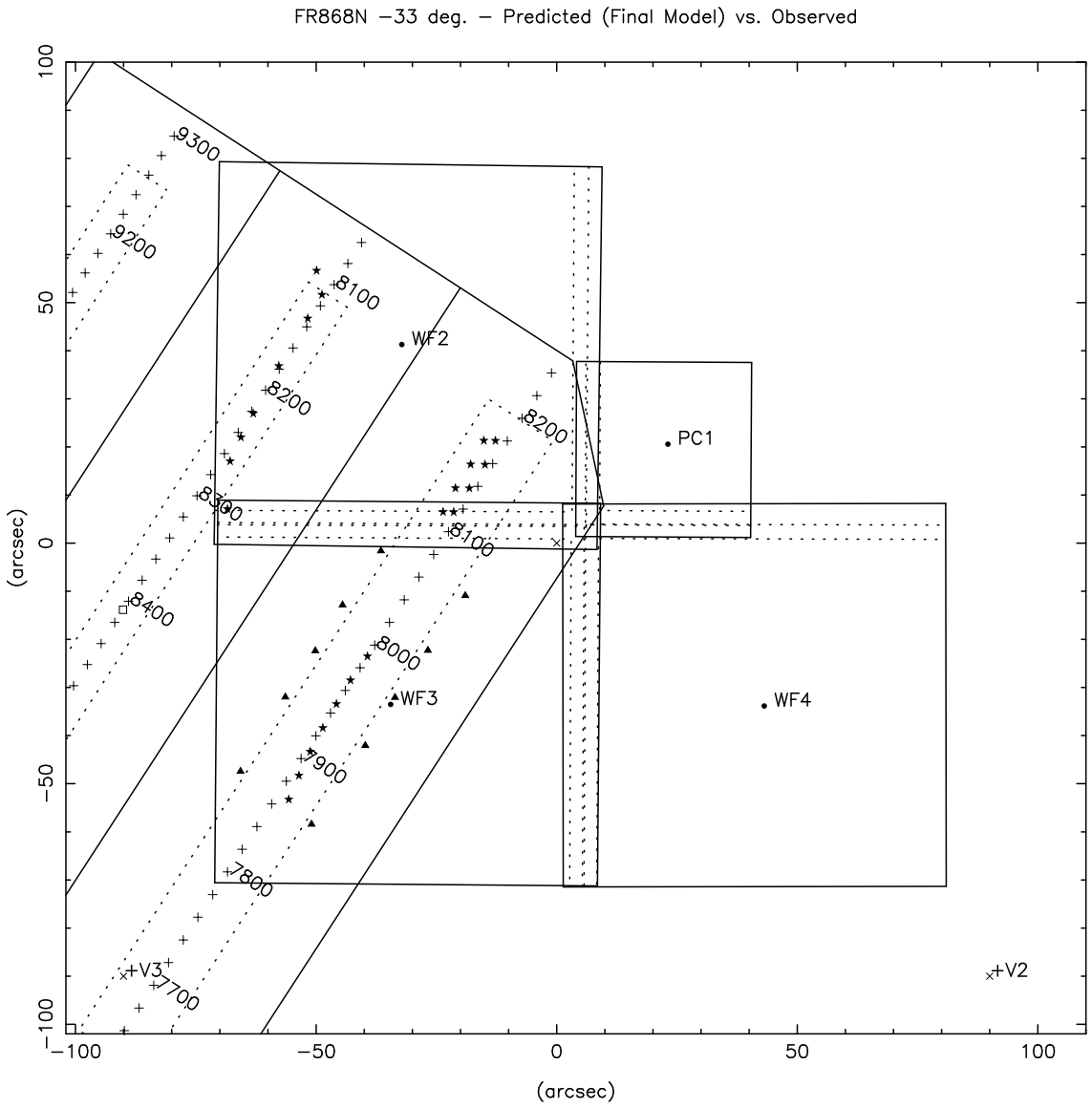

4. Building the TRANS Tables.

The observation planning software requires a table of POS TARGs which are used when scheduling LRF observations. This table contains eight columns, as follows:

> Columns 1 and 2: These are the starting and ending wavelengths (Angstroms) for an arbitrary wavelength range.
>
> Column 3: The filter to be used, along with any rotation. For example, FR533N33 implies the FR533N ramp filter rotated by -33 degrees.
>
> Column 4: The aperture location which the POS TARGs will use as their starting point.
>
> Columns 5 and 6: A POS TARG set which corresponds to the first wavelength of the range.
>
> Columns 7 and 8: A second POS TARG set which corresponds to the end of the wavelength range.

The TRANS observation planning software takes the "central wavelength" given by the proposer, and then locates the first line in the table containing that wavelength. Based on the supplied central wavelength, and the starting and ending wavelengths, the software then performs a linear interpolation between the two POS TARGs. This final interpolated POS TARG, along with the aperture given by Column 4, is used to schedule the observation.

Construction of the LRF-TRANS table begins by examining plots such as Figure 9, then specifying the properties of wavelength "runs." Each run is characterized by its wavelength limits, the filter, ramp number, and rotation to be used, and the desired CCD. In many cases a given wavelength can be observed at several different settings. We have chosen the runs so as to provide a minimum 10 arcsecond diameter unvignetted field of view wherever possible. Care was taken to stay at least 3 arcseconds away from CCD edges, so as to preserve a 10 arcsecond clear aperture, even in the presence of normal pointing errors. In cases where settings were possible on both the PC and WFC CCDs, a preference was given for the WFC, since the larger pixels would give a better signal-to-noise ratio in the presence of readout noise.

Given this table of wavelength runs, the transformations between LRF wavelength and CCD pixel (X,Y) derived in the previous sections (Equations 1, 2, and 3; Tables 3, 4, and 9) were used to assign CCD pixel locations to the ends of each run. Table 10 illustrates the results. The observation planning software requires a table in POS TARG units; this is easily computed from the pixel table by using the pixel scales in Cox (1994) and the standard "-FIX" aperture locations. The "-FIX" apertures are used, since they are constant in time, and the results are shown in Table 11.

There are also instances where some wavelengths cannot be reached, if a 10 arcsecond unvignetted aperture is to be supported. These wavelengths fall just off the CCDs at the ends of the ramps, or in the vignetted regions where the CCD join, or in the un-imaged

region surrounding the PC. In these cases, we have created additional lines in the TRANS table where the unavailable wavelengths are observed at the nearest reachable setting. In effect, this causes the observation to occur away from the peak of the LRF filter bandpass, with a corresponding reduction in throughput. These cases are indicated in the pixel TRANS table (Table 10) where the maximum percent throughput loss is indicated in the "VIGNETTING" column. Differences between the observer's requested central wavelength and the nearest reachable wavelength of up to ~0.2% were allowed.

5. The Interim TRANS Table.

When the initial work on the LRF-TRANS table was being performed, the commanding codes for operating the +15 degree rotation of the LRF filters did not exist. Hence, an "interim" LRF-TRANS table was constructed which would enable observation at most wavelengths using only the zero, -18, and -33 degree rotations of the LRF filters. Once the +15 degree rotation was enabled, a "final" table would be created which eliminated the wavelength gaps.

The interim table is listed in Tables 10 and 11, and the corresponding wavelength runs are plotted in Figure 10. The wavelength runs are plotted as heavy lines. Ramp locations which serve multiple wavelengths, i.e. the "vignetted" settings in Table 10, are indicated by large circles.

We note that the wavelength runs of the outermost ramps on each filter (the #1 and #4 ramps) have been manually forced (displaced) about 2 arcseconds inward on the filter, so as to move the promised 10 arcsecond apertures farther from the CCD edges. This reduces the possibility that pointing errors might cause the CCD edges to intrude into the promised 10 arcsecond diameter unvignetted aperture. A 10 arcsecond diameter unvignetted aperture is supported at all settings in the interim table.

This interim table contains 8 gaps in wavelength. These are small ranges which could not be reached without considerable light loss (e.g. between 4182 and 4190 Angstroms). Proposal lines requesting central wavelengths in these gaps generated error messages in the TRANS software and did not schedule, and would await the final LRF-TRANS table.

The accuracy of the wavelength / aperture mapping provided by this table is ~0.7 arcseconds in the wavelength direction, or ~1 Angstrom at 3700 Angstrom setting, and ~3 Angstroms at the 9800 Angstrom setting. The accuracy in the transverse direction is ~0.5 arcseconds.

Table 10: LRF-TABLE Version 28856 in CCD Pixels (Installed 09-May-1995).

λ_1	λ_2	FILTER	APERTURE	CCD Pixel				VIGNETTING
				X1	Y1	X2	Y2	
3710	3800	FR418N	WF4-FIX	750.0	736.8	161.5	737.7	
3800	3878	FR418N33	WF3-FIX	669.5	559.2	395.1	128.9	
3878	3881	FR418N18	PC1-FIX	402.3	225.0	402.3	225.0	<2%
3881	3907	FR418N18	PC1-FIX	402.3	225.0	515.4	579.5	
3907	3929	FR418N33	WF2-FIX	128.4	286.7	250.1	209.9	
3929	4008	FR418N18	WF2-FIX	562.7	233.0	130.1	367.1	
4008	4038	FR418N	PC1-FIX	541.3	632.7	543.3	256.5	
4038	4100	FR418N18	WF3-FIX	425.3	130.8	532.4	469.9	
4100	4177	FR418N	WF4-FIX	309.0	276.2	750.3	275.5	
4177	4182	FR418N	WF4-FIX	750.3	275.5	750.3	275.5	<3%
4190	4195	FR418N	WF3-FIX	247.5	748.1	247.5	748.1	<3%
4195	4210	FR418N	WF3-FIX	247.5	748.1	248.2	665.9	
4210	4308	FR418N	WF3-FIX	248.2	665.9	252.7	128.5	
4308	4313	FR418N	WF3-FIX	252.7	128.5	252.7	128.5	<3%
4332	4337	FR418N	WF2-FIX	127.9	247.6	127.9	247.6	<3%
4337	4446	FR418N	WF2-FIX	127.9	247.6	725.4	255.7	
4446	4550	FR418N	WF2-FIX	691.7	716.2	180.6	709.2	
4550	4562	FR418N	WF2-FIX	180.6	709.2	121.7	708.4	
4562	4567	FR418N	WF2-FIX	121.7	708.4	121.7	708.4	<2%
4582	4593	FR418N	WF3-FIX	713.7	125.6	713.7	125.6	<13%
4593	4720	FR418N	WF3-FIX	713.7	125.6	708.5	749.9	
4720	4733	FR418N	WF3-FIX	708.5	749.9	708.5	749.9	<13%
4733	4746	FR533N	WF3-FIX	689.3	748.9	689.3	748.9	<19%
4746	4863	FR533N	WF3-FIX	689.3	748.9	694.4	135.5	
4863	4873	FR533N	WF3-FIX	694.4	135.5	694.4	135.5	<9%
4892	4897	FR533N	WF2-FIX	137.8	689.4	137.8	689.4	<3%
4897	4900	FR533N	WF2-FIX	137.8	689.4	153.6	689.6	
4900	5013	FR533N	WF2-FIX	153.6	689.6	745.9	697.7	
5013	5020	FR533N18	WF2-FIX	693.4	642.4	662.9	651.8	
5020	5153	FR533N	WF2-FIX	737.3	236.6	130.0	228.4	
5153	5158	FR533N	WF2-FIX	130.0	228.4	130.0	228.4	<1%
5183	5188	FR533N	WF3-FIX	233.5	127.4	233.5	127.4	<2%
5188	5310	FR533N	WF3-FIX	233.5	127.4	228.8	684.7	
5310	5322	FR533N	WF3-FIX	228.8	684.7	228.3	739.5	
5322	5327	FR533N	WF3-FIX	228.3	739.5	228.3	739.5	<0.5%
5334	5339	FR533N	WF4-FIX	750.9	294.7	750.9	294.7	<2%
5339	5450	FR533N	WF4-FIX	750.9	294.7	277.2	295.5	
5450	5528	FR533N18	WF3-FIX	504.4	445.3	404.1	127.6	
5528	5566	FR533N	PC1-FIX	585.3	277.5	583.4	632.3	

Table 10: LRF-TABLE Version 28856 in CCD Pixels (Installed 09-May-1995).

λ_1	λ_2	FILTER	APERTURE	CCD Pixel				VIGNETTING
				X1	Y1	X2	Y2	
5566	5671	FR533N18	WF2-FIX	124.1	348.8	552.3	216.1	
5671	5700	FR533N33	WF2-FIX	224.8	203.2	122.3	267.7	
5700	5741	FR533N18	PC1-FIX	558.8	577.0	444.9	220.1	
5741	5743	FR533N33	WF3-FIX	370.8	126.5	370.8	126.5	<0.3%
5743	5910	FR533N33	WF3-FIX	370.8	126.5	745.9	714.9	
5910	6007	FR533N	WF4-FIX	333.8	747.6	738.8	746.9	
6007	6192	FR680N	WF2-FIX	750.3	706.9	122.9	698.4	
6192	6198	FR680N	WF2-FIX	122.9	698.4	122.9	698.4	<2%
6221	6238	FR680N	WF3-FIX	703.6	128.1	703.6	128.1	<13%
6238	6409	FR680N	WF3-FIX	703.6	128.1	698.8	708.2	
6409	6584	FR680N	WF3-FIX	237.8	705.6	242.6	127.0	
6584	6587	FR680N	WF3-FIX	242.6	127.0	242.6	127.0	
6584	6591	FR680N	WF3-FIX	242.6	127.0	242.6	127.0	<2%
6624	6631	FR680N	WF2-FIX	125.9	237.5	125.9	237.5	<2%
6631	6800	FR680N	WF2-FIX	125.9	237.5	684.5	245.1	
6800	6921	FR680N18	WF2-FIX	480.1	248.0	129.9	356.6	
6921	6976	FR680N	PC1-FIX	563.3	639.2	565.3	274.6	
6976	7061	FR680N18	WF3-FIX	413.2	126.0	490.8	371.7	
7061	7241	FR680N	WF4-FIX	203.0	286.4	748.3	285.6	
7241	7246	FR680N	WF4-FIX	748.3	285.6	748.3	285.6	<1%
7246	7251	FR680N	WF4-FIX	749.6	743.5	749.6	743.5	<1%
7251	7420	FR680N	WF4-FIX	749.6	743.5	213.3	744.3	
7420	7600	FR680N33	WF3-FIX	688.9	608.4	381.6	126.4	
7600	7602	FR680N33	WF3-FIX	381.6	126.4	381.6	126.4	<0.3%
7602	7605	FR680N18	PC1-FIX	427.0	230.0	427.0	230.0	<0.2%
7605	7658	FR680N18	PC1-FIX	427.0	230.0	538.9	580.6	
7658	7690	FR680N33	WF2-FIX	126.2	276.1	212.1	222.0	
7690	7830	FR868N	WF4-FIX	711.5	751.3	316.5	751.9	
7830	8072	FR868N33	WF3-FIX	728.2	705.8	360.9	129.7	
8072	8074	FR868N33	WF3-FIX	360.9	129.7	360.9	129.7	<0.3%
8074	8077	FR868N18	PC1-FIX	471.5	231.0	471.5	231.0	<0.2%
8077	8140	FR868N18	PC1-FIX	471.5	231.0	589.7	601.5	
8140	8300	FR868N18	WF2-FIX	527.6	213.2	126.2	337.6	
8300	8362	FR868N	PC1-FIX	605.4	644.1	607.3	287.9	
8362	8460	FR868N18	WF3-FIX	393.1	126.1	470.6	371.7	
8460	8661	FR868N	WF4-FIX	196.9	305.7	724.7	304.9	

Table 10: LRF-TABLE Version 28856 in CCD Pixels (Installed 09-May-1995).

λ_1	λ_2	FILTER	APERTURE	CCD Pixel				VIGNETTING
				X1	Y1	X2	Y2	
8661	8910	FR868N	WF3-FIX	218.3	731.6	223.4	125.3	
8910	8920	FR868N	WF3-FIX	223.4	125.3	223.4	125.3	<3%
8964	8973	FR868N	WF2-FIX	125.7	218.2	125.7	218.2	<1%
8973	8980	FR868N	WF2-FIX	125.7	218.2	142.7	218.5	
8980	9200	FR868N	WF2-FIX	142.7	218.5	678.2	225.8	
9200	9415	FR868N	WF2-FIX	668.4	686.5	162.2	679.6	
9415	9430	FR868N	WF2-FIX	162.2	679.6	126.8	679.2	
9430	9440	FR868N	WF2-FIX	126.8	679.2	126.8	679.2	<4%
9478	9501	FR868N	WF3-FIX	684.3	135.4	684.3	135.4	<6%
9501	9762	FR868N	WF3-FIX	684.3	135.4	679.2	750.2	

Table 11: LRF-TABLE Version 28856 in POS TARG units.

LAM1	LAM2	FILTER	APERTURE	POS TARG (arcseconds)			
				POSX1	POSY1	POSX2	POSY2
3710	3800	FR418N	WF4-FIX	31.46	-32.58	31.55	26.05
3800	3878	FR418N33	WF3-FIX	-25.19	-13.41	2.13	29.43
3878	3881	FR418N18	PC1-FIX	-0.81	-9.08	-0.81	-9.08
3881	3907	FR418N18	PC1-FIX	-0.81	-9.08	4.34	7.06
3907	3929	FR418N33	WF2-FIX	12.68	-29.39	20.33	-17.27
3929	4008	FR418N18	WF2-FIX	18.03	13.86	4.67	-29.22
4008	4038	FR418N	PC1-FIX	5.52	9.48	5.61	-7.65
4038	4100	FR418N18	WF3-FIX	-0.88	29.24	-11.54	-4.52
4100	4177	FR418N	WF4-FIX	-14.43	11.36	-14.50	-32.61
4177	4182	FR418N	WF4-FIX	-14.50	-32.61	-14.50	-32.61
4190	4195	FR418N	WF3-FIX	16.83	-32.22	16.83	-32.22
4195	4210	FR418N	WF3-FIX	16.83	-32.22	16.76	-24.03
4210	4308	FR418N	WF3-FIX	16.76	-24.03	16.31	29.47
4308	4313	FR418N	WF3-FIX	16.31	29.47	16.31	29.47
4332	4337	FR418N	WF2-FIX	16.57	-29.44	16.57	-29.44
4337	4446	FR418N	WF2-FIX	16.57	-29.44	15.77	30.07
4446	4550	FR418N	WF2-FIX	-30.10	26.71	-29.40	-24.19
4550	4562	FR418N	WF2-FIX	-29.39	-24.19	-29.31	-30.06
4562	4567	FR418N	WF2-FIX	-29.31	-30.06	-29.31	-30.06
4582	4593	FR418N	WF3-FIX	-29.59	29.76	-29.59	29.76
4593	4720	FR418N	WF3-FIX	-29.59	29.76	-29.07	-32.40

Table 11: LRF-TABLE Version 28856 in POS TARG units.

LAM1	LAM2	FILTER	APERTURE	POS TARG (arcseconds)			
				POSX1	POSY1	POSX2	POSY2
4720	4733	FR418N	WF3-FIX	-29.07	-32.40	-29.07	-32.40
4733	4746	FR533N	WF3-FIX	-27.16	-32.30	-27.16	-32.30
4746	4863	FR533N	WF3-FIX	-27.16	-32.30	-27.67	28.77
4863	4873	FR533N	WF3-FIX	-27.67	28.77	-27.67	28.77
4892	4897	FR533N	WF2-FIX	-27.42	-28.45	-27.42	-28.45
4897	4900	FR533N	WF2-FIX	-27.42	-28.45	-27.44	-26.88
4900	5013	FR533N	WF2-FIX	-27.45	-26.88	-28.25	32.11
5013	5020	FR533N18	WF2-FIX	-22.75	26.88	-23.68	23.84
5020	5153	FR533N	WF2-FIX	17.67	31.25	18.48	-29.23
5153	5158	FR533N	WF2-FIX	18.48	-29.23	18.48	-29.23
5183	5188	FR533N	WF3-FIX	18.22	29.58	18.22	29.58
5188	5310	FR533N	WF3-FIX	18.22	29.58	18.69	-25.91
5310	5322	FR533N	WF3-FIX	18.69	-25.91	18.74	-31.36
5322	5327	FR533N	WF3-FIX	18.74	-31.36	18.74	-31.36
5334	5339	FR533N	WF4-FIX	-12.58	-32.67	-12.58	-32.67
5337	5339	FR533N	WF4-FIX	-12.58	-32.67	-12.58	-32.67
5339	5450	FR533N	WF4-FIX	-12.58	-32.67	-12.50	14.53
5450	5528	FR533N18	WF3-FIX	-8.75	-2.07	1.23	29.56
5528	5566	FR533N	PC1-FIX	7.53	-6.69	7.44	9.46
5566	5671	FR533N18	WF2-FIX	6.49	-29.82	19.71	12.83
5671	5700	FR533N33	WF2-FIX	20.99	-19.79	14.57	-30.00
5700	5741	FR533N18	PC1-FIX	6.32	6.94	1.13	-9.31
5741	5743	FR533N33	WF3-FIX	4.55	29.67	4.55	29.67
5743	5910	FR533N33	WF3-FIX	4.55	29.67	-32.80	-28.91
5910	6007	FR533N	WF4-FIX	32.54	8.89	32.47	-31.46
6007	6192	FR680N	WF2-FIX	-29.17	32.55	-28.32	-29.94
6192	6198	FR680N	WF2-FIX	-28.32	-29.94	-28.32	-29.94
6221	6238	FR680N	WF3-FIX	-28.58	29.51	-28.58	29.51
6238	6409	FR680N	WF3-FIX	-28.58	29.51	-28.11	-28.25
6409	6584	FR680N	WF3-FIX	17.79	-27.99	17.31	29.62
6584	6587	FR680N	WF3-FIX	17.31	29.62	17.31	29.62
6584	6591	FR680N	WF3-FIX	17.31	29.62	17.31	29.62
6624	6631	FR680N	WF2-FIX	17.58	-29.64	17.58	-29.64
6631	6800	FR680N	WF2-FIX	17.58	-29.64	16.82	25.99
6800	6921	FR680N18	WF2-FIX	16.53	5.64	5.72	-29.24
6921	6976	FR680N	PC1-FIX	6.52	9.78	6.62	-6.82
6976	7061	FR680N18	WF3-FIX	0.33	29.72	-7.40	5.26
7061	7241	FR680N	WF4-FIX	-13.41	21.92	-13.49	-32.41
7241	7246	FR680N	WF4-FIX	-13.49	-32.41	-13.49	-32.41
7246	7251	FR680N	WF4-FIX	32.13	-32.54	32.13	-32.54
7251	7420	FR680N	WF4-FIX	32.13	-32.54	32.21	20.89

Table 11: LRF-TABLE Version 28856 in POS TARG units.

LAM1	LAM2	FILTER	APERTURE	POS TARG (arcseconds)			
				POSX1	POSY1	POSX2	POSY2
7420	7600	FR680N33	WF3-FIX	-27.12	-18.31	3.47	29.68
7600	7602	FR680N33	WF3-FIX	3.47	29.68	3.47	29.68
7602	7605	FR680N18	PC1-FIX	0.32	-8.86	0.32	-8.86
7605	7658	FR680N18	PC1-FIX	0.32	-8.86	5.41	7.11
7658	7690	FR680N33	WF2-FIX	13.73	-29.61	19.12	-21.05
7690	7830	FR868N	WF4-FIX	32.91	-28.74	32.97	10.61
7830	8072	FR868N33	WF3-FIX	-31.03	-28.01	5.54	29.35
8072	8074	FR868N33	WF3-FIX	5.54	29.35	5.54	29.35
8074	8077	FR868N18	PC1-FIX	2.34	-8.81	2.34	-8.81
8077	8140	FR868N18	PC1-FIX	2.34	-8.81	7.73	8.06
8140	8300	FR868N18	WF2-FIX	20.00	10.37	7.61	-29.61
8300	8362	FR868N	PC1-FIX	8.44	10.00	8.53	-6.22
8362	8460	FR868N18	WF3-FIX	2.33	29.71	-5.39	5.26
8460	8661	FR868N	WF4-FIX	-11.49	22.53	-11.57	-30.06
8661	8910	FR868N	WF3-FIX	19.73	-30.57	19.23	29.79
8910	8920	FR868N	WF3-FIX	19.23	29.79	19.23	29.79
8964	8973	FR868N	WF2-FIX	19.50	-29.66	19.50	-29.66
8973	8980	FR868N	WF2-FIX	19.50	-29.66	19.47	-27.96
8980	9200	FR868N	WF2-FIX	19.47	-27.96	18.74	25.37
9200	9415	FR868N	WF2-FIX	-27.14	24.39	-26.45	-26.02
9415	9430	FR868N	WF2-FIX	-26.44	-26.02	-26.40	-29.55
9430	9440	FR868N	WF2-FIX	-26.40	-29.55	-26.40	-29.55
9478	9501	FR868N	WF3-FIX	-26.66	28.78	-26.66	28.78
9501	9762	FR868N	WF3-FIX	-26.66	28.78	-26.15	-32.43

Figure 10.a. Wavelength runs for interim TRANS table on FR418N.

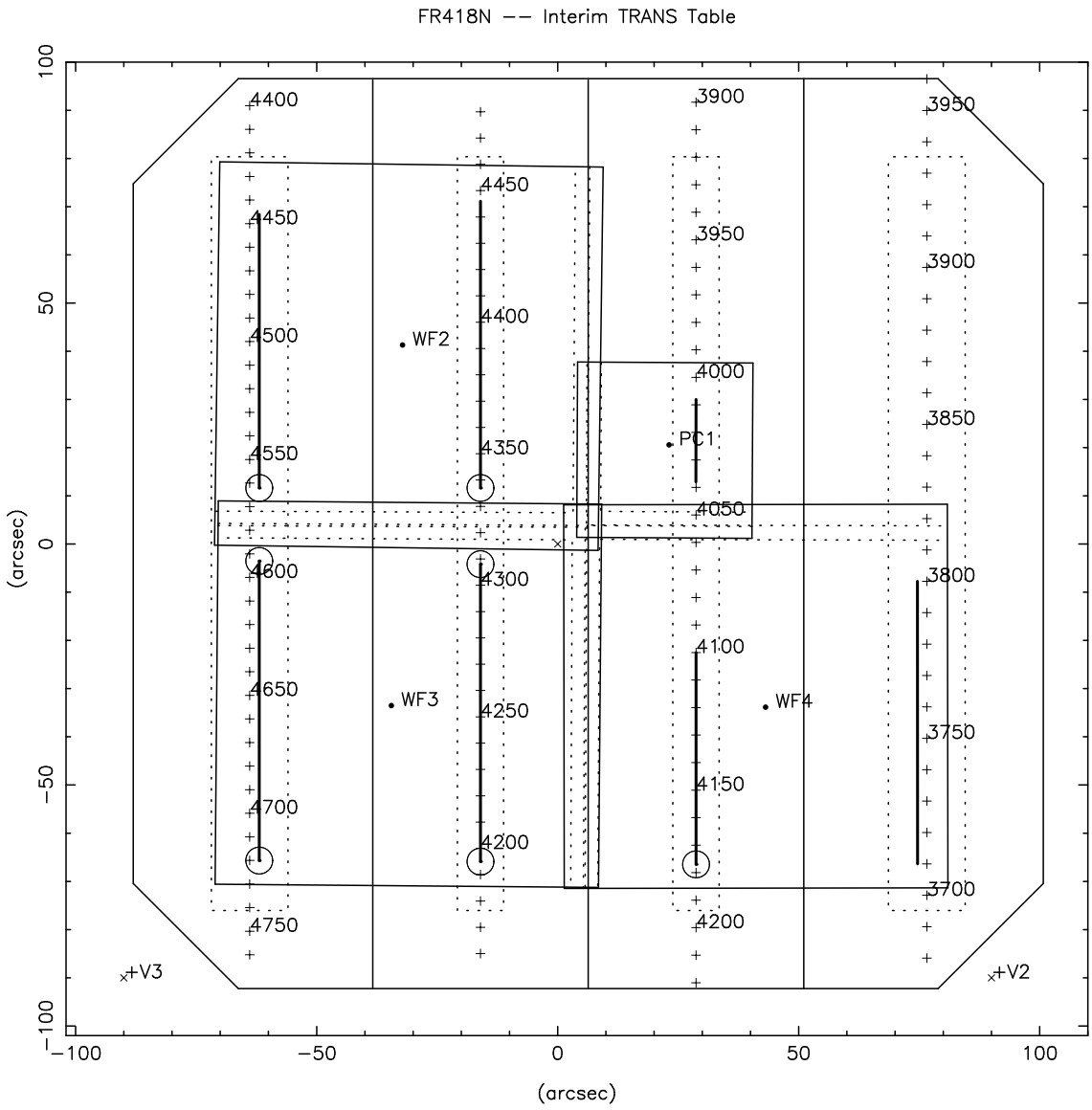

Figure 10.b. Wavelength runs for interim TRANS table on FR418N18.

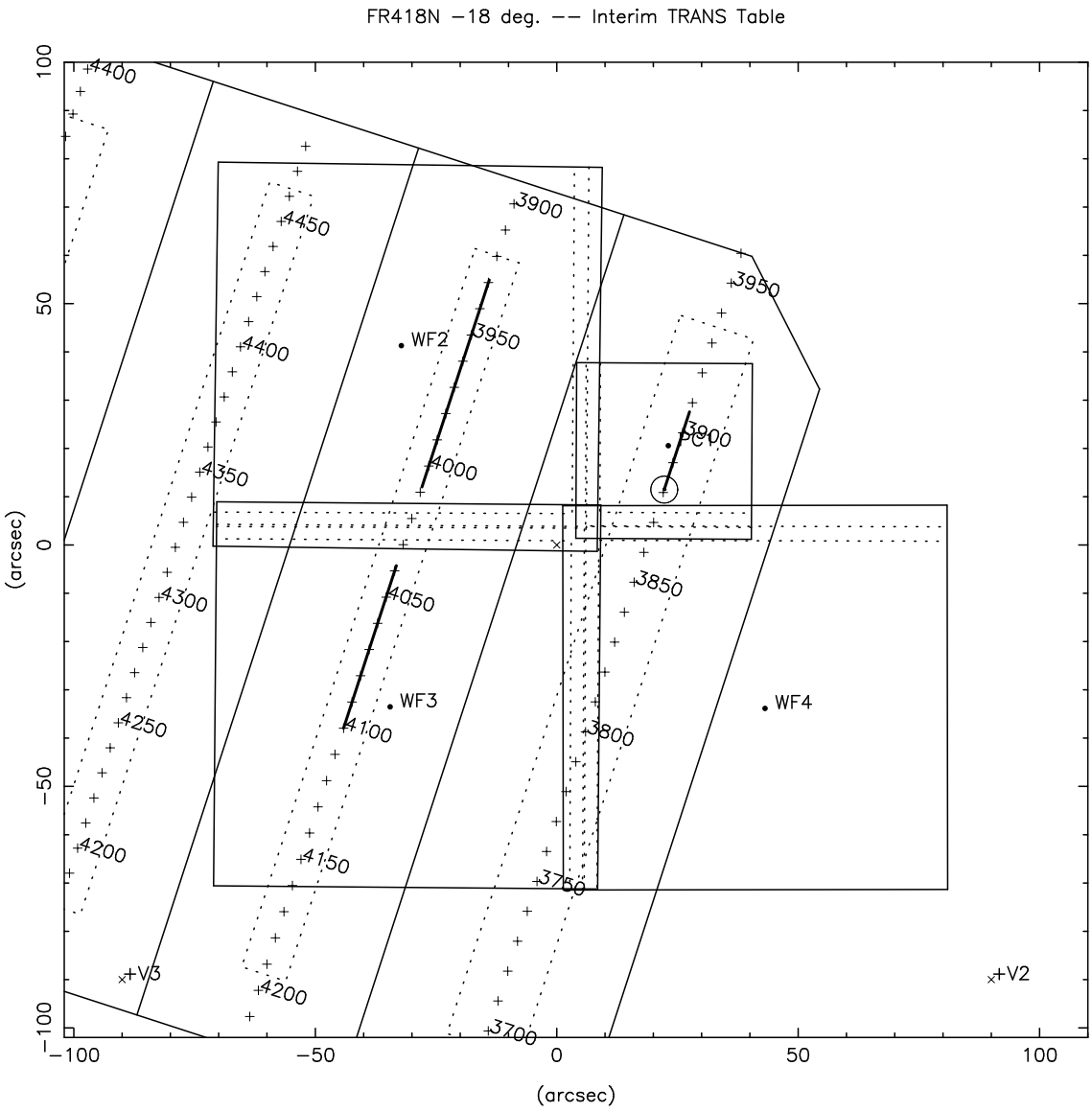

Figure 10.c. Wavelength runs for interim TRANS table on FR418N33.

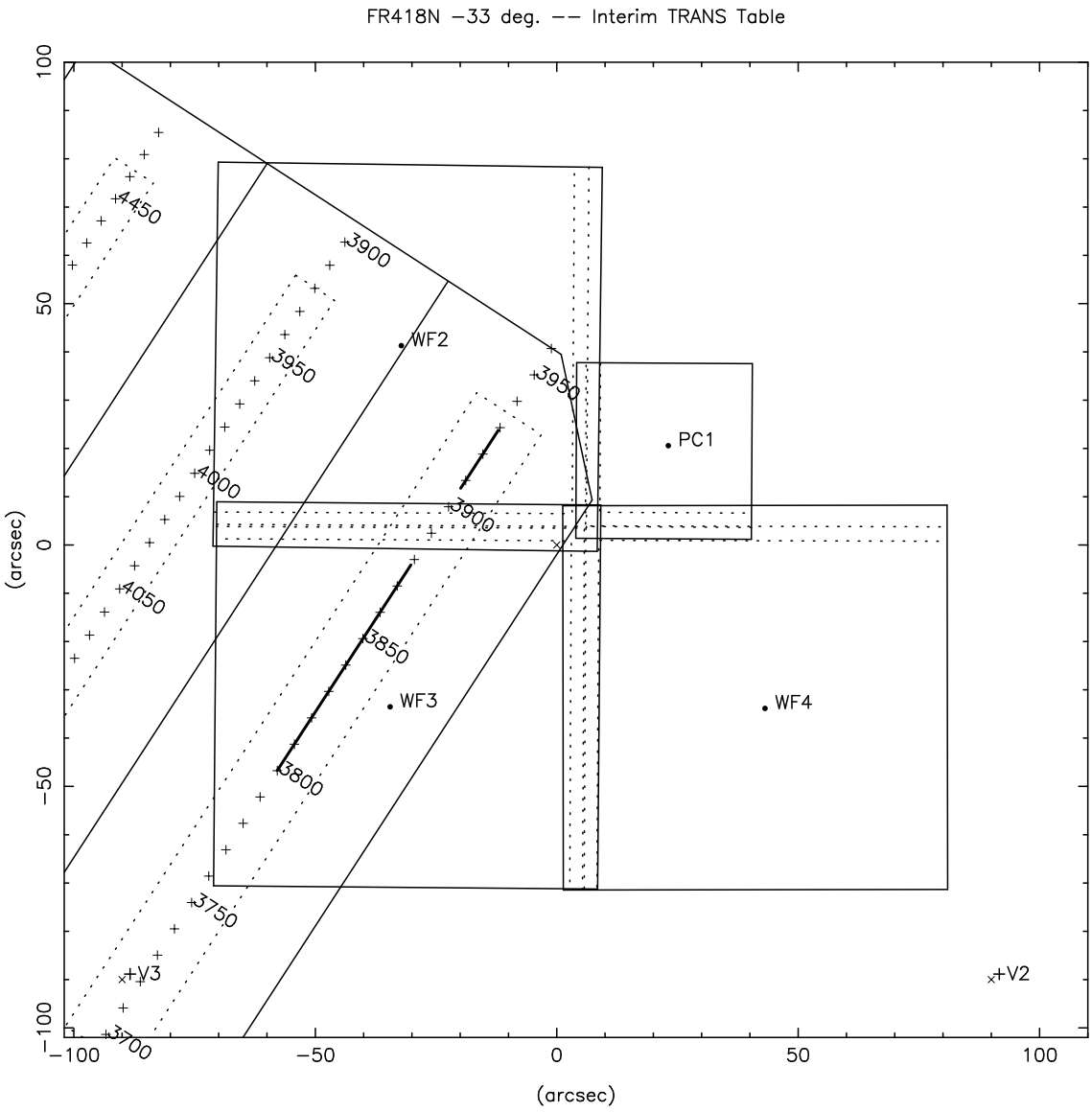

Figure 10.d. Wavelength runs for interim TRANS table on FR533N.

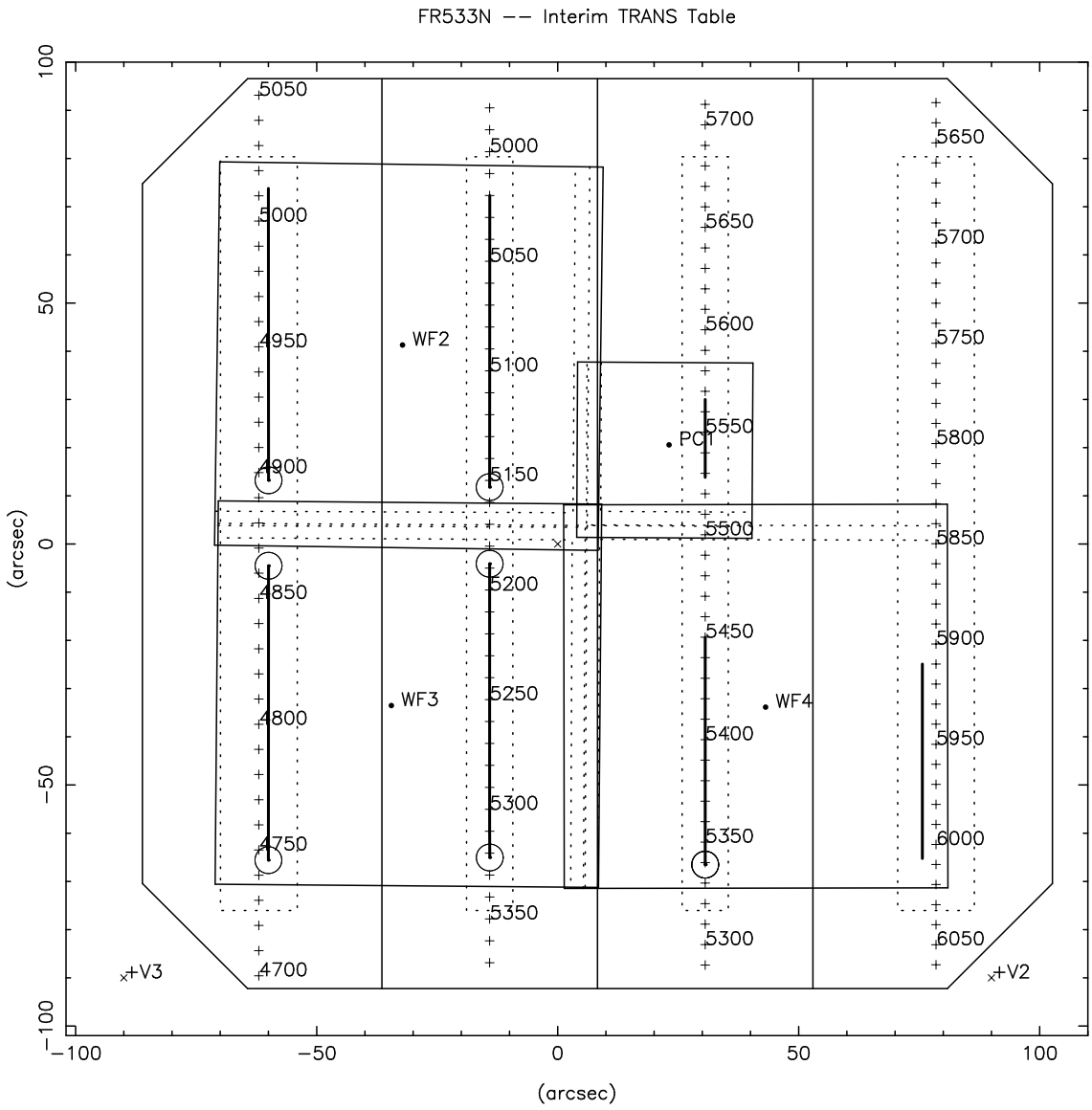

Figure 10.e. Wavelength runs for interim TRANS table on FR533N18.

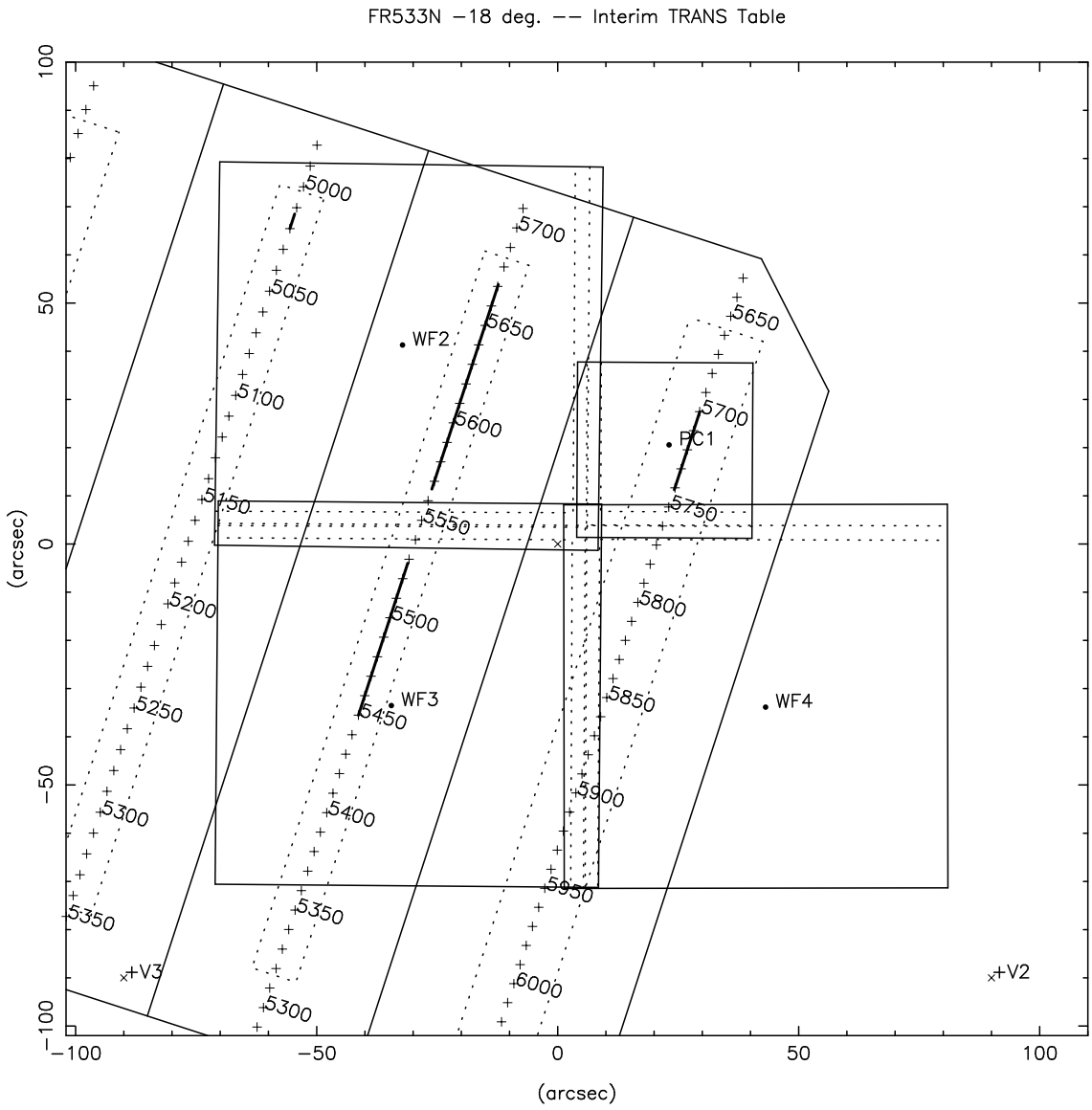

Figure 10.f. Wavelength runs for interim TRANS table on FR533N33.

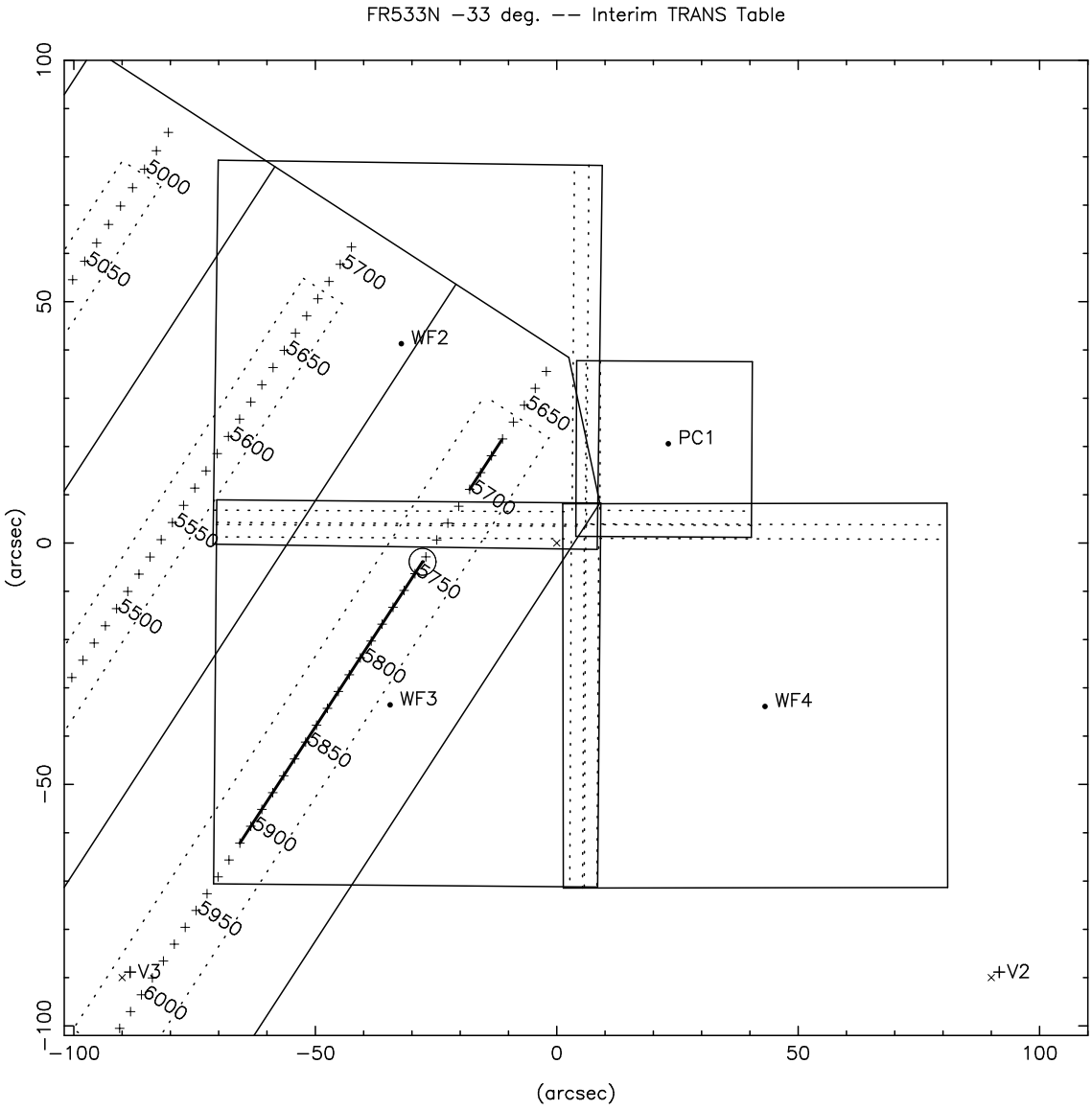

Figure 10.g. Wavelength runs for interim TRANS table on FR680N.

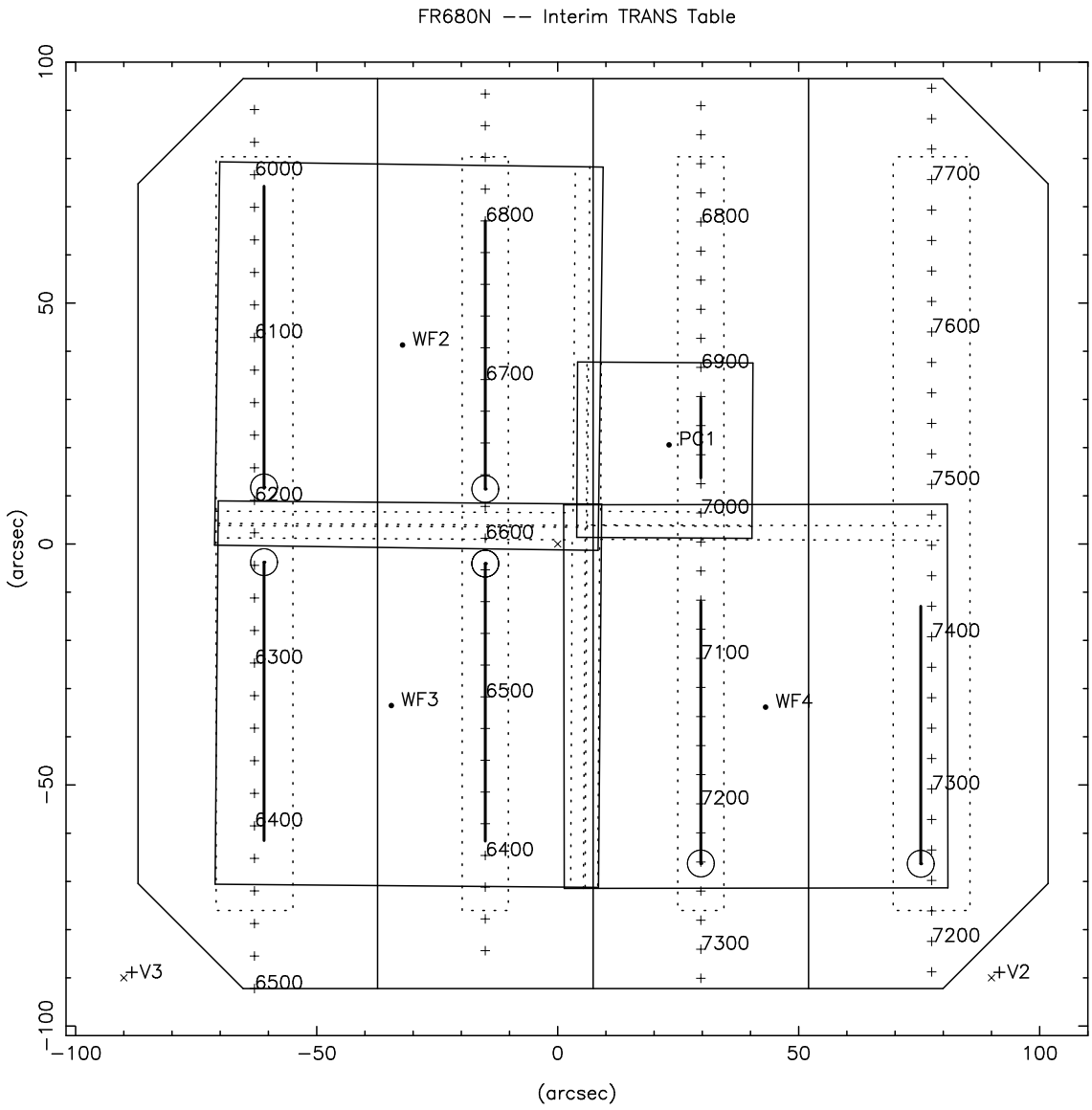

Figure 10.h. Wavelength runs for interim TRANS table on FR680N18.

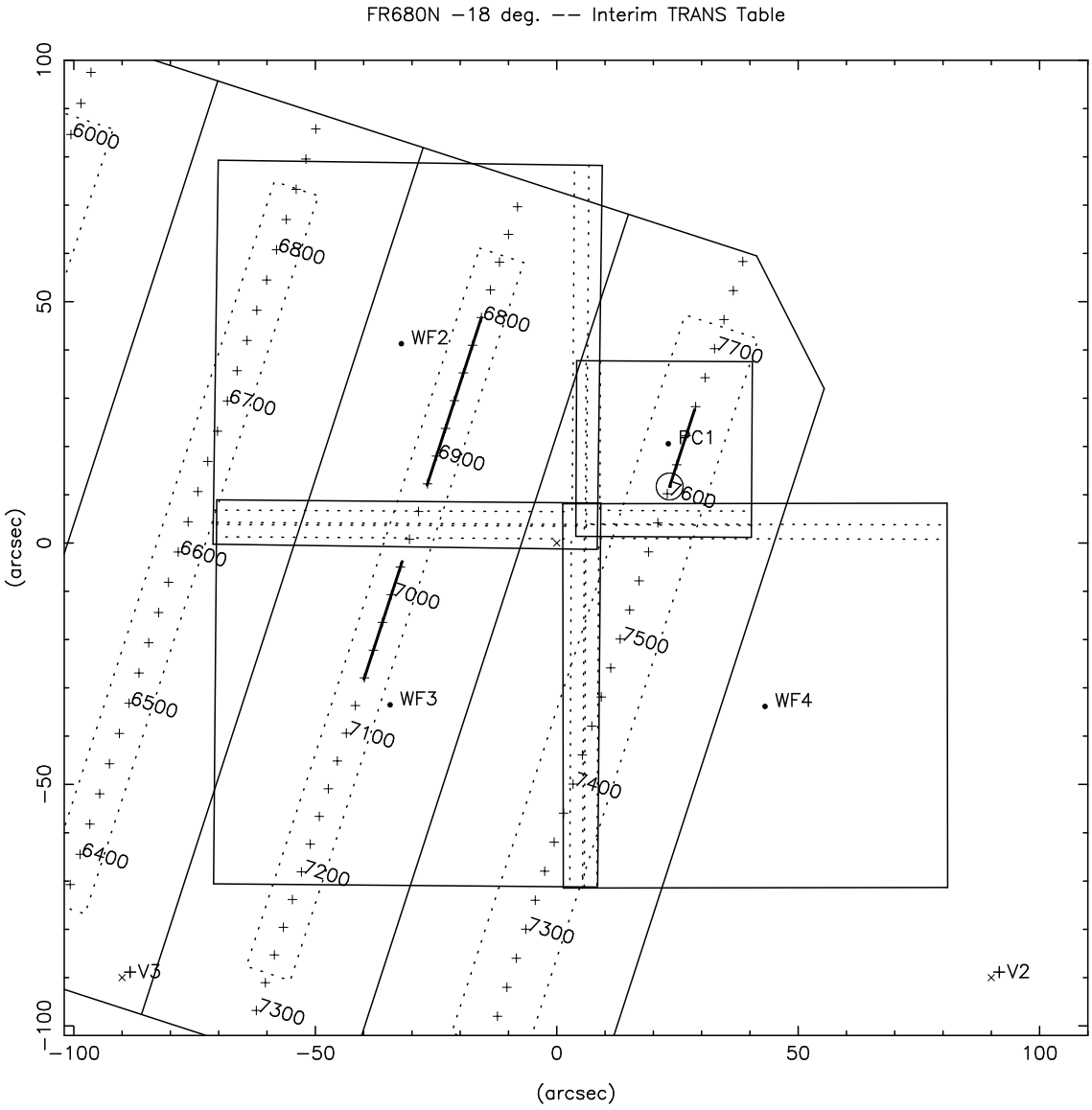

Figure 10.i. Wavelength runs for interim TRANS table on FR680N33.

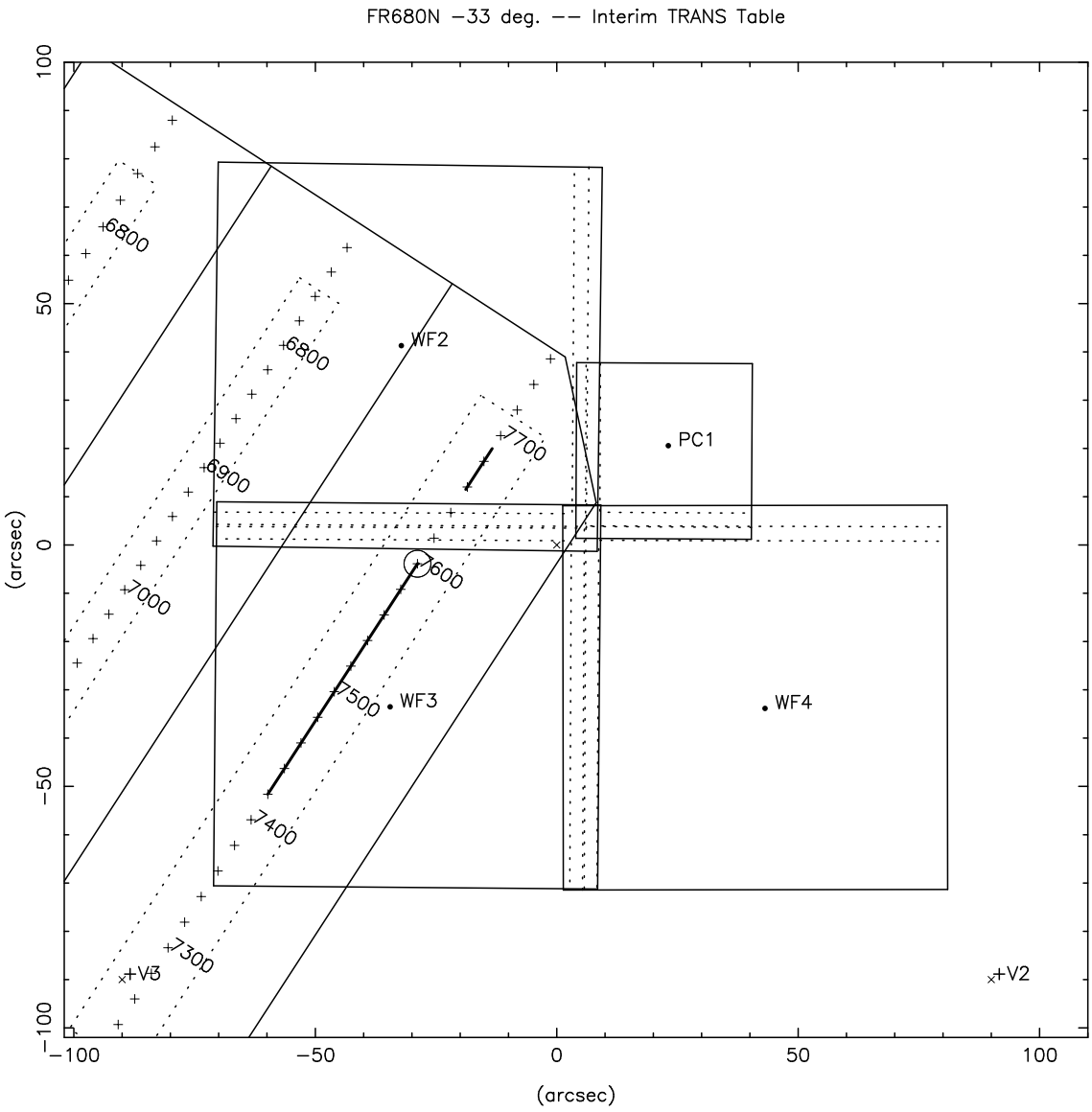

Figure 10.j. Wavelength runs for interim TRANS table on FR868N.

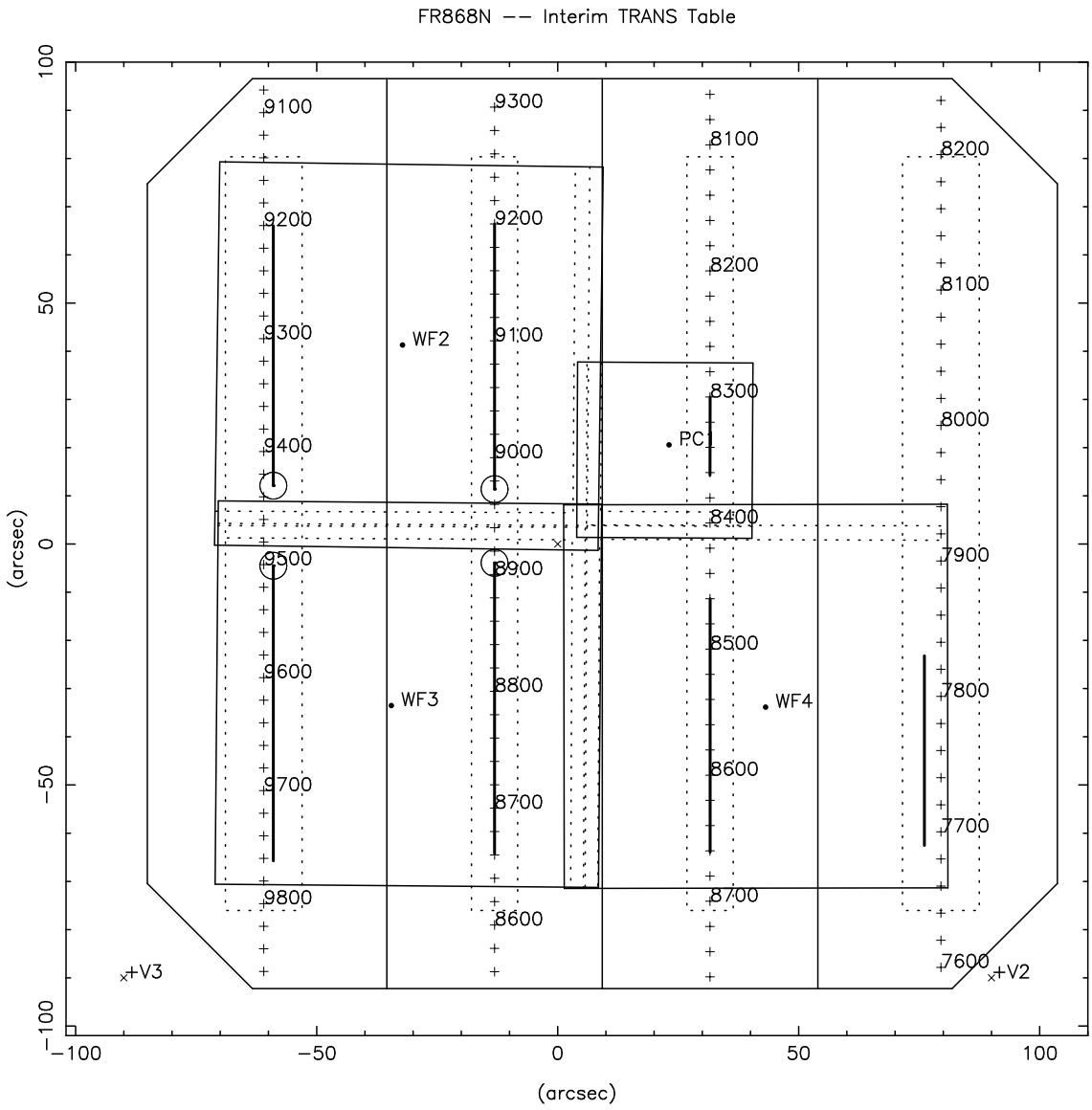

Figure 10.k. Wavelength runs for interim TRANS table on FR868N18.

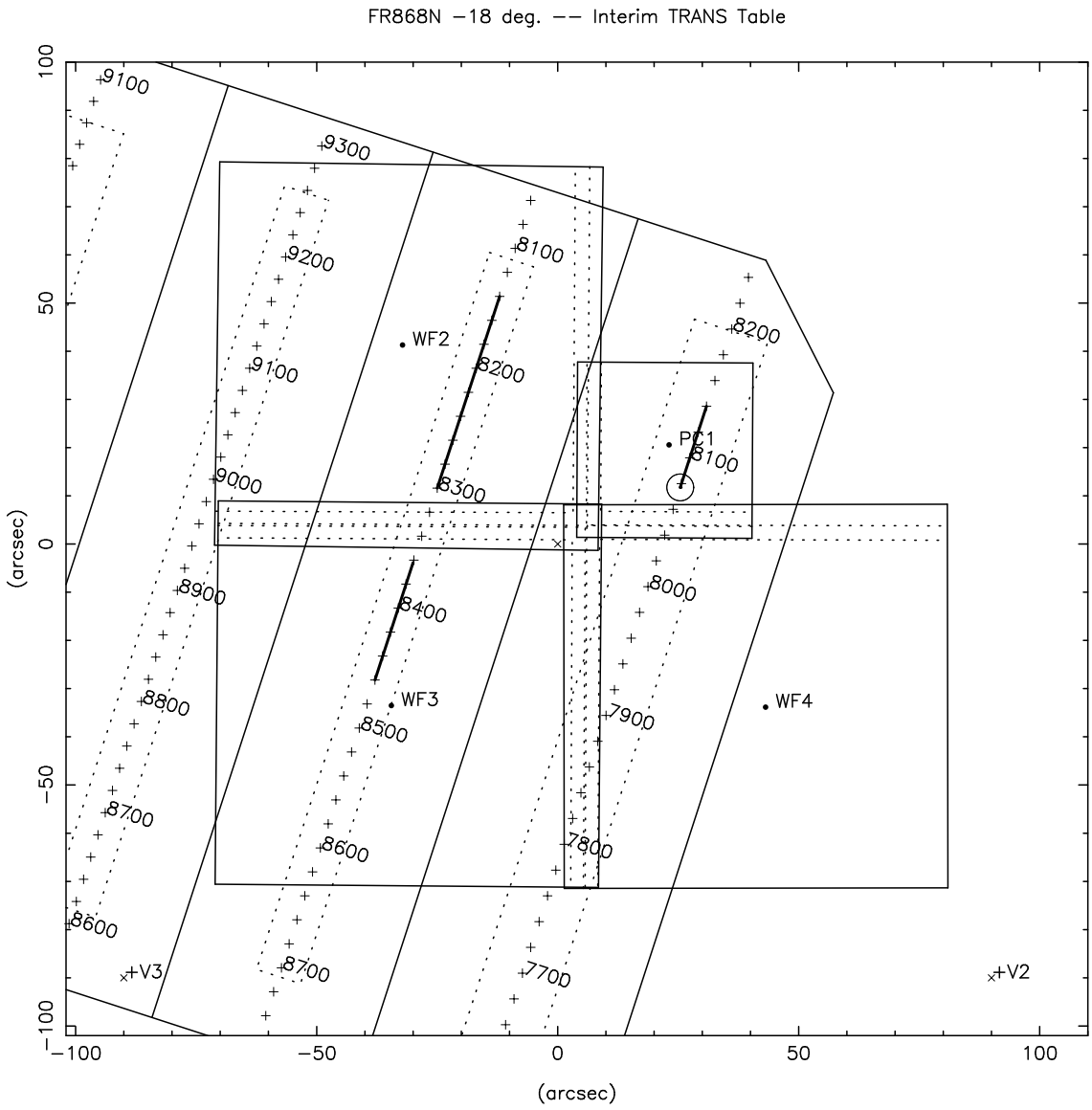

Figure 10.l. Wavelength runs for interim TRANS table on FR868N33.

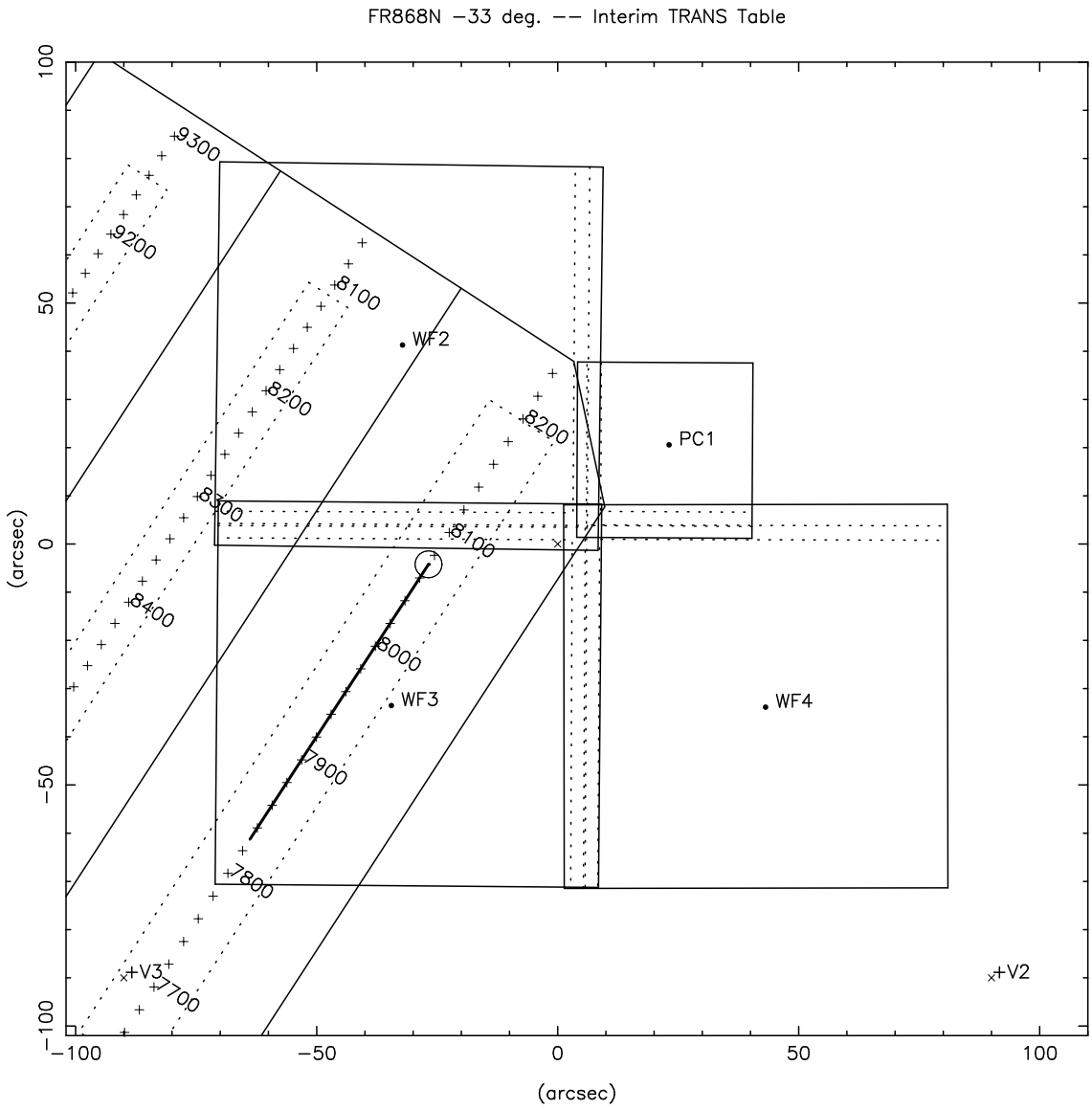

6. The Final TRANS table (used for proposals submitted >1 July 1995).

Once commanding codes for the +15 degree filter rotations were completed, a second, “final” table was created and installed in TRANS. The final table is listed in Tables 12 and 13, and the corresponding wavelength runs are plotted in Figure 11. The wavelength runs are plotted as heavy lines. As before, ramp locations which serve multiple wavelengths, i.e. the “vignetted” settings in Table 12, are indicated by large circles.

As with the interim TRANS table, the wavelength runs of the outermost ramps on each filter (the #1 and #4 ramps) have been manually forced (displaced) about 2 arcseconds inward on the filter, so as to move the promised 10 arcsecond apertures farther from the CCD edges. This reduces the possibility that pointing errors might cause the CCD edges to intrude into the promised 10 arcsecond diameter unvignetted aperture.

A 10 arcsecond diameter unvignetted field of view is supported for nearly all wavelengths. There are, however, three small wavelength ranges where the clear field of view is reduced. These are all on the PC CCD, and involve the +15 degree filter rotation, where the unvignetted region of the filter lies partially off the CCD. The wavelength ranges from 5176 to 5183 Angstroms, and from 6587 to 6590 Angstroms, both have the clear field of view reduced to ~9 arcseconds. For the wavelength range 8920 to 8945 Angstroms the field of view is reduced to ~7.5 arcseconds diameter. These are indicated by “FOV” in the VIGNETTING column of Table 12.

The final table has no gaps in the wavelength coverage, largely due to the addition of the +15 degree filter rotation.

The accuracy of the wavelength / aperture mapping provided by this table is ~0.7 arcseconds in the wavelength direction, or ~1 Angstrom at the 3700 Angstrom setting, and ~3 Angstroms at the 9800 Angstrom setting. The accuracy in the transverse direction is ~0.5 arcseconds.

Table 12: LRF-TABLE Version 29290 in CCD Pixels (Installed 29-June-1995)

λ_1	λ_2	FILTER	APERTURE	CCD Pixel				VIGNETTING
				X1	Y1	X2	Y2	
3710	3800	FR418N	WF4-FIX	750.0	736.8	161.5	737.7	
3800	3878	FR418N33	WF3-FIX	669.5	559.2	395.1	128.9	
3878	3881	FR418N18	PC1-FIX	402.3	225.0	402.3	225.0	<2%
3881	3907	FR418N18	PC1-FIX	402.3	225.0	515.4	579.5	
3907	3929	FR418N33	WF2-FIX	128.4	286.7	250.1	209.9	
3929	4008	FR418N18	WF2-FIX	562.7	233.0	130.1	367.1	
4008	4038	FR418N	PC1-FIX	541.3	632.7	543.3	256.5	
4038	4100	FR418N18	WF3-FIX	425.3	130.8	532.4	469.9	
4100	4177	FR418N	WF4-FIX	309.0	276.2	750.3	275.5	
4177	4182	FR418N	WF4-FIX	750.3	275.5	750.3	275.5	<3%
4182	4186	FR418P15	WF4-FIX	596.5	515.9	596.5	515.9	<2%

Table 12: LRF-TABLE Version 29290 in CCD Pixels (Installed 29-June-1995)

λ_1	λ_2	FILTER	APERTURE	CCD Pixel				VIGNETTING
				X1	Y1	X2	Y2	
4186	4210	FR418P15	WF4-FIX	596.5	515.9	469.4	482.1	
4210	4308	FR418N	WF3-FIX	248.2	665.9	252.7	128.5	
4308	4337	FR418P15	PC1-FIX	690.2	264.6	598.4	599.9	
4337	4446	FR418N	WF2-FIX	127.9	247.6	725.4	255.7	
4446	4550	FR418N	WF2-FIX	691.7	716.2	180.6	709.2	
4550	4571	FR418P15	WF2-FIX	230.0	253.8	130.7	225.8	
4571	4582	FR418P15	WF2-FIX	130.7	225.8	130.7	225.8	<11%
4582	4593	FR418N	WF3-FIX	713.7	125.6	713.7	125.6	<13%
4593	4720	FR418N	WF3-FIX	713.7	125.6	708.5	749.9	
4720	4733	FR418N	WF3-FIX	708.5	749.9	708.5	749.9	<13%
4733	4746	FR533N	WF3-FIX	689.3	748.9	689.3	748.9	<19%
4746	4863	FR533N	WF3-FIX	689.3	748.9	694.4	135.5	
4863	4873	FR533N	WF3-FIX	694.4	135.5	694.4	135.5	<9%
4873	4884	FR533P15	WF2-FIX	128.3	205.1	128.3	205.1	<12%
4884	4900	FR533P15	WF2-FIX	128.3	205.1	209.0	227.9	
4900	5013	FR533N	WF2-FIX	153.6	689.6	745.9	697.7	
5013	5020	FR533N18	WF2-FIX	693.4	642.4	662.9	651.8	
5020	5153	FR533N	WF2-FIX	737.3	236.6	130.0	228.4	
5153	5176	FR533P15	PC1-FIX	637.9	614.9	698.6	393.3	
5176	5183	FR533P15	PC1-FIX	698.6	393.3	698.6	325.9	FOV 9″
5183	5188	FR533N	WF3-FIX	233.5	127.4	233.5	127.4	<2%
5188	5310	FR533N	WF3-FIX	233.5	127.4	228.8	684.7	
5310	5335	FR533P15	WF4-FIX	482.8	505.5	593.1	534.9	
5335	5337	FR533P15	WF4-FIX	593.1	534.9	593.1	534.9	<1%
5337	5339	FR533N	WF4-FIX	750.9	294.7	750.9	294.7	<1%
5339	5450	FR533N	WF4-FIX	750.9	294.7	277.2	295.5	
5450	5528	FR533N18	WF3-FIX	504.4	445.3	404.1	127.6	
5528	5566	FR533N	PC1-FIX	585.3	277.5	583.4	632.3	
5566	5671	FR533N18	WF2-FIX	124.1	348.8	552.3	216.1	
5671	5700	FR533N33	WF2-FIX	224.8	203.2	122.3	267.7	
5700	5741	FR533N18	PC1-FIX	558.8	577.0	444.9	220.1	
5741	5743	FR533N33	WF3-FIX	370.8	126.5	370.8	126.5	<0.3%
5743	5910	FR533N33	WF3-FIX	370.8	126.5	745.9	714.9	
5910	6007	FR533N	WF4-FIX	333.8	747.6	738.8	746.9	
6007	6192	FR680N	WF2-FIX	750.3	706.9	122.9	698.4	
6192	6208	FR680P15	WF2-FIX	177.1	228.4	124.9	213.6	
6208	6221	FR680P15	WF2-FIX	124.9	213.6	124.9	213.6	<8%
6221	6238	FR680N	WF3-FIX	703.6	128.1	703.6	128.1	<13%
6238	6409	FR680N	WF3-FIX	703.6	128.1	698.8	708.2	
6409	6584	FR680N	WF3-FIX	237.8	705.6	242.6	127.0	
6584	6587	FR680N	WF3-FIX	242.6	127.0	242.6	127.0	<1%

Table 12: LRF-TABLE Version 29290 in CCD Pixels (Installed 29-June-1995)

λ_1	λ_2	FILTER	APERTURE	CCD Pixel				VIGNETTING
				X1	Y1	X2	Y2	
6587	6590	FR680P15	PC1-FIX	699.1	294.3	699.1	315.3	FOV 9″
6590	6631	FR680P15	PC1-FIX	699.1	315.3	620.9	601.2	
6631	6800	FR680N	WF2-FIX	125.9	237.5	684.5	245.1	
6800	6921	FR680N18	WF2-FIX	480.1	248.0	129.9	356.6	
6921	6976	FR680N	PC1-FIX	563.3	639.2	565.3	274.6	
6976	7061	FR680N18	WF3-FIX	413.2	126.0	490.8	371.7	
7061	7241	FR680N	WF4-FIX	203.0	286.4	748.3	285.6	
7241	7246	FR680N	WF4-FIX	748.3	285.6	748.3	285.6	<1%
7246	7251	FR680N	WF4-FIX	749.6	743.5	749.6	743.5	<1%
7251	7420	FR680N	WF4-FIX	749.6	743.5	213.3	744.3	
7420	7600	FR680N33	WF3-FIX	688.9	608.4	381.6	126.4	
7600	7602	FR680N33	WF3-FIX	381.6	126.4	381.6	126.4	<0.3%
7602	7605	FR680N18	PC1-FIX	427.0	230.0	427.0	230.0	<0.2%
7605	7658	FR680N18	PC1-FIX	427.0	230.0	538.9	580.6	
7658	7690	FR680N33	WF2-FIX	126.2	276.1	212.1	222.0	
7690	7830	FR868N	WF4-FIX	711.5	751.3	316.5	751.9	
7830	8072	FR868N33	WF3-FIX	728.2	705.8	360.9	129.7	
8072	8074	FR868N33	WF3-FIX	360.9	129.7	360.9	129.7	<0.3%
8074	8077	FR868N18	PC1-FIX	471.5	231.0	471.5	231.0	<0.2%
8077	8140	FR868N18	PC1-FIX	471.5	231.0	589.7	601.5	
8140	8300	FR868N18	WF2-FIX	527.6	213.2	126.2	337.6	
8300	8362	FR868N	PC1-FIX	605.4	644.1	607.3	287.9	
8362	8460	FR868N18	WF3-FIX	393.1	126.1	470.6	371.7	
8460	8661	FR868N	WF4-FIX	196.9	305.7	724.7	304.9	
8661	8910	FR868N	WF3-FIX	218.3	731.6	223.4	125.3	
8910	8920	FR868N	WF3-FIX	223.4	125.3	223.4	125.3	<3%
8920	8945	FR868P15	PC1-FIX	701.1	339.1	701.1	467.5	FOV 7.5″
8945	8980	FR868P15	PC1-FIX	701.1	467.5	651.9	647.3	
8980	9200	FR868N	WF2-FIX	142.7	218.5	678.2	225.8	
9200	9415	FR868N	WF2-FIX	668.4	686.5	162.2	679.6	
9415	9456	FR868P15	WF2-FIX	219.9	220.5	127.0	194.2	
9456	9478	FR868P15	WF2-FIX	127.0	194.2	127.0	194.2	<13%
9478	9501	FR868N	WF3-FIX	684.3	135.4	684.3	135.4	<6%
9501	9762	FR868N	WF3-FIX	684.3	135.4	679.2	750.2	

Table 13: LRF-TABLE Version 29290 in POS TARG units

LAM1	LAM2	FILTER	APERTURE	POS TARG (arcseconds)			
				POSX1	POSY1	POSX2	POSY2
3710	3800	FR418N	WF4-FIX	31.46	-32.58	31.55	26.05
3800	3878	FR418N33	WF3-FIX	-25.19	-13.41	2.13	29.43
3878	3881	FR418N18	PC1-FIX	-0.81	-9.08	-0.81	-9.08
3881	3907	FR418N18	PC1-FIX	-0.81	-9.08	4.34	7.06
3907	3929	FR418N33	WF2-FIX	12.68	-29.39	20.33	-17.27
3929	4008	FR418N18	WF2-FIX	18.03	13.86	4.67	-29.22
4008	4038	FR418N	PC1-FIX	5.52	9.48	5.61	-7.65
4038	4100	FR418N18	WF3-FIX	-0.88	29.24	-11.54	-4.52
4100	4177	FR418N	WF4-FIX	-14.43	11.36	-14.50	-32.61
4177	4182	FR418N	WF4-FIX	-14.50	-32.61	-14.50	-32.61
4182	4186	FR418P15	WF4-FIX	9.45	-17.29	9.45	-17.29
4186	4210	FR418P15	WF4-FIX	9.45	-17.29	6.09	-4.62
4210	4308	FR418N	WF3-FIX	16.76	-24.03	16.31	29.47
4308	4337	FR418P15	PC1-FIX	12.30	-7.28	8.12	7.99
4337	4446	FR418N	WF2-FIX	16.57	-29.44	15.77	30.07
4446	4550	FR418N	WF2-FIX	-30.10	26.71	-29.40	-24.19
4550	4571	FR418P15	WF2-FIX	15.95	-19.27	18.74	-29.16
4571	4582	FR418P15	WF2-FIX	18.74	-29.16	18.74	-29.16
4582	4593	FR418N	WF3-FIX	-29.59	29.76	-29.59	29.76
4593	4720	FR418N	WF3-FIX	-29.59	29.76	-29.07	-32.40
4720	4733	FR418N	WF3-FIX	-29.07	-32.40	-29.07	-32.40
4733	4746	FR533N	WF3-FIX	-27.16	-32.30	-27.16	-32.30
4746	4863	FR533N	WF3-FIX	-27.16	-32.30	-27.67	28.77
4863	4873	FR533N	WF3-FIX	-27.67	28.77	-27.67	28.77
4873	4884	FR533P15	WF2-FIX	20.80	-29.40	20.80	-29.40
4884	4900	FR533P15	WF2-FIX	20.80	-29.40	18.53	-21.36
4900	5013	FR533N	WF2-FIX	-27.45	-26.88	-28.25	32.11
5013	5020	FR533N18	WF2-FIX	-22.75	26.88	-23.68	23.84
5020	5153	FR533N	WF2-FIX	17.67	31.25	18.48	-29.23
5153	5176	FR533P15	PC1-FIX	9.92	8.67	12.68	-1.42
5176	5183	FR533P15	PC1-FIX	12.68	-1.42	12.68	-4.49
5183	5188	FR533N	WF3-FIX	18.22	29.58	18.22	29.58
5188	5310	FR533N	WF3-FIX	18.22	29.58	18.69	-25.91
5310	5335	FR533P15	WF4-FIX	8.42	-5.96	11.35	-16.95
5335	5337	FR533P15	WF4-FIX	11.35	-16.95	11.35	-16.95
5337	5339	FR533N	WF4-FIX	-12.58	-32.67	-12.58	-32.67
5339	5450	FR533N	WF4-FIX	-12.58	-32.67	-12.50	14.53
5450	5528	FR533N18	WF3-FIX	-8.75	-2.07	1.23	29.56
5528	5566	FR533N	PC1-FIX	7.53	-6.69	7.44	9.46

Table 13: LRF-TABLE Version 29290 in POS TARG units

LAM1	LAM2	FILTER	APERTURE	POS TARG (arcseconds)			
				POSX1	POSY1	POSX2	POSY2
5566	5671	FR533N18	WF2-FIX	6.49	-29.82	19.71	12.83
5671	5700	FR533N33	WF2-FIX	20.99	-19.79	14.57	-30.00
5700	5741	FR533N18	PC1-FIX	6.32	6.94	1.13	-9.31
5741	5743	FR533N33	WF3-FIX	4.55	29.67	4.55	29.67
5743	5910	FR533N33	WF3-FIX	4.55	29.67	-32.80	-28.91
5910	6007	FR533N	WF4-FIX	32.54	8.89	32.47	-31.46
6007	6192	FR680N	WF2-FIX	-29.17	32.55	-28.32	-29.94
6192	6208	FR680P15	WF2-FIX	18.48	-24.54	19.96	-29.74
6208	6221	FR680P15	WF2-FIX	19.96	-29.74	19.96	-29.74
6221	6238	FR680N	WF3-FIX	-28.58	29.51	-28.58	29.51
6238	6409	FR680N	WF3-FIX	-28.58	29.51	-28.11	-28.25
6409	6584	FR680N	WF3-FIX	17.79	-27.99	17.31	29.62
6584	6587	FR680N	WF3-FIX	17.31	29.62	17.31	29.62
6587	6590	FR680P15	PC1-FIX	12.71	-5.93	12.71	-4.97
6590	6631	FR680P15	PC1-FIX	12.71	-4.97	9.15	8.05
6631	6800	FR680N	WF2-FIX	17.58	-29.64	16.82	25.99
6800	6921	FR680N18	WF2-FIX	16.53	5.64	5.72	-29.24
6921	6976	FR680N	PC1-FIX	6.52	9.78	6.62	-6.82
6976	7061	FR680N18	WF3-FIX	0.33	29.72	-7.40	5.26
7061	7241	FR680N	WF4-FIX	-13.41	21.92	-13.49	-32.41
7241	7246	FR680N	WF4-FIX	-13.49	-32.41	-13.49	-32.41
7246	7251	FR680N	WF4-FIX	32.13	-32.54	32.13	-32.54
7251	7420	FR680N	WF4-FIX	32.13	-32.54	32.21	20.89
7420	7600	FR680N33	WF3-FIX	-27.12	-18.31	3.47	29.68
7600	7602	FR680N33	WF3-FIX	3.47	29.68	3.47	29.68
7602	7605	FR680N18	PC1-FIX	0.32	-8.86	0.32	-8.86
7605	7658	FR680N18	PC1-FIX	0.32	-8.86	5.41	7.11
7658	7690	FR680N33	WF2-FIX	13.73	-29.61	19.12	-21.05
7690	7830	FR868N	WF4-FIX	32.91	-28.74	32.97	10.61
7830	8072	FR868N33	WF3-FIX	-31.03	-28.01	5.54	29.35
8072	8074	FR868N33	WF3-FIX	5.54	29.35	5.54	29.35
8074	8077	FR868N18	PC1-FIX	2.34	-8.81	2.34	-8.81
8077	8140	FR868N18	PC1-FIX	2.34	-8.81	7.73	8.06
8140	8300	FR868N18	WF2-FIX	20.00	10.37	7.61	-29.61
8300	8362	FR868N	PC1-FIX	8.44	10.00	8.53	-6.22
8362	8460	FR868N18	WF3-FIX	2.33	29.71	-5.39	5.26
8460	8661	FR868N	WF4-FIX	-11.49	22.53	-11.57	-30.06
8661	8910	FR868N	WF3-FIX	19.73	-30.57	19.23	29.79
8910	8920	FR868N	WF3-FIX	19.23	29.79	19.23	29.79
8920	8945	FR868P15	PC1-FIX	12.80	-3.89	12.80	1.96
8945	8980	FR868P15	PC1-FIX	12.80	1.96	10.56	10.14

Table 13: LRF-TABLE Version 29290 in POS TARG units

LAM1	LAM2	FILTER	APERTURE	POS TARG (arcseconds)			
				POSX1	POSY1	POSX2	POSY2
8980	9200	FR868N	WF2-FIX	19.47	-27.96	18.74	25.37
9200	9415	FR868N	WF2-FIX	-27.14	24.39	-26.45	-26.02
9415	9456	FR868P15	WF2-FIX	19.27	-20.28	21.89	-29.53
9456	9478	FR868P15	WF2-FIX	21.89	-29.53	21.89	-29.53
9478	9501	FR868N	WF3-FIX	-26.66	28.78	-26.66	28.78
9501	9762	FR868N	WF3-FIX	-26.66	28.78	-26.15	-32.43

Figure 11.a. Wavelength runs for final TRANS table on FR418P15.

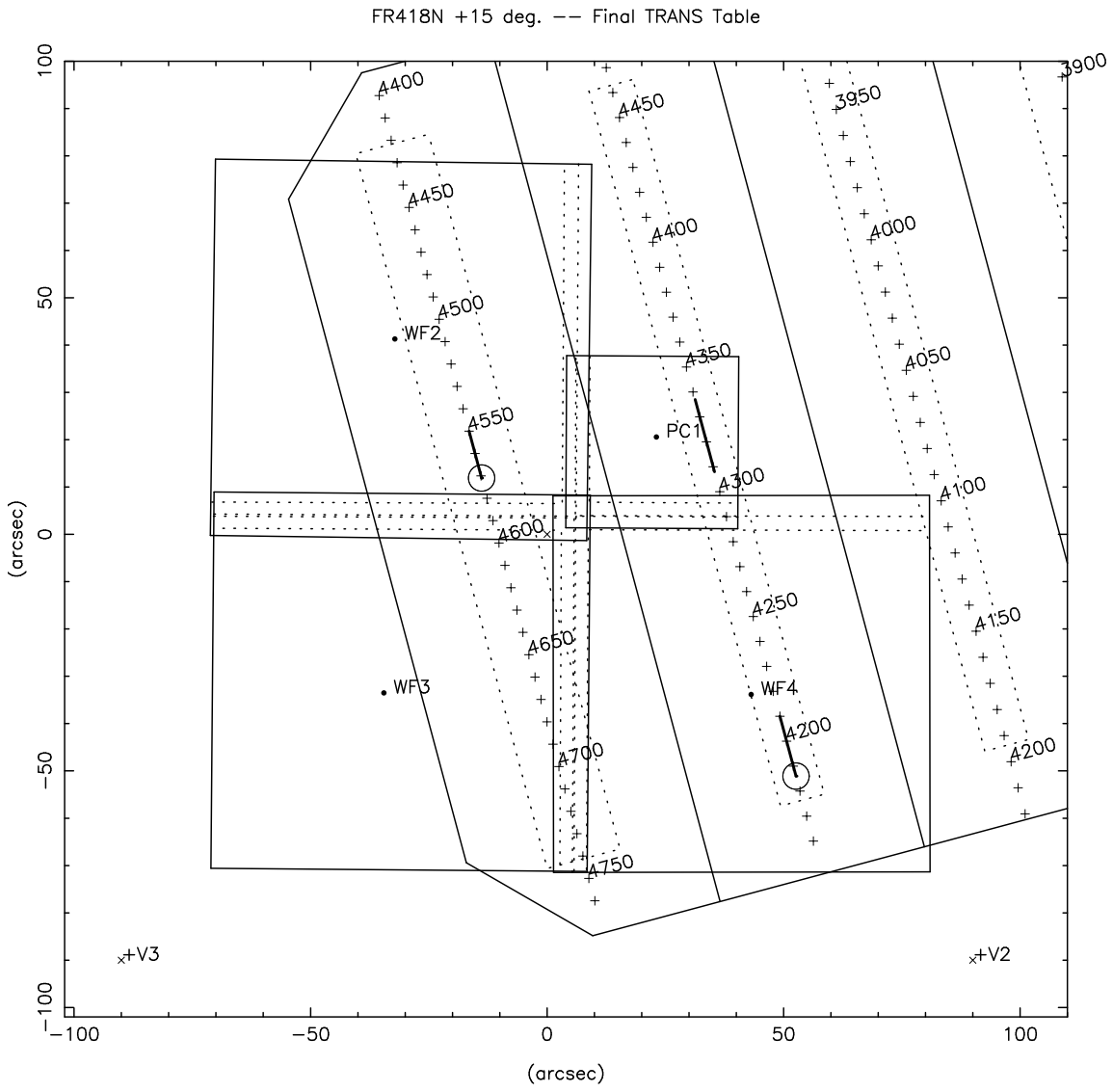

Figure 11.b. Wavelength runs for final TRANS table on FR418N.

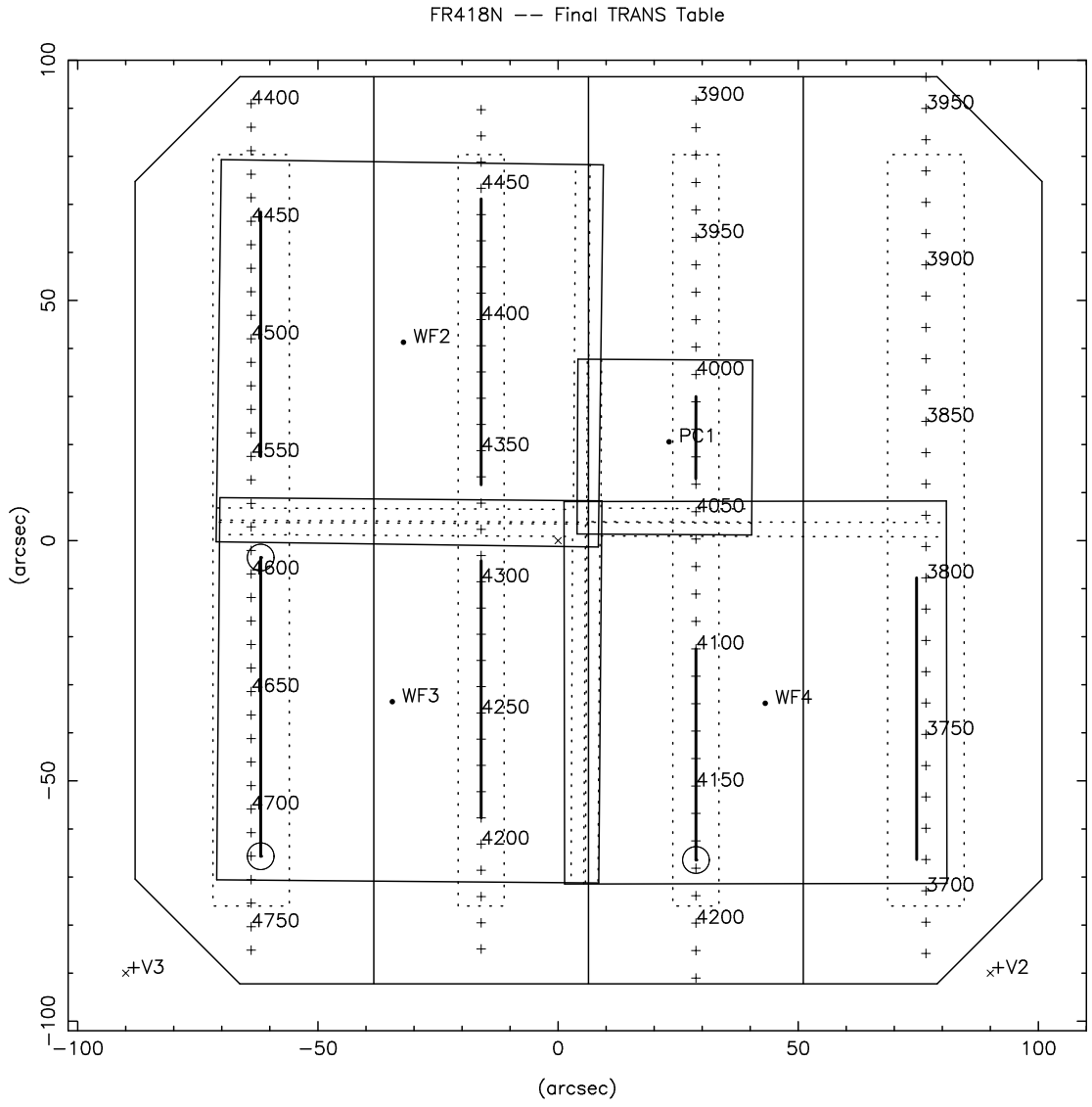

Figure 11.c. Wavelength runs for final TRANS table on FR418N18.

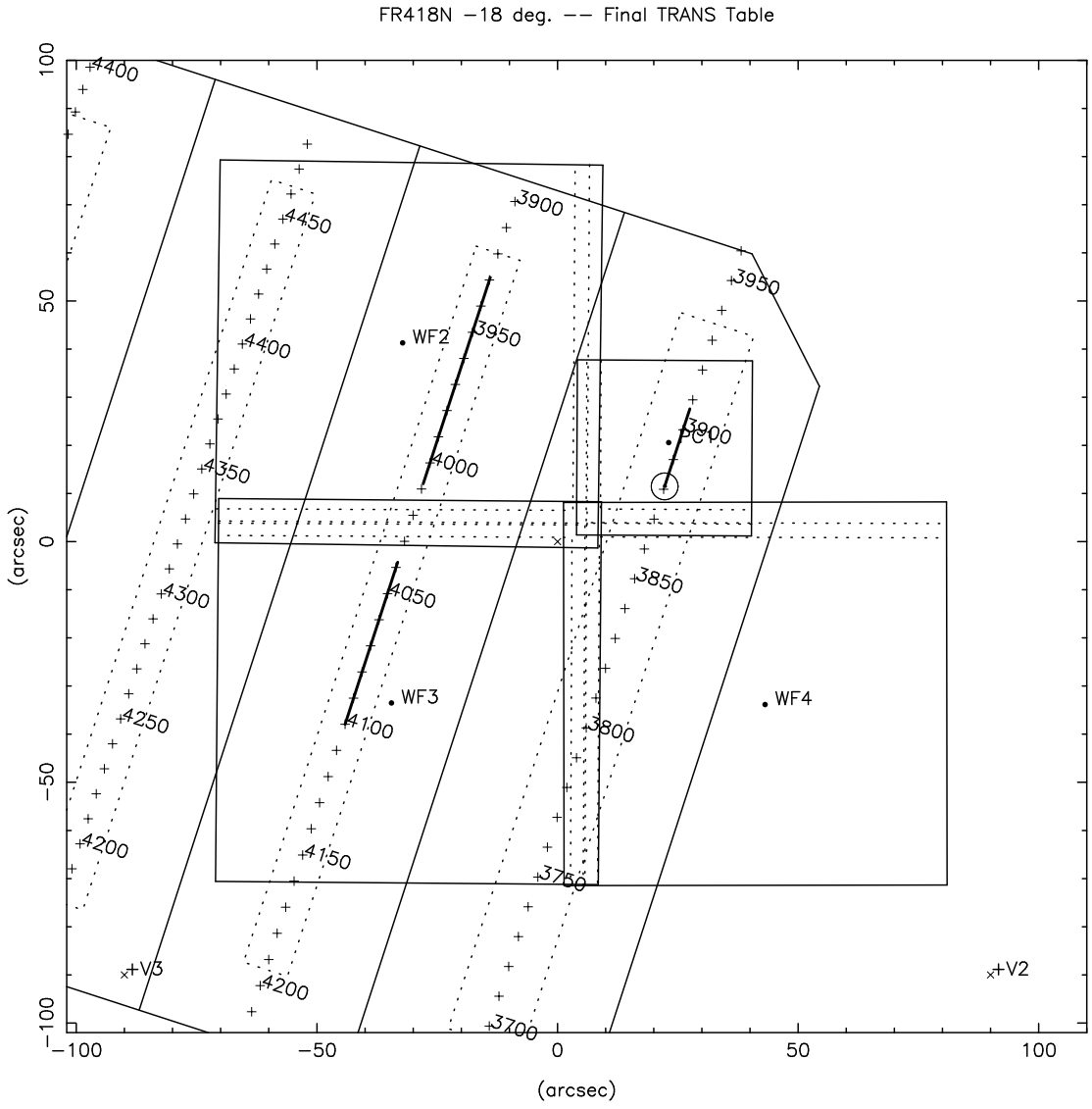

Figure 11.d. Wavelength runs for final TRANS table on FR418N33.

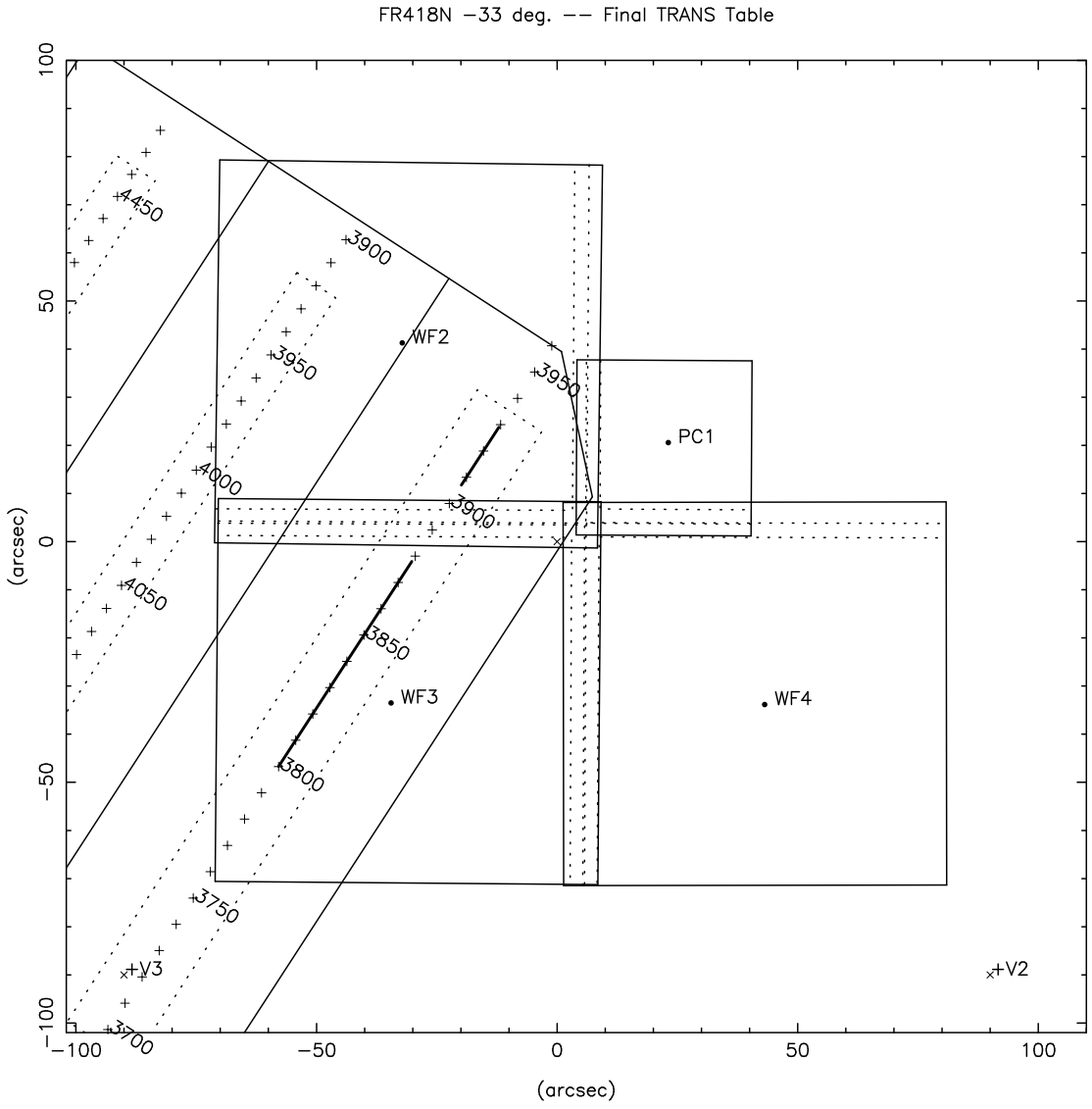

Figure 11.e. Wavelength runs for final TRANS table on FR533P15.

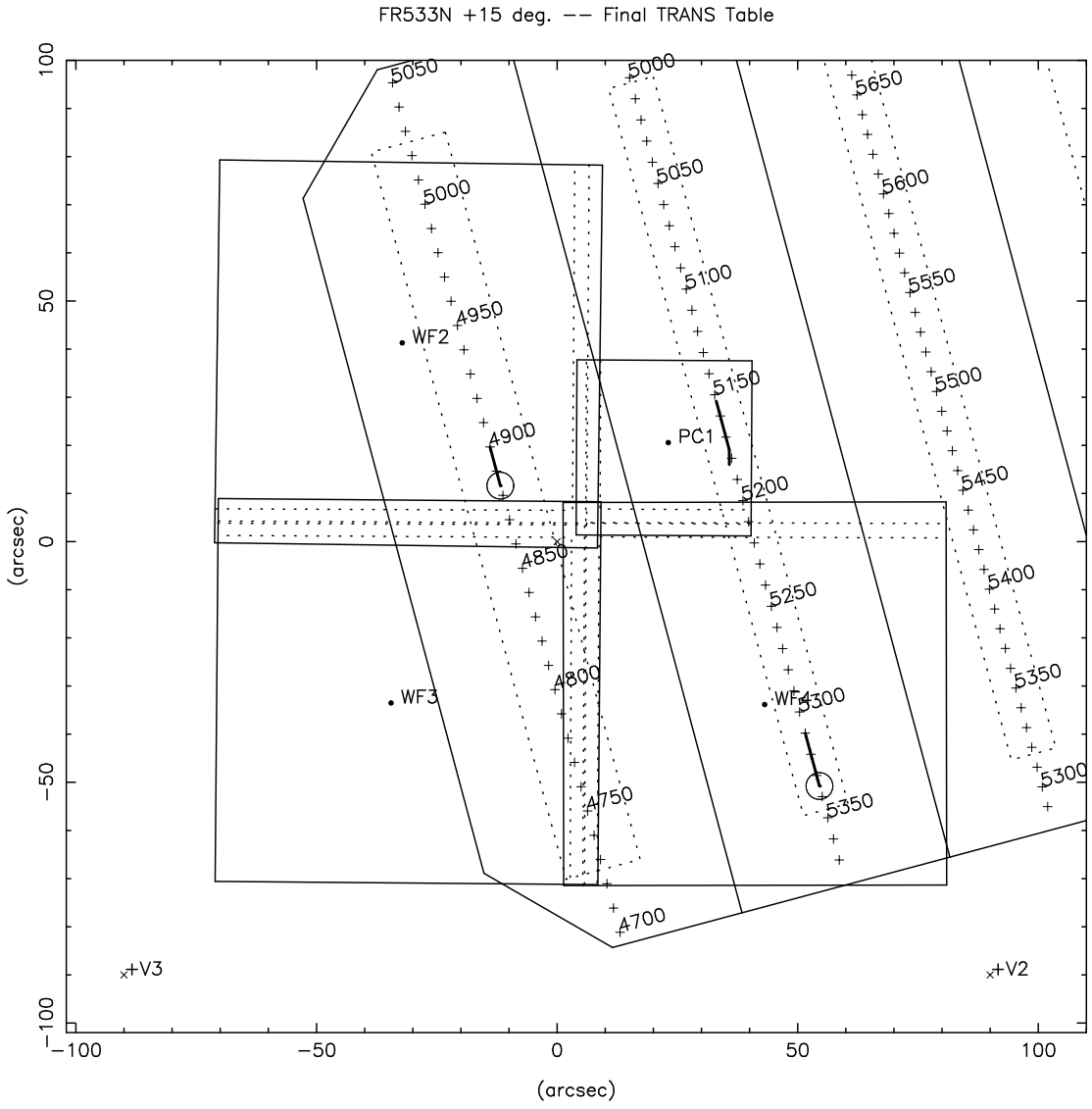

Figure 11.f. Wavelength runs for final TRANS table on FR533N.

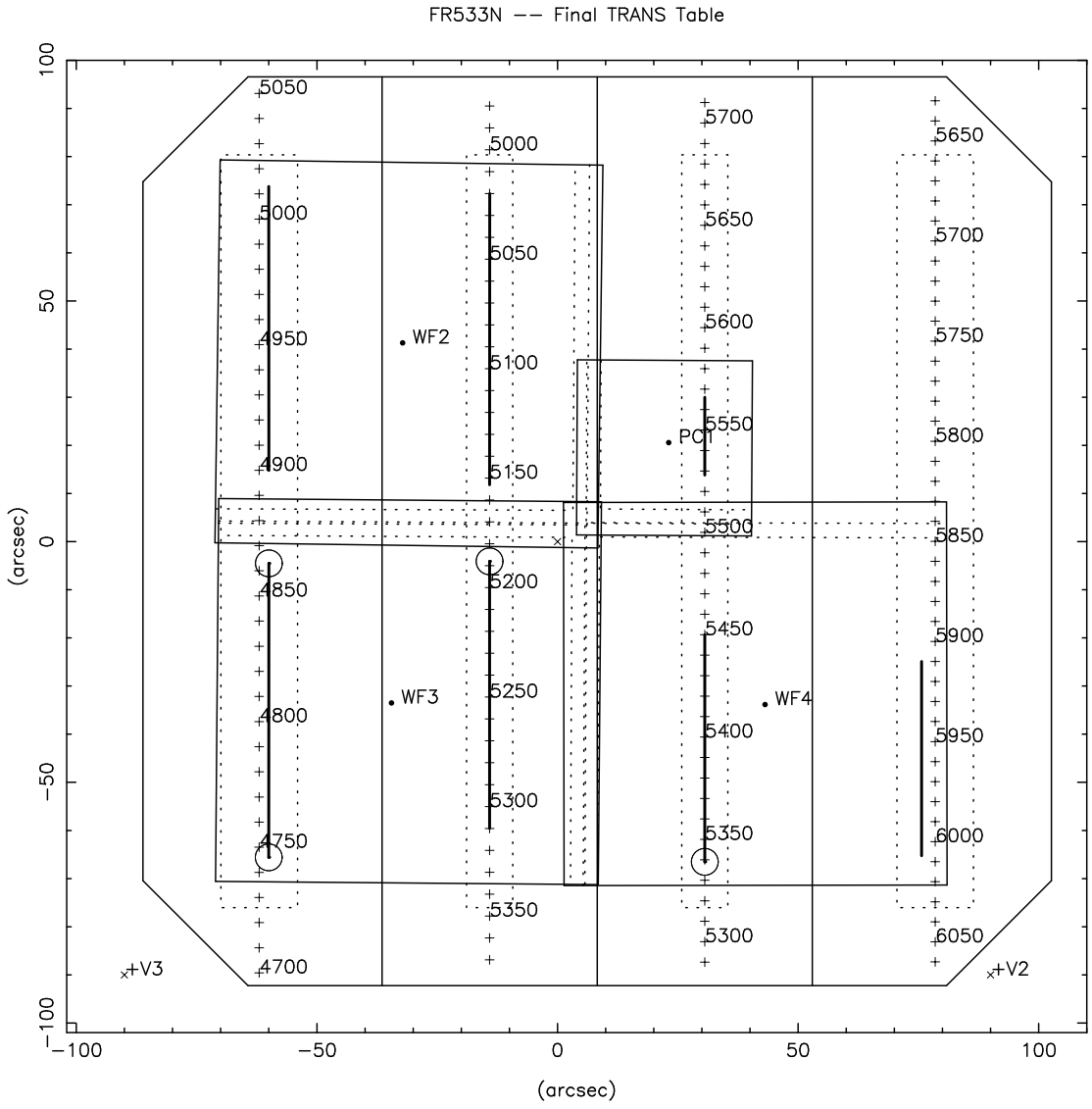

Figure 11.g. Wavelength runs for final TRANS table on FR533N18.

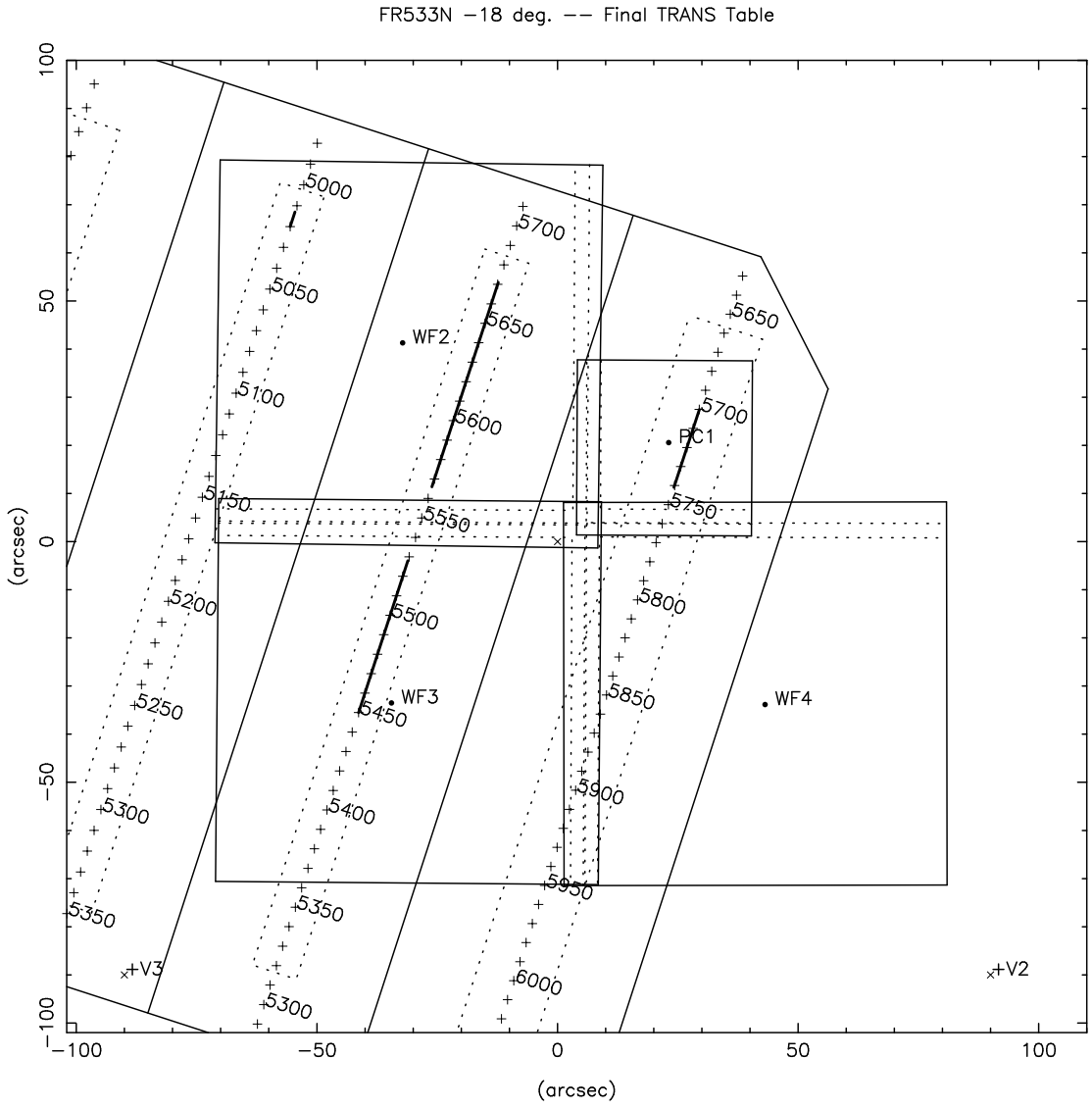

Figure 11.h. Wavelength runs for final TRANS table on FR533N33.

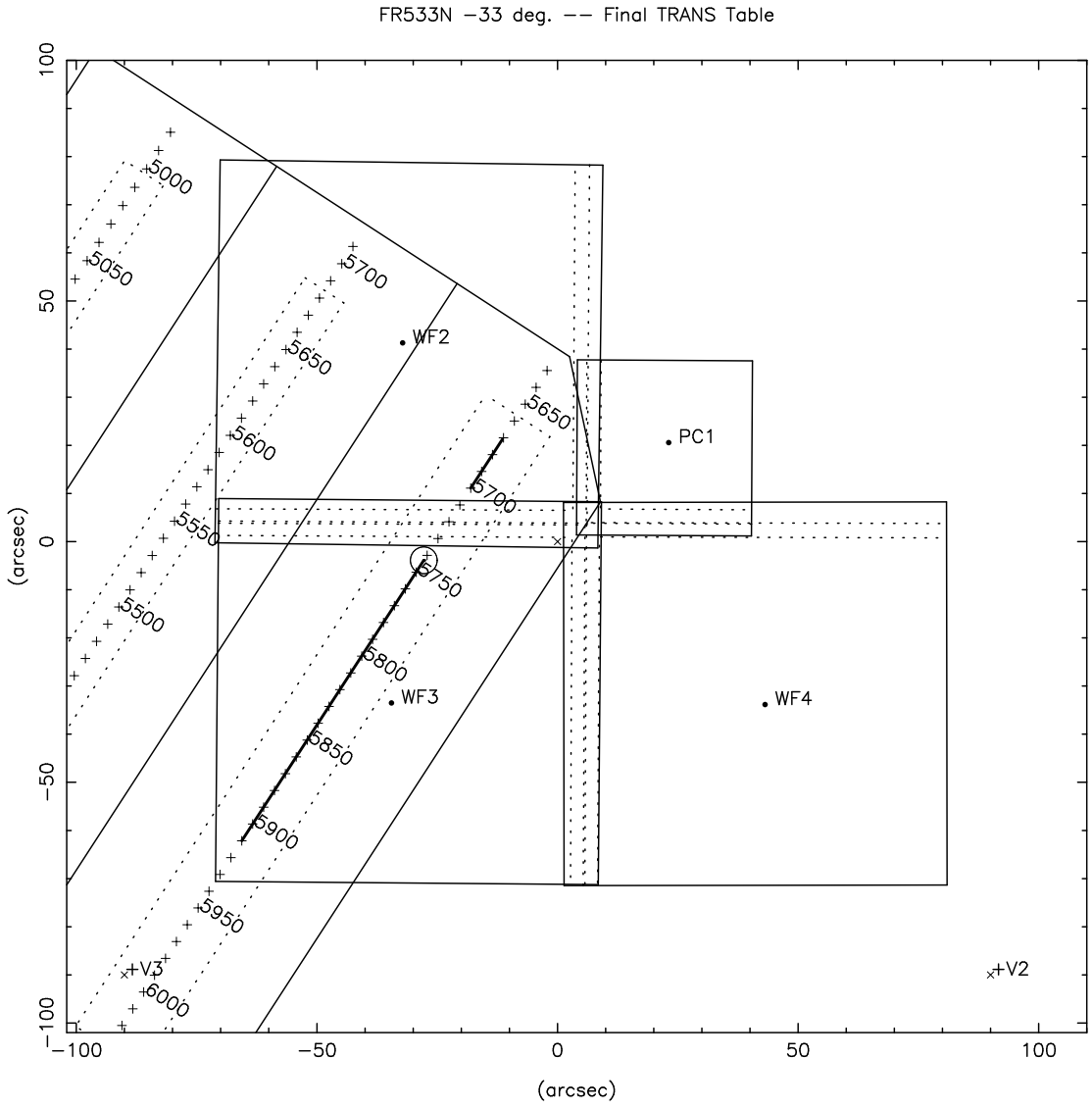

Figure 11.i. Wavelength runs for final TRANS table on FR680P15.

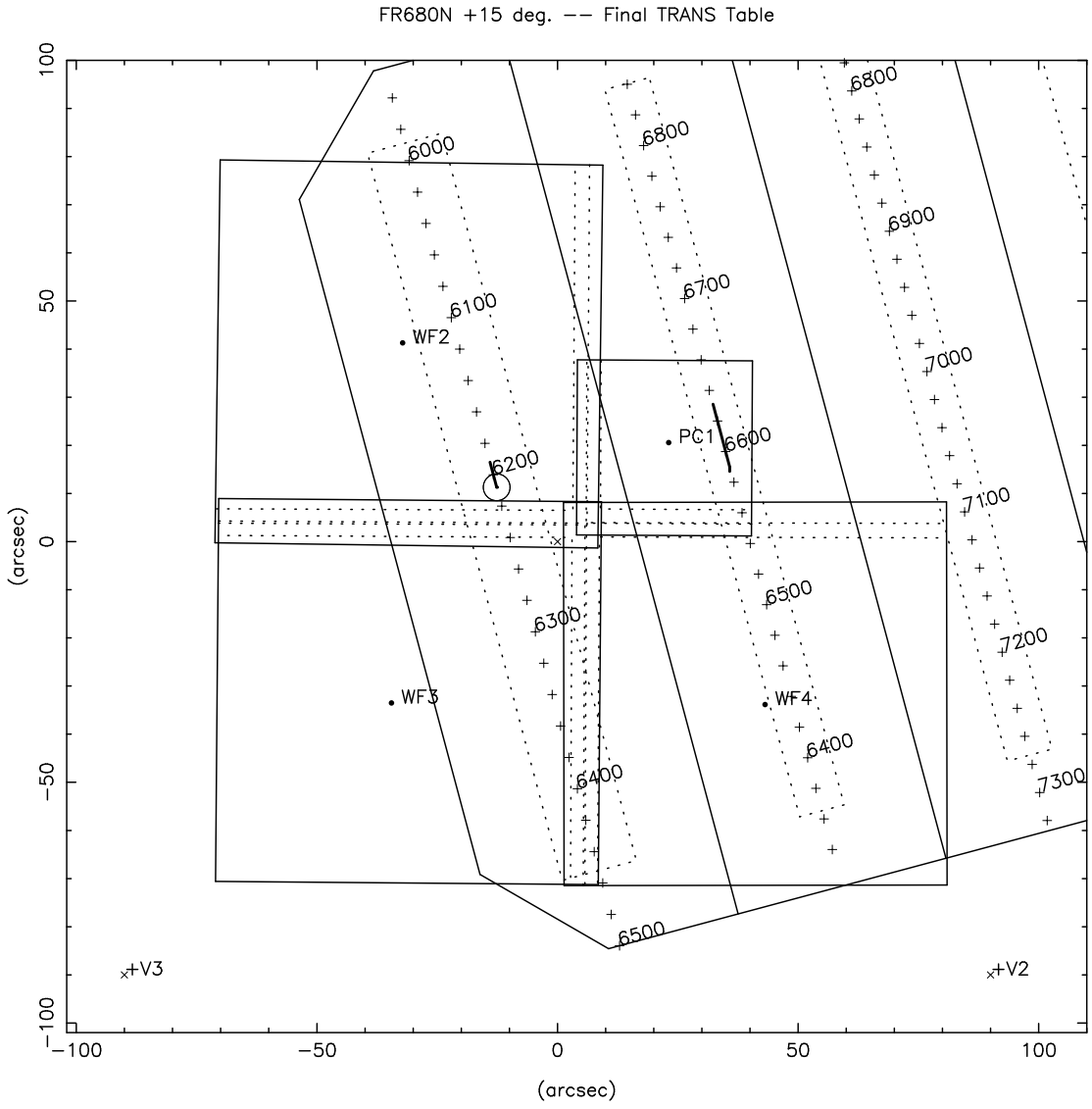

Figure 11.j. Wavelength runs for final TRANS table on FR680N.

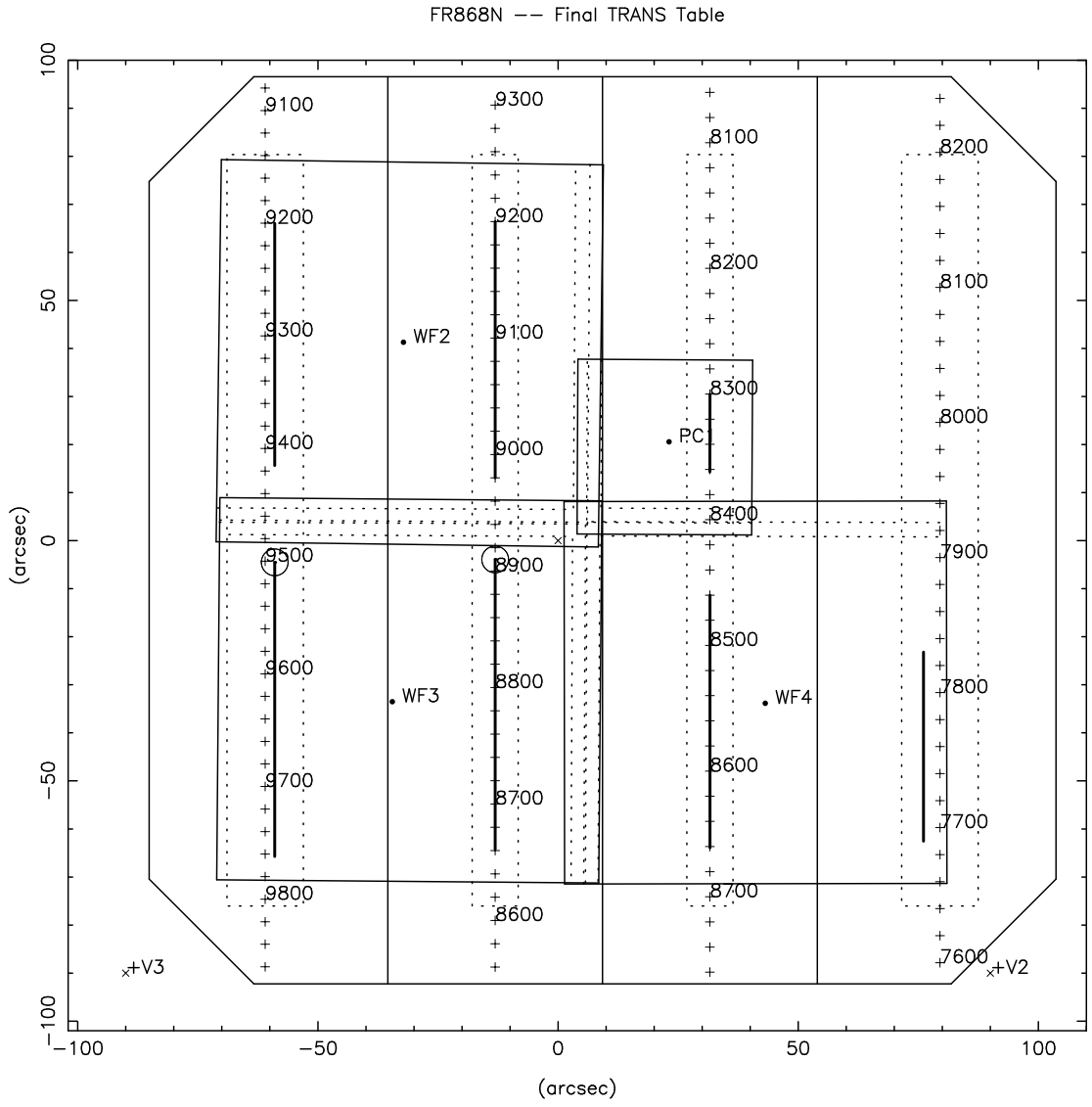

Figure 11.k. Wavelength runs for final TRANS table on FR680N18.

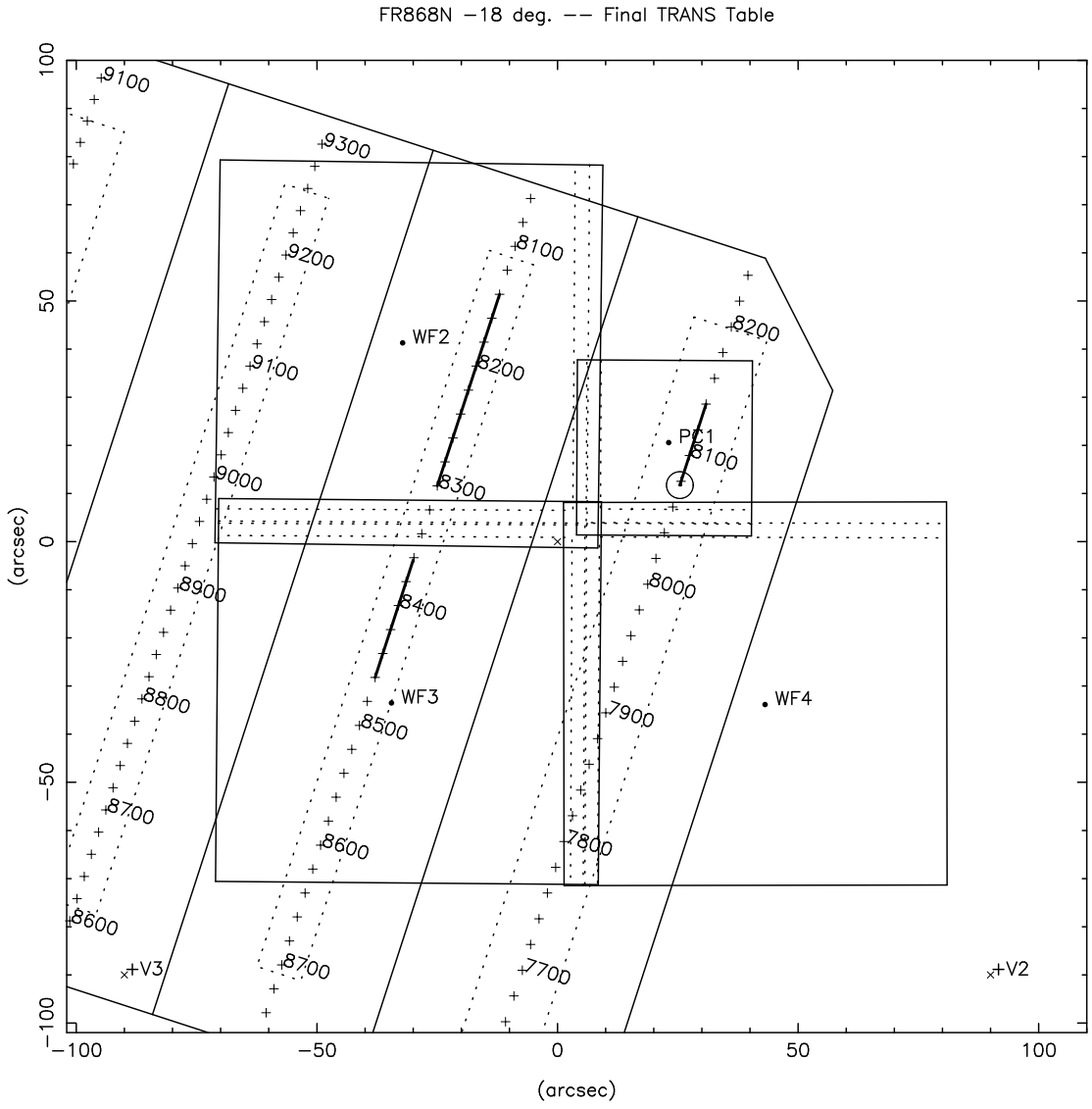

Figure 11.l. Wavelength runs for final TRANS table on FR680N33.

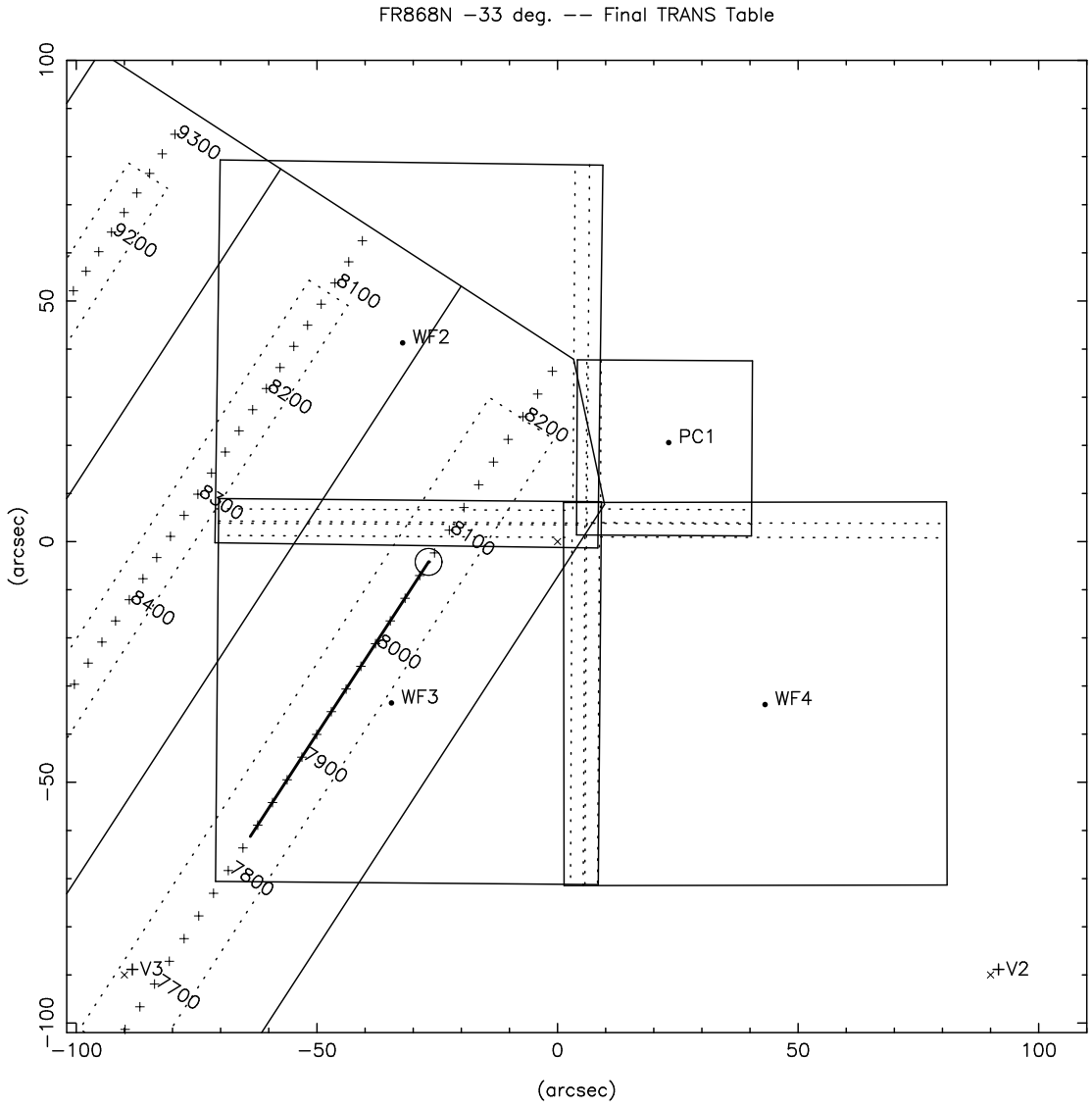

Figure 11.m. Wavelength runs for final TRANS table on FR868P15.

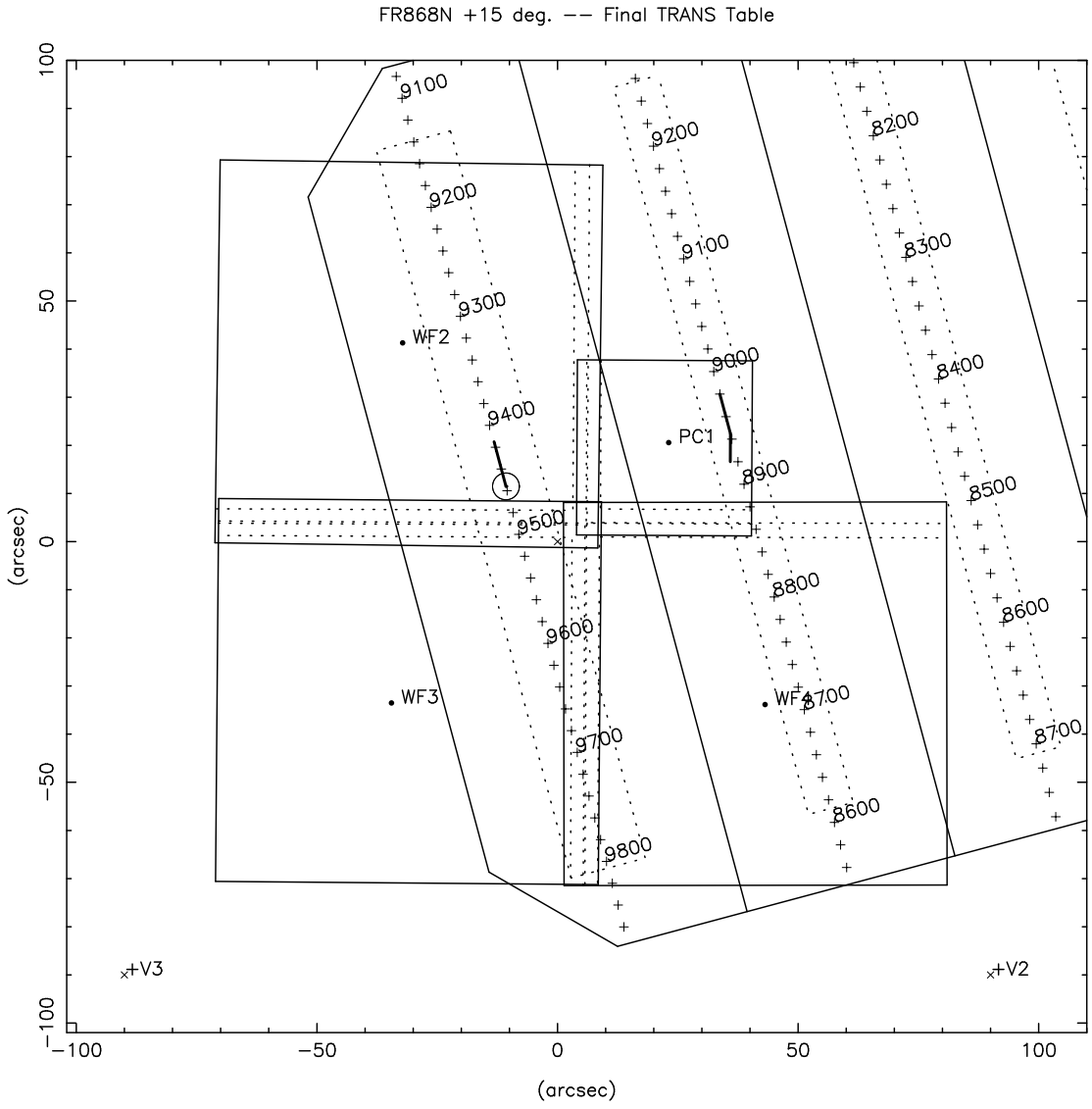

Figure 11.n. Wavelength runs for final TRANS table on FR868N.

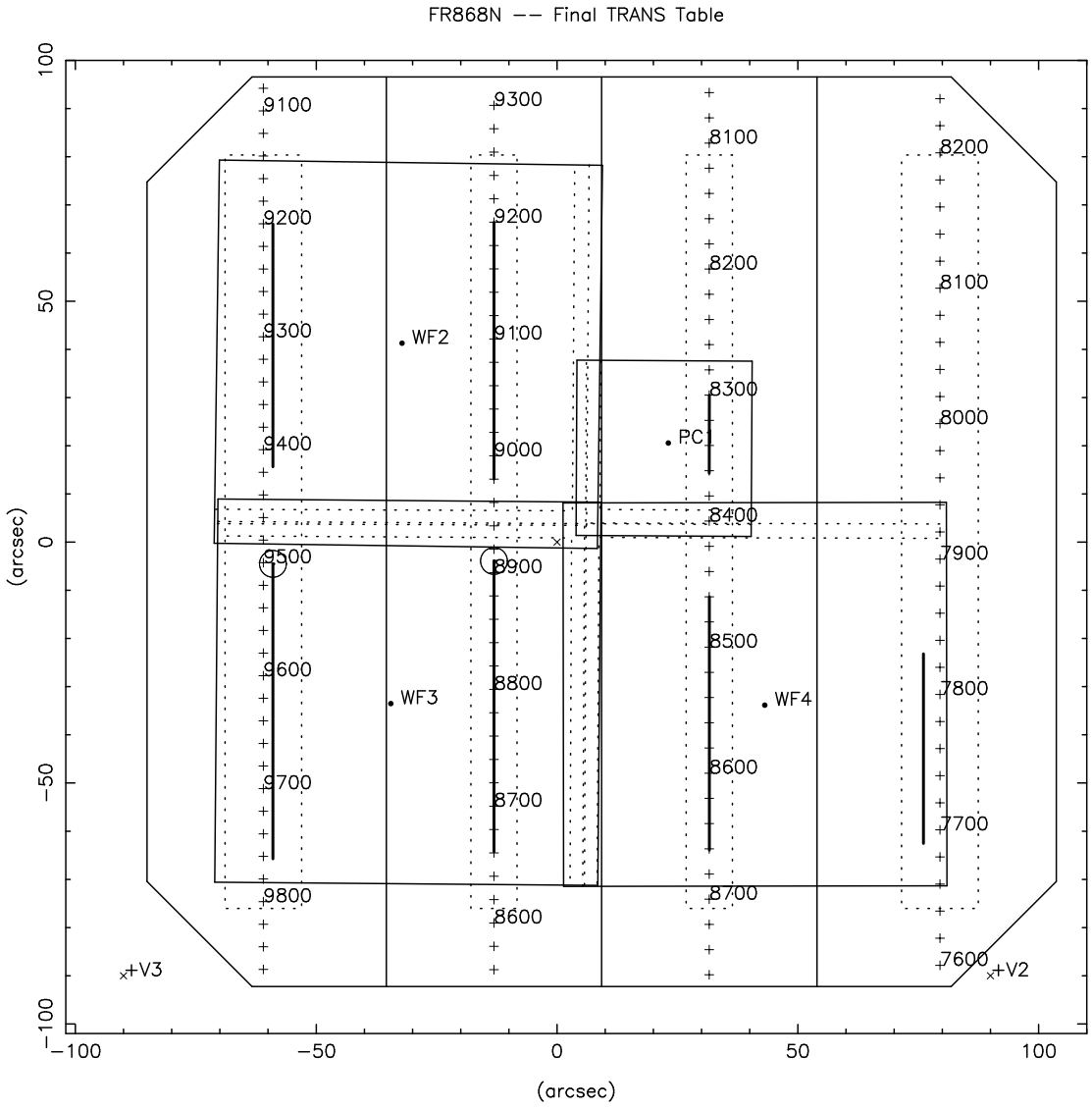

Figure 11.o. Wavelength runs for final TRANS table on FR868N18.

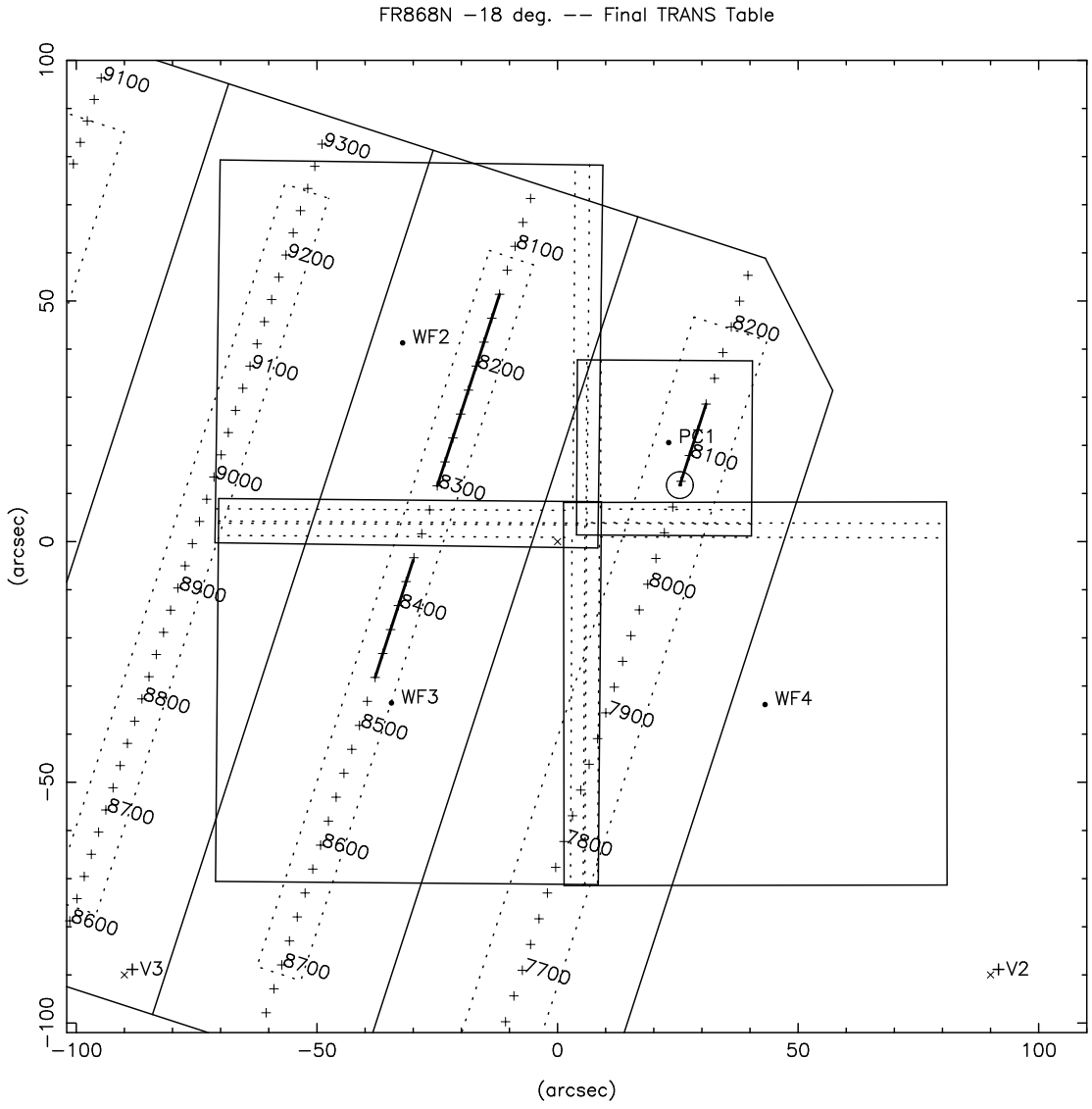

Figure 11.p. Wavelength runs for final TRANS table on FR868N33.

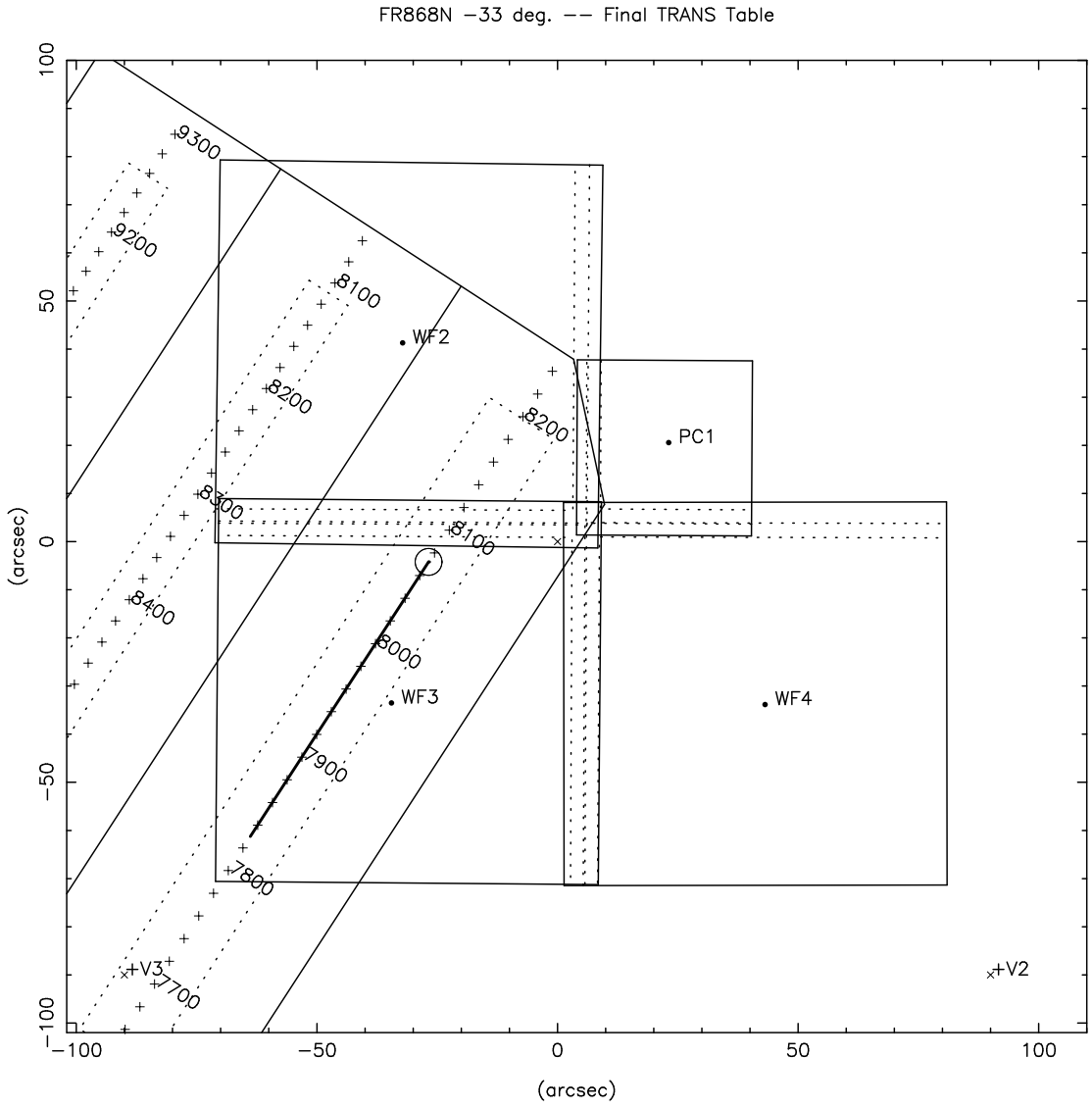

7. Information for Observers: Proposal Status, Tools, and Calibration

In this Section we review implementation of early LRF proposals, and review general calibration procedures for LRF data.

7.1 Implementation of Early LRF Proposals

Early LRF observers will want to know which TRANS table was used to implement their proposals. The table below summarizes this information as of 22 May 1996. Later proposals not listed will all use the "final" TRANS table. As it turns out, there is only one proposal where differences between the interim and final tables have any importance -- proposal 5957 (Sparks=PI). In this proposal the exposures of 3C98, 3C136.1, 3C171, 3C268.4, 3C277.1, 3C284, and 3C297 used settings unique to the interim table, and will require special photometric calibration. STScI will provide these calibrations.

All other proposals using the interim table (DB28856), use portions of it which are identical to the final table. This means that all photometric calibrations, etc., will be identical to those derived for the final table.

Table 14: Status of Early Ramp Proposals - as of 22 May 1996

Proposal	Proposal Type	TRANS version # Date LRF Table	Comments
4709	CAL	---	Internal Monitor
4721	CAL	---	Decontamination Proposal
5215	SCI	---	Scheduled with POS TARGS
5411	SCI	---	Units without LRFs executed; LRFs transferred to Proposal 6332
5561	CAL	---	Internal Monitor
5616	SCI	#77 06-01-95 DB28856	Completed
5635	ENG	#47 03-28-94 DB26391	Partial Filter Stepping Test
5655	CAL	---	Internal Monitor
5758	SCI	#79 07-06-95 DB29290	1 unit; Scheduling
5765	SCI	#77 06-09-95 DB28856	Completed
5832	SCI	#76 05-31-95 DB28856	Completed
5848	SCI	#75 05-10-95 DB28856	Completed; only unit 01 had WFPC2
5909	SCI	DB29290	Completed
5923	SCI	***[a]	In Implementation
5924	SCI	#83 09-06-95 DB29290	12 units; all TRANSed with DB29290; Completed
5927	SCI	***	In Scheduling
5930	SCI	#78 06-30-95 DB29290	Completed

Table 14: Status of Early Ramp Proposals - as of 22 May 1996

Proposal	Proposal Type	TRANS version # Date LRF Table	Comments
5932	SCI	#78 06-28-95 DB28856	Uses Older Table for all 8 units; Completed
5956	SCI	***	In Implementation
5957	SCI	#78 06-16-95 DB28856	Uses Older Table for all units; Snapshot Program ongoing
5966	SCI	***	In Implementation
6140	CAL	---	The Ramp Filter Proposal
6149	SCI	#77 06-13-95 DB28856	Completed
6183	CAL	---	Decontamination Proposal
6189	CAL	---	Internal Monitor
6219	SCI	#81 08-14-95 DB29290	Completed
6231	SCI	#76 05-18-95 DB28856	Completed
6250	CAL	---	Internal Monitor
6332	SCI	#82 08-24-95 DB29290	7 units; Completed

a. *** Not yet in SOGS

7.2 Software Tools and Calibration

We now briefly review the status of LRF calibration as of early May 1996. LRF observers should be aware of our LRF Calibration WWW page, and check it periodically for updates:

http://www.stsci.edu/ftp/instrument_news/WFPC2/Wfpc2_lrf/lrf_calibration.html

The first question observers usually have is ‘‘where is my target?’’ Both Table 12 and Figure 12 serve to answer this question. Also, the LRF calculator tool on WWW (see above address) allows observers to easily compute target locations.

Regarding flat-field calibration: As of this writing, LRF images are not corrected for flat field in the calibration pipeline. We recommend using a narrow band filter flat taken at a nearby wavelength. Preliminary tests indicate that this technique should flatten data to an accuracy of ~2%. There are various fundamental problems with taking flats in the ramps themselves (e.g. unknown spectrum of lamp, pinholes in the filters, etc.) and much effort will be needed to attain the same accuracy already provided by narrow band flats.

There are two methods for attaining photometric calibration. The WFPC2 Exposure Time Calculator has the capability to estimate count rates in the LRF filters for a wide variety of targets. The accuracy for stellar sources will be poor in the vicinity of strong absorption

features, but the calculations for emission lines and power laws should be accurate to a few percent.

The alternate method is to use the SYNPHOT synthetic photometry package; this allows accurate calculation using detailed stellar spectra, as well as a wide selection of non-stellar spectra. The necessary LRF tables have recently been installed in SYNPHOT. Observers will need to obtain and install the latest SYNPHOT tables, if they do not already have them (i.e. need versions later than April 1996). The SYNPHOT tables and information on installing them can be obtained at

http://www.stsci.edu/ftp/instrument_news/WFPC2/Wfpc2_phot/wfpc2_synphot.html

To specify an LRF filter in SYNPHOT, one merely includes ‘‘LRF#xxxx’’ in the PHOTMODE, where xxxx in the central wavelength setting specified on the Phase 2 proposal. It is important to use the Phase 2 setting here, regardless of the wavelength of the emission line, since this controls the physical setting of the filter and hence the bandpass location and shape. Also CCD WF3 should be specified, as the flats are normalized on that CCD. For example, if the Phase 2 proposal requested central wavelength 4584.2 Angstrons, the mode might be specified as:

MODE=WFPC2,3,LRF#4584.2

Note that the wavelength should be given only to the first decimal place; inaccurate results may occur if the wavelength is specified to 2 or mode decimal places. This is due to the way “jumps” between ramps are handled in the SYNPHOT LRF table.

Future calibration work will include a series of on-orbit standard star observations to check the throughput values (proposals 6194 and 6939), as well as observations of emission line targets to verify and monitor the wavelength calibration. Additional internal observations (VISFLATS or perhaps Earth flats) will also be made where the ramps are crossed with narrow band filters; these will help monitor the wavelength stability of the ramp filters, as well as that of the narrow band filters.

8. References

Biretta, J. A. and Sparks, W. B. 1995, “WFPC2 Polarization Observations: Strategies, Apertures, and Calibration Plans,” WFPC2 Instrument Science Report 95-01.

Cox, C. 1994, “The WFPC2 Scales and Alignments” Science Observatory Branch Report SOB-94-10-21.

Evans, R. 1992, “WFPC-2 Ramp Filter Predictors” JPL Interoffice Memorandum DM# 2031 (Dec. 30, 1992).

Scowen, P. 1995. private communication.

Trauger, J. 1993. private communication.